Report 3819

VAL SHIP RESEARCH AND DEVELOPMENT CENTER
Bethesda, Maryland 20034

MOTIONS AND HULL-INDUCED BRIDGING-STRUCTURE LOADS FOR A SMALL WATERPLANE AREA, TWIN-HULLED, ATTACK AIRCRAFT CARRIER IN WAVES

by

Harry D. Jones
and
David M. Gerzina

SHIP PERFORMANCE DEPARTMENT
RESEARCH AND DEVELOPMENT REPORT

August 1973

Report 3819

MOTIONS AND HULL-INDUCED BRIDGING STRUCTURE LOADS FOR A SMALL WATERPLANE AREA, TWIN-HULLED, ATTACK AIRCRAFT CARRIER IN WAVES

The Naval Ship Research and Development Center is a U. S. Navy center for laboratory effort directed at achieving improved sea and air vehicles. It was formed in March 1967 by merging the David Taylor Model Basin at Carderock, Maryland with the Marine Engineering Laboratory at Annapolis, Maryland.

Naval Ship Research and Development Center

Bethesda, Md. 20034

MAJOR NSRDC ORGANIZATIONAL COMPONENTS

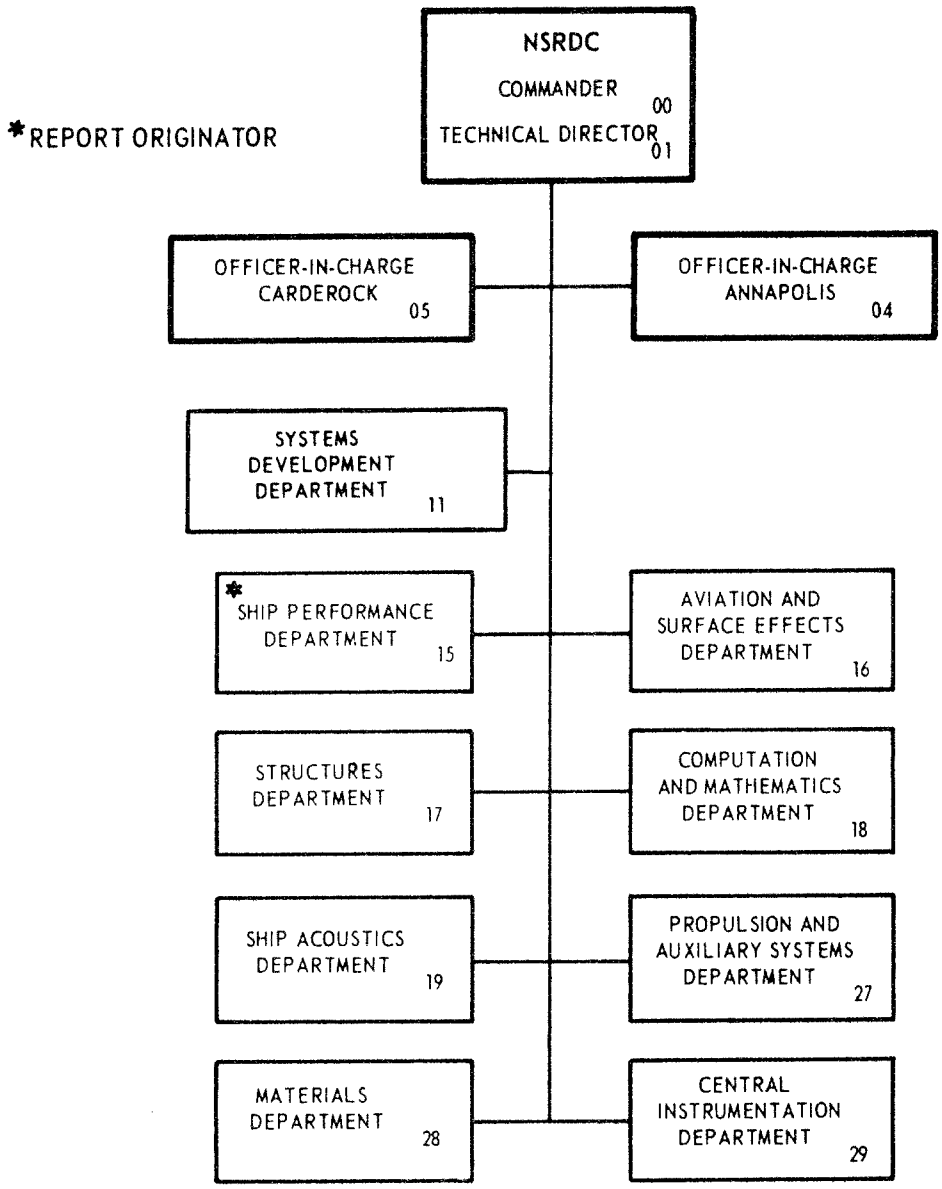

NDW-NSRDC 3960/44 (REV. 8/71)

GPO 917-872

TABLE OF CONTENTS

LIST OF FIGURES

Page

Page

Page

NOTATION

B	Beam
BM	Bending moment
CG	Center of gravity
E	Area under spectrum
F_n	Froude number
FS	Full scale
FW	Freshwater
GM_t	Transverse metacentric height
H	Draft
HS	Hull separation—distance between closest points
KG	Vertical center of gravity
LBP or L	Length between perpendiculars
LCG	Longitudinal center of gravity
LWL	Waterline length
SW	Seawater
TCG	Transverse center of gravity
TF	Transverse force
YM	Yaw moment
Δ	Displacement
ΔT	Added thrust
ζ_A	Wave amplitude
λ	Wavelength
σ	Standard deviation of an irregular signal
χ	Heading angle
ω_e	Frequency of wave encounter

ABSTRACT

An experimental investigation was performed with a model in the maneuvering and seakeeping facility at the Naval Ship Research and Development Center to determine the characteristics of a proposed small waterplane area, twin-hulled, attack aircraft carrier in waves. Motions of the model were measured, together with the forces and moments induced by the hulls on the cross structure spanning the two hulls. Experimental data were compiled in head, bow, beam, quartering, and following regular waves in addition to long-crested, irregular head and beam waves. Some powering measurements were also made in regular head waves.

ADMINISTRATIVE INFORMATION

This work was authorized and funded under the Naval Ship Systems Command Exploratory Development Applied Hydromechanics Program, Budget Program 32, Work Unit 1-1568-205.

INTRODUCTION

In addition to the specific purpose of investigating the behavior in waves of a SWATH (small waterplane area, twin hull) CVA (attack aircraft carrier) these experiments form part of a program to generate a body of knowledge about the characteristics of CVA catamarans with various hull proportions. This program is similar to that used in determining the characteristics of the ASR (submarine rescue ship) catamaran.[1]

The SWATH model was tested in the free-running condition, with no rigid constraints on the motion responses. Regular wave data were measured for Froude numbers of 0, 0.153, and 0.306—corresponding to 0, 15, and 30 knots, full scale (FS)—and five headings to the wave direction, i.e., head 180-degrees, bow 135-degrees, beam 90-degrees, quartering 45-degrees, and following 0-degree waves, for the catamaran hulls at their designed spacings. An additional hull spacing was also tested for the same three speeds, with headings restricted to head, bow, and beam waves. Irregular wave data were measured for head and beam seas at F_n = 0.153 for the designed hull spacing.

The model did not possess a bridging structure; hence, no wave-induced impact loads on the bridging structures were obtained. The use of instrumented flexures between the two hulls permitted determining loads on the bridging structure due to relative hull motions.

---

[1]Wahab, R. et al., "On the Behavior of the ASR Catamaran in Waves," Marine Technology, Vol. 8, No. 3 (Jul 1971).

MODEL PARTICULARS

Ship and model particulars for the SWATH CVA are given in Table 1 with the lines shown in Figure 1. The 17-ft model was constructed of mahogany and was designated "Model 5266."

TABLE 1 – SHIP AND MODEL PARTICULARS FOR THE SMALL WATERPLANE AREA, TWIN-HULLED, ATTACK AIRCRAFT CARRIER MODEL 5266

(Scale Ratio 50)

Particular	Unit of Measure	Ship	Model
Length (LBP)	Feet	850	17
Length (LWL)	Feet	751	15.02
Beam each Hull (B)	Feet	30.42	0.608
Midship Maximum Breadth	Feet	70	1.4
Draft (H)	Feet	69.5	1.39
Displacement each Hull ($\Delta/2$)	Long Tons	50,500 SW*	0.394 FW*
Longitudinal Center of Gravity (LCG), Aft of FP	Feet	419.9	8.398
Longitudinal Radius of Gyration	–	0.26 L*	0.26 L
Vertical Center of Gravity (KG)	Feet	78	1.56
Design Hull Separation (HS)	Feet	207	4.14
Distance between Centerlines at Station 10	Feet	279	5.57
Transverse Metacentric Height (GM_t)	Feet	92	1.84
Natural Heave Period	Seconds	19.80	2.8
Natural Pitch Period	Seconds	33.59	4.75
Natural Roll Period	Seconds	25.46	3.6
Second Hull Separation (HS)	Feet	157	3.14
Distance between Centerlines at Station 10	Feet	229	4.57
Transverse Metacentric Height (GM_t)	Feet	43.05	0.861
Natural Heave Period	Seconds	19.80	2.8
Natural Pitch Period	Seconds	30.41	4.3
Natural Roll Period	Seconds	32.53	4.6

*SW is seawater; FW is freshwater; L is length between perpendiculars.

Each of the twin hulls was equipped with outward turning propellers, and a narrow strip of sandpaper was fitted to each hull at Station 1/2 to stimulate turbulent flow in the boundary layer. The two hulls were ballasted and trimmed to the designed waterline (DWL) individually, to give identical values for the longitudinal radius of gyration and vertical center of gravity; see Table 1. The model was not fitted with a bridging structure; however, two "strain-gaged" flexures were used to span the two hulls to permit measuring the forces and moments acting between the hulls. These particular flexures were also used to determine the load characteristics for the ASR catamaran[1] and the conventional (CONCAT) CVA catamaran, previously studied by the Center.

INSTRUMENTATION

The study of motions and hull-induced bridging structure loads for a SWATH CVA model was carried out in the maneuvering and seakeeping facility (MASK) at the Center. Throughout the experiments the model was self-propelled with no rigid constraints on the motion responses, i.e., the model was free to move in all six degrees of freedom.

The model was powered by two 5-horsepower, d-c motors--one mounted on each hull. The model speed was controlled manually through these motors and was regulated in accordance with the preset carriage speed. Sway and yaw signals were used as input to the steering servo units on each hull, which corrected the rudder angle and held the model on course. Tethering lines, required for acceleration and deceleration of the model, along with power cables and transducer signal cables were the only interconnections from the carriage to the model. While data were being recorded, these lines and cables were slack and did not affect the model responses.

Various types of instrumentation and transducers were used in collecting data during the experiments. Angular measurements such as pitch, roll, and yaw were measured by using gyroscopes mounted on the hull decks. Ultrasonic transducers were used to measure linear displacements. The relative bow motion (RBM) sonic probe was mounted along the longitudinal center line of the model at a position approximately 0.13 L aft of Station 0. Sonic probes were also used on the side and stern of the model to measure sway and surge, respectively. Heave, port and starboard hull-bow motions, and port and starboard hull-stern motions were measured with accelerometers. The heave accelerometer was mounted at a point coincident with both longitudinal (LCG) and transverse centers of gravity (TCG), while the bow-motion accelerometers were positioned 0.24 L aft of Station 0 on the port and starboard hulls. Similarly, the stern-motion accelerometers were placed 0.24 L forward of Station 20 on the two hulls. Propeller thrust was measured, using dynamometers mounted in the port hull on both the inboard and outboard shafts.

The hulls were connected by a combination of block gages and flexure beams, equipped with a network of strain gages. This arrangement enabled measuring six loads used in calculating the five relative forces and moments due to the relative motions between the hulls. These beams were centered about

the LCG and TCG of the model with the vertical center of the beams 33.05 inches above the keel. The following information was derived using the instrumented flexure beams:

Bending Moment	Moment tending to produce relative roll between hulls
Torsion Moment	Moment tending to produce relative pitch between hulls
Yawing Moment	Moment tending to produce relative yaw between hulls
Shear Force	Force tending to produce relative heave between two hulls
Transverse Force	Force tending to produce relative sway between hulls

EXPERIMENTAL PROCEDURE

The large SWATH CVA model was tested in regular waves and long-crested, irregular waves as well as in calm water. The regular-wave program consisted of testing the model at its designed hull separation of 4.14 ft, i.e., distance between closest points,* at headings of 180, 135, 90, 45, and 0 degrees. At each heading the model was tested at three model speeds of 0, 2.12, and 4.24 knots—equivalent to Froude numbers of 0, 0.153, and 0.306. The ratio of wave length-to-ship length (λ/L) during these experiments ranged from approximately 0.40 to 4.90. Owing to the large range in λ/L covered during these tests, nominal wave steepness ($2\zeta_A/\lambda$) had to be changed from 1/50 for the shorter period waves to 1/100 for the longer period waves. The two nominal steepnesses were used in an effort to keep the wave height in a range that would result in reasonable motions and loads for the model. In several cases waves of both steepnesses were used as a linearity check. In addition, added thrust measurements were made at 180-degree heading for three nominal wave steepnesses of 1/50, 1/75, and 1/100.

Similar regular wave experiments were also conducted with the hull separation less than designed, i.e., 3.14 ft, for the same three speeds with heading limited to head, bow, and beam waves.

The irregular head-wave experiments were performed at a model speed of 2.12 knots, i.e., F_n = 0.153, for the hulls at their designed spacing. Two existing magnetic tape programs, designated "Programs 1 and 6," were used to generate the unidirectional irregular waves. These programs were each used to generate two significant wave heights. Similar experiments were conducted in irregular beam seas. For each condition, approximately 300 seconds of data were collected, corresponding to about one-half hour of full-scale operation.

In addition to the previously described experiments, the model was tested in calm water at both 2.12 and 4.24 knots to determine the trim at each speed as well as the calm water thrust.

*Distance between hull centerlines is also given in Table 1.

DATA ANALYSIS

Throughout the experiments the model responses were recorded in analog form on magnetic tape. Later these analog tape data were digitized and put in a form suitable for analysis on an IBM 7090 computer.

The regular wave-data analysis consisted of determining the Fourier transform coefficients for the fundamental frequency of the wave-height signal and the coefficients of each of the other signals at the same frequency. Mean-level offsets, amplitudes, and phases of each of the signals were then determined. To obtain correct phase relationships, all phases were calculated relative to the wave as it passed the CG of the model, a positive phase angle indicating a lead of response before wave. Corrections to the CG location were accounted for by the mean-level offsets of the surge and sway signals and by the distance from the expected position of the model to the wave-height probe. Spectral analysis was made of irregular wave data. The significant double amplitude values of the oscillatory motions, forces, and moments were obtained from area E under the spectra, using the relationship

$$\text{significant value} = 2.83\sqrt{E}$$

where $E = 2\sigma^2$.

Figures 2 and 3 indicate the sign conventions used for presenting motions and structural loads in the experimental results.

RESULTS AND DISCUSSION

Figure 4 shows calm water-mean values of bending moment, yaw moment, transverse force, trim, and relative bow motion (displacement) for the full-scale SWATH at its designed hull separation. These parameters are shown as ranges, for the two given Froude numbers of 0.153 and 0.306. The change seen in the relative bow displacement with forward speed due to trim and sinkage indicates a significant decrease in height at the position of the forward structure which could imply an increase in the probability of bridging-structure slamming.* The change in trim angle with forward speed could however present a problem to aircraft operations. These possible problems did not arise for the CONCAT CVA because the changes in trim and relative bow displacement were negligible with forward speed. The mean values for the loads presented here are, in general, about one-half the values given for the CONCAT CVA.

---

*Data presented later in Figure 20 do not show excessive relative bow-motion responses, except in following waves, when compared to data for monohull ships. It is possible that this decrease in height may not lead to a significant problem in bridging-structure slamming.

Figure 5 gives long-crested, irregular head-sea wave results for tape Programs 1 and 6 as full-scale predictions of spectral energy and compares them with theoretical Pierson spectra for comparable significant wave heights. The significant double amplitude values of heave, pitch, and relative bow motion as well as port bow and stern and starboard bow and stern motions are given in Figures 6 and 7 as functions of significant wave height. Different symbols distinguish the two tape programs used, with straight lines faired through the data points for each program. With a sufficient variation in frequency of maximum energy content, these plots can be used to estimate significant motions for any given long-crested, irregular head wave of known significant wave height and frequency of maximum energy. The discrepancies in significant port and starboard stern motions are thought to be due to a faulty transducer on the port stern. Figures 8 and 9 show comparisons of nondimensional transfer functions of the motions derived from both the regular and irregular wave tests. In general, the agreement is quite good, which would indicate that results of regular wave, nondimensional transfer functions for other headings would suffice for predicting unidirectional, irregular wave responses for those seaway conditions.

Figure 10 is a spectral energy graph for beam waves, similar to Figure 5. However, it can be seen that the frequency of maximum energy content varies only slightly between the two programs. Significant values of the motions, forces, and moments for beam waves are given in Figures 11 through 13. These plots do not lend themselves to predictions in other seaways as did the significant value graphs of head waves, owing to the minimal difference in the frequency of maximum energy content between the two tape programs used. The scatter seen in heave in Figure 11 is probably due to a low signal-to-noise ratio of the heave accelerometer with such small heave signals. Figures 14 through 16 are comparisons of nondimensional transfer functions for the motions, forces, and moments between the regular and irregular wave results. Comparisons for the beam-wave experiments are good; however, they are not as good as for the head-wave results. In general, the regular wave results are less in the lower frequency range tested.

For the designed hull spacing, regular-wave, nondimensional transfer functions for the motions are presented in Figures 17 through 24. Comparing SWATH CVA data with those for the CONCAT CVA, it is seen that a larger range of λ/L was tested for the modified catamaran. This was done to obtain resonance peak values which occurred in this range. However, for this size of ship and higher λ/L's, i.e., those more than approximately 2.5, do not represent realistic waves normally found in nature. For the range from λ/L = 0.5 to 2.5, SWATH results are generally higher at zero speed and lower at speed, except some of the results for quartering and following waves. Another exception was the nondimensional, roll-transfer function. This was negligible for all headings to approximately λ/L = 4.0, when an extreme peak was encountered at zero speed in beam and oblique seas. The motions, indicated by the transfer functions in Figures 17 through 24, have shown an inverse relationship to forward speed from what has generally been expected. They show a general decrease with forward speed rather than an increase, which is usually expected for both monohulls and conventional catamarans. Some exceptions occur in quartering and following waves when an increase in motion is seen going from 15 to 30 knots; however, at 30 knots the motion rarely exceeds that measured at zero speed. The heave transfer function at 0 and 30 knots

and the relative bow-motion, transfer function in following waves are also larger than would normally be expected and could present a problem in bridging-structure slamming.

Figures 25 through 29 present the nondimensional forces and moments for SWATH. The nondimensional transverse force is of the same general shape for both CONCAT and SWATH CVA's. Both showed a peak at about the same λ/L, with the amplitude of SWATH at least twice as large at the peak. The exception to this trend is at speed for the 180-degree heading, at which virtually no response was recorded for the modified CVA. No similarities in shape are seen for the nondimensional shear force results. In all instances SWATH amplitudes are much less, with maximums tending to occur near both extremes of the λ/L scale. The nondimensional moments for both SWATH and CONCAT CVA's have basically the same shape. Peak amplitudes for SWATH are in general twice as large as for CONCAT CVA's. The SWATH has virtually no response at a 90-degree heading for nondimensional torsion moment, while a maximum occurred for CONCAT. It is seen in Figures 25 through 29 that the maximum loads acting on the bridging structure occur at wavelengths generally much shorter than those where the motion resonances occur. This phenomenon may be caused by the fact that the waves, usually around λ/L = 1.0, are such that with a hull form of this type large differential forces are generated on the hulls. Since natural periods are so much longer than those corresponding to λ/L = 1.0, most of the wave energy goes into bridging-structure loading. Peaks may also be seen in the vertical shear force in Figure 26, corresponding in wavelength to the peaks seen in the rolling motion. This effect is probably due to inertial loadings, resulting from large motions of the hull mass.

Figures 30 through 42 show phase angles for the previously described motions, forces, and moments for the modified catamaran at its designed spacing. The phase angles are restricted within a 360-degree interval, making some of the faired curves appear discontinuous. A positive phase angle indicates that the response is leading the wave.

Figures 43 through 55 are nondimensional transfer functions of motions, forces, and moments for the modified catamaran at a second hull separation of 157 ft. For these experiments, the model hulls were 1 foot closer together, equivalent to a reduction of full-scale hull separation of 50 ft. The results for the three headings tested showed little difference from the designed hull-spacing results. Generally the responses have been of the same shape and size for both hull spacings tested. Phase angle plots for the second hull separation are given in Figures 56 through 68; as would be expected, the phase comparisons for the two hull separations are generally similar and follow the same trends.

Figures 69 and 70 present added thrust curves for a range of ratios of wave length-to-ship length and the two test speeds, i.e., F_n = 0.153 and 0.306. These graphs also include curves of the parabolic relationship $\Delta T = A\,\zeta_A^{\,2}$ that were determined using the least-square-fit criteria to the experimental data.

During experiments with this model, it showed an excellent stability on course. This, however, made it difficult to maneuver at speed.

CONCLUDING REMARKS

Comparisons made in the preceding section between SWATH and CONCAT CVA's data give an indication of the advantages, i.e., a general decrease in motions with forward speed, and disadvantages, i.e., a general increase in hull-induced, bridging-structure loads, for SWATH. The information presented gives an indication of the maximum motions and loads to be expected with a SWATH CVA. In many instances maximum responses occurred in wave conditions not normally found. Results of the irregular and regular wave comparisons indicate the reliability of making irregular wave predictions from regular wave results for other headings.

In general, measured motions indicate that the ship performs best at speeds with possible difficulty arising at zero speed and in following seas, especially should a much smaller ship of this design be considered. The high, hull-induced, bridging-structure loads present a problem in that required added strength will possibly create a change in displacement to which a weight-controlled, low waterplane catamaran of this type is very sensitive.

RECOMMENDATIONS

Further consideration should be given to the possible occurrence of bridging-structure slamming in head and following seas. In head seas, the motions are small and in some cases almost nonexistent; however, the combination of this characteristic and the reduction in forward structure height due to trim and sinkage could result in slamming due to wave height alone. In following seas, the relative motion may be sufficient to cause bridging-structure slamming, especially when coupled with the reduced forward structure height due to ship speed. The change in trim with speed could possibly be prevented by redesigning the lower or pod portion of the hulls. An alternate method of reducing the change in trim would be a ballasting system, whereby the trim could be adjusted as necessary.

From experimental observations, it is recommended that the maneuvering characteristics at designed speed should be considered.

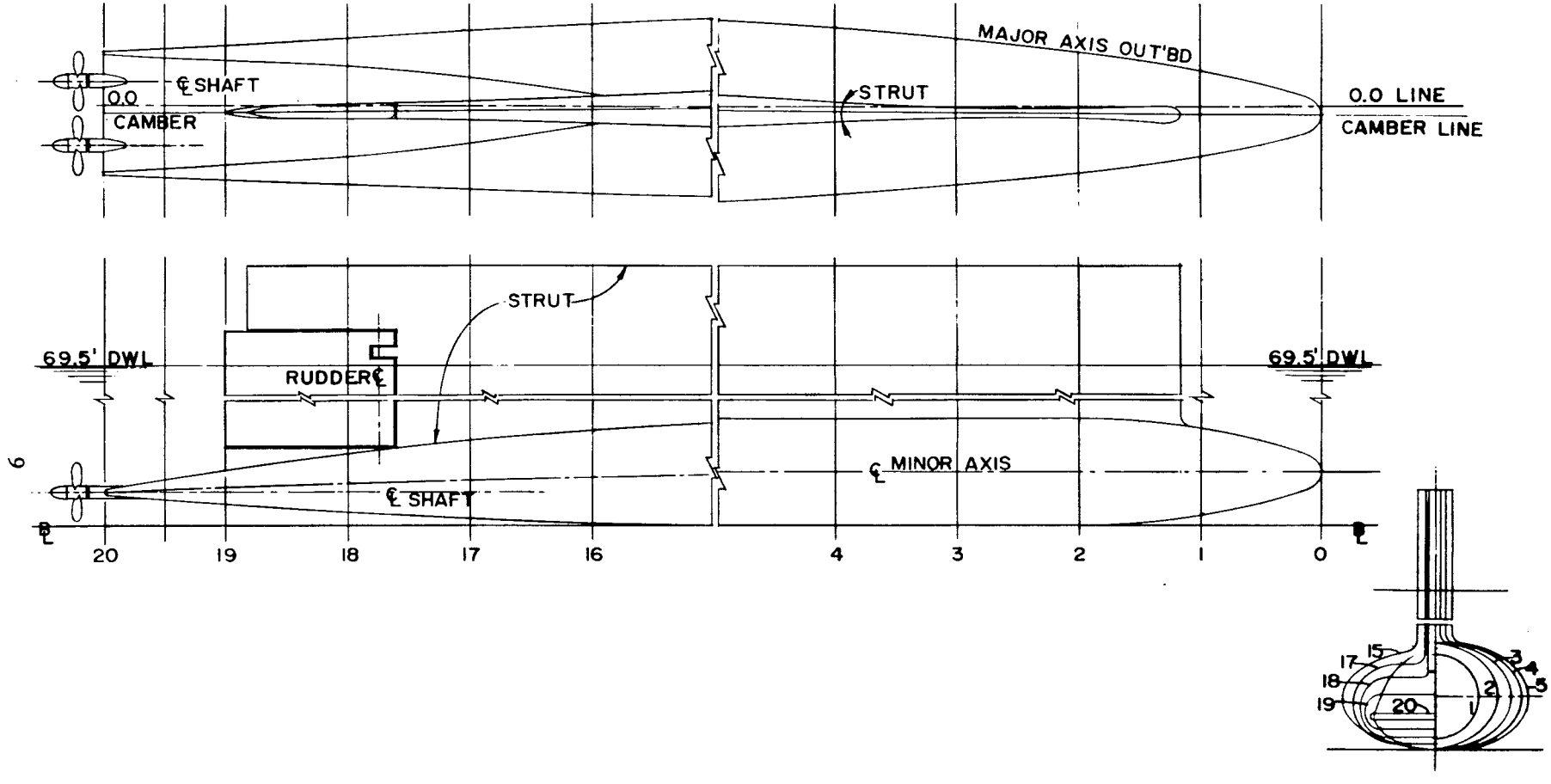

Figure 1 – Small Waterplane Area, Twin-Hulled, Attack Aircraft Carrier Model 5266

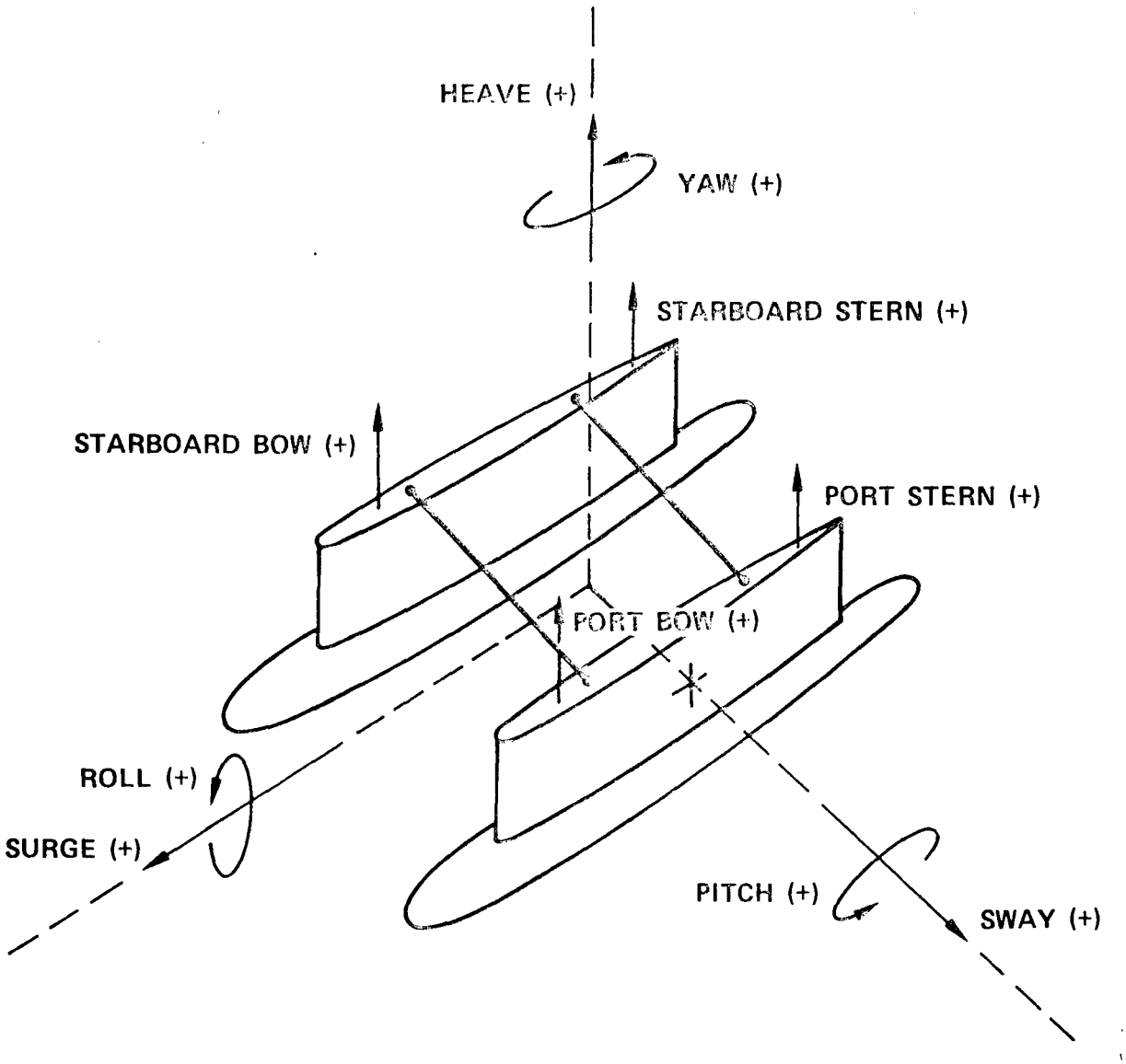

Figure 2 – Sign Convention Used for Motions in Presentation of Experiment Results

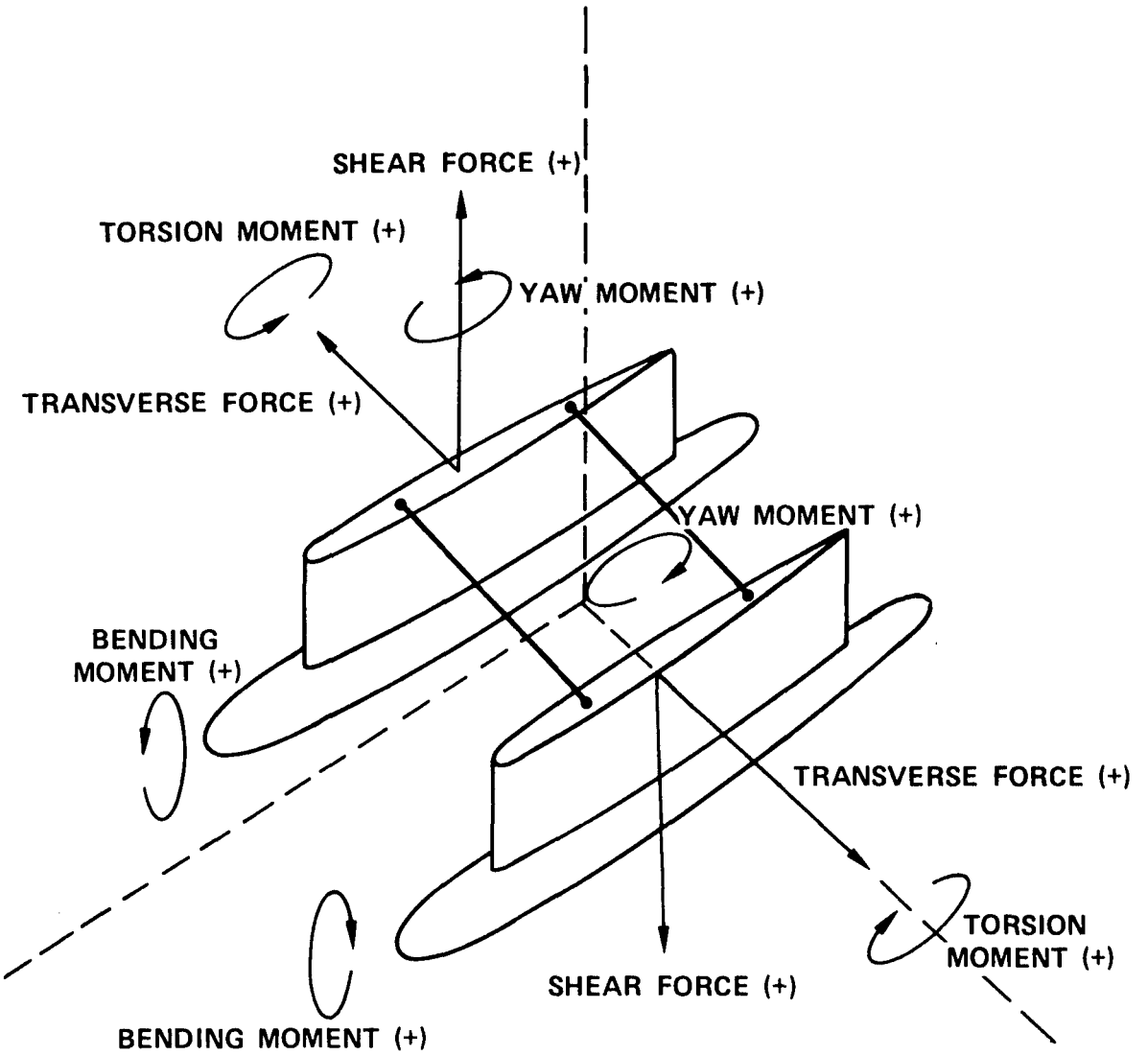

Figure 3 – Sign Convention Used for Structural Loads in Presentation of Experiment Results

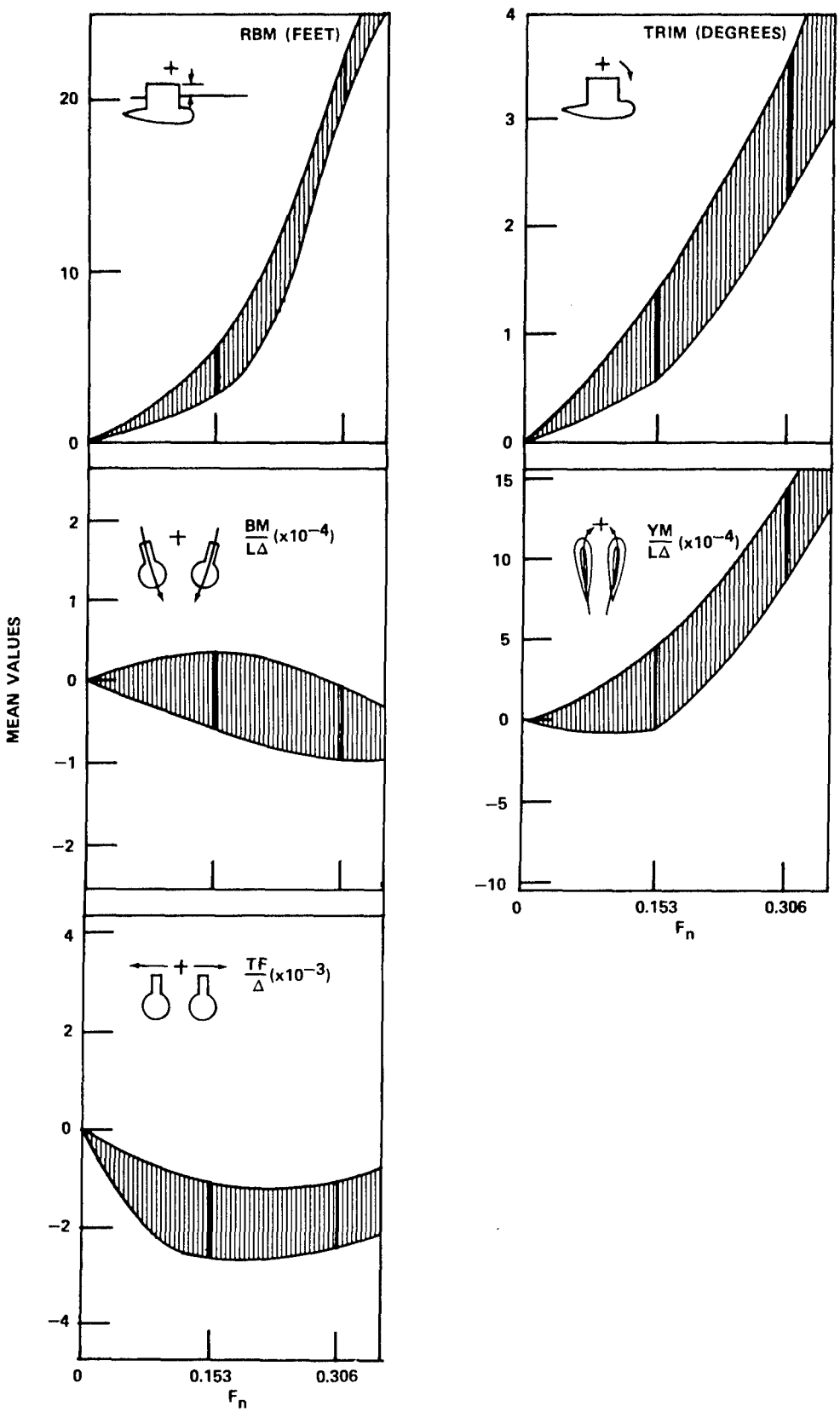

Figure 4 – Calm Water Mean Values versus Froude Number for a Hull Separation of 207 Feet

$\chi = 180^{o}$

SIGNIFICANT WAVE HEIGHTS

Prog. 1 - 11.2'	Prog. 1 - 30.3'
Prog. 6 - 9.7'	Prog. 6 - 20.6'
Pierson - 10.4'	Pierson - 25.5'

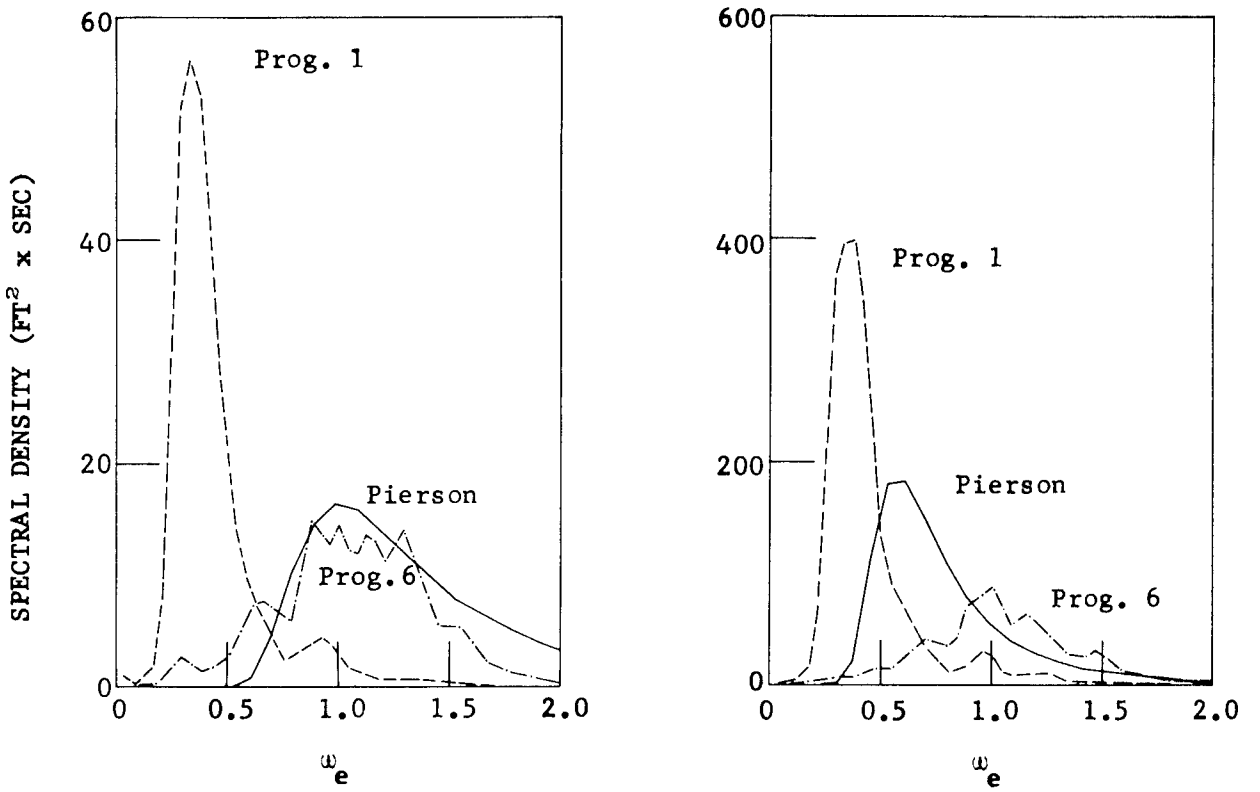

Figure 5 – Spectral Energy of Long-Crested, Irregular Sea-Test Conditions with Theoretical Pierson Predictions for F_n = 0.153, Full Scale

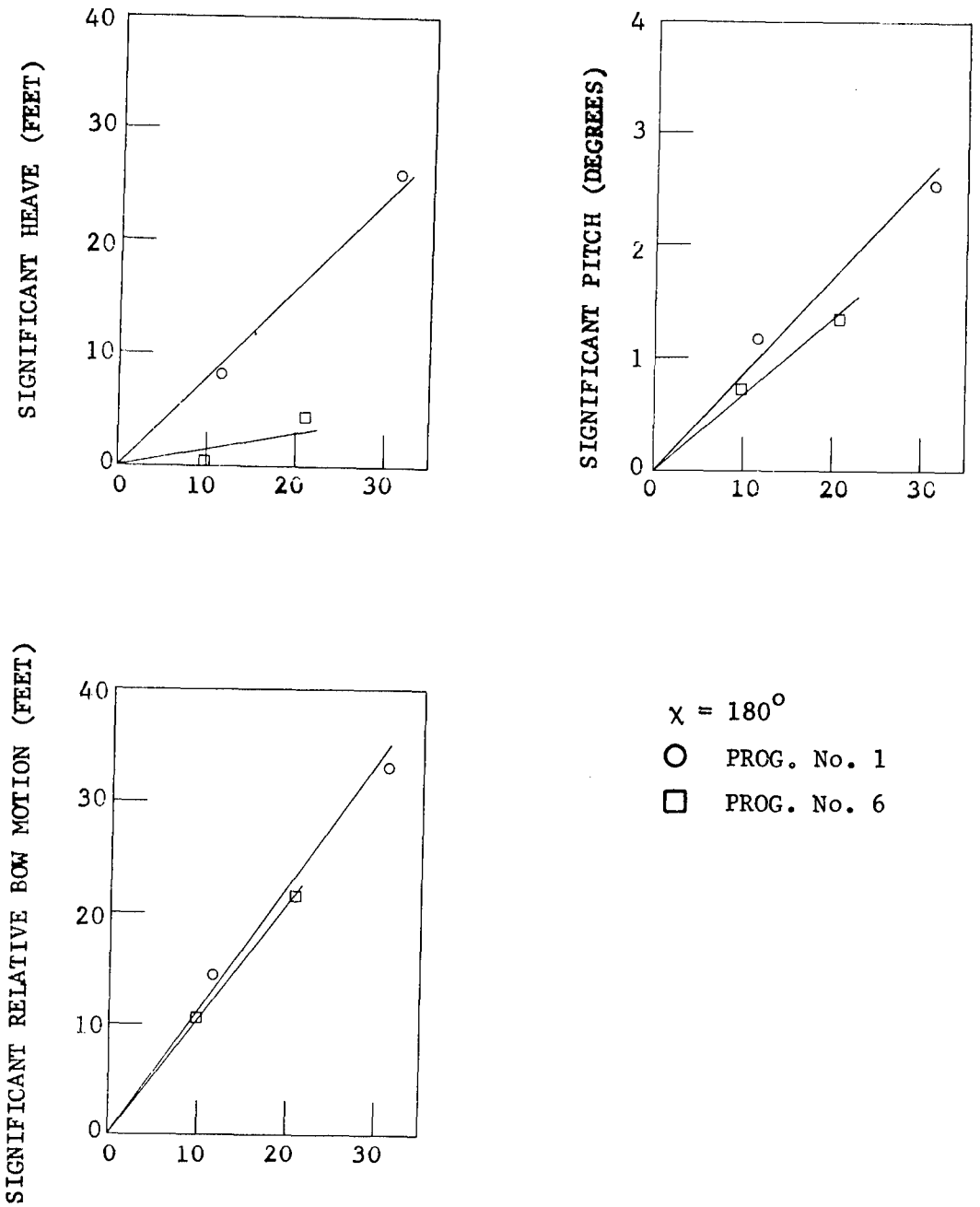

Figure 6 – Significant Heave, Pitch, and Relative Bow Motion versus Significant Wave Height for F_n = 0.153, Full Scale

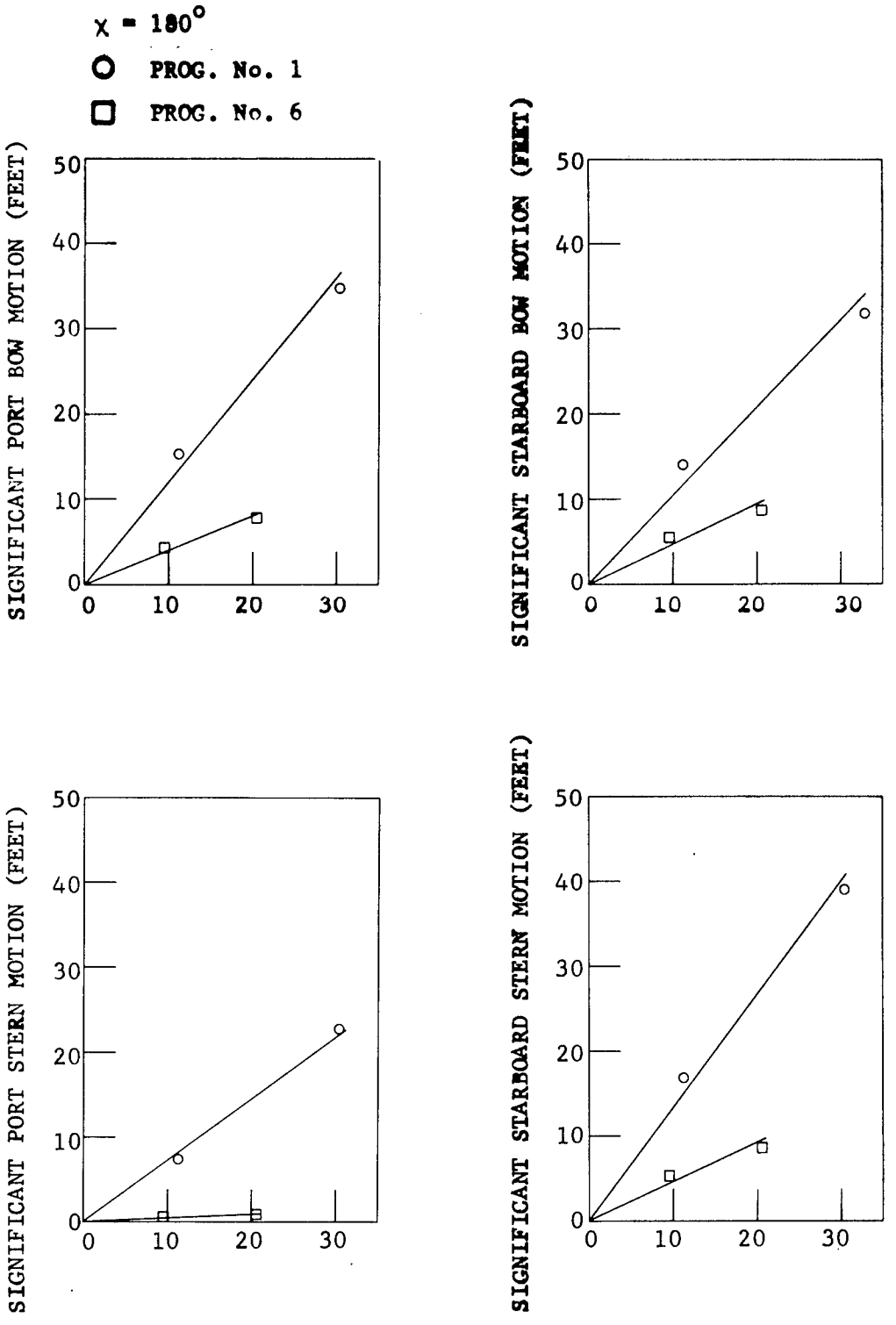

Figure 7 – Significant Port Bow and Stern and Starboard Bow and Stern Motions versus Significant Wave Height for F_n = 0.153, Full Scale

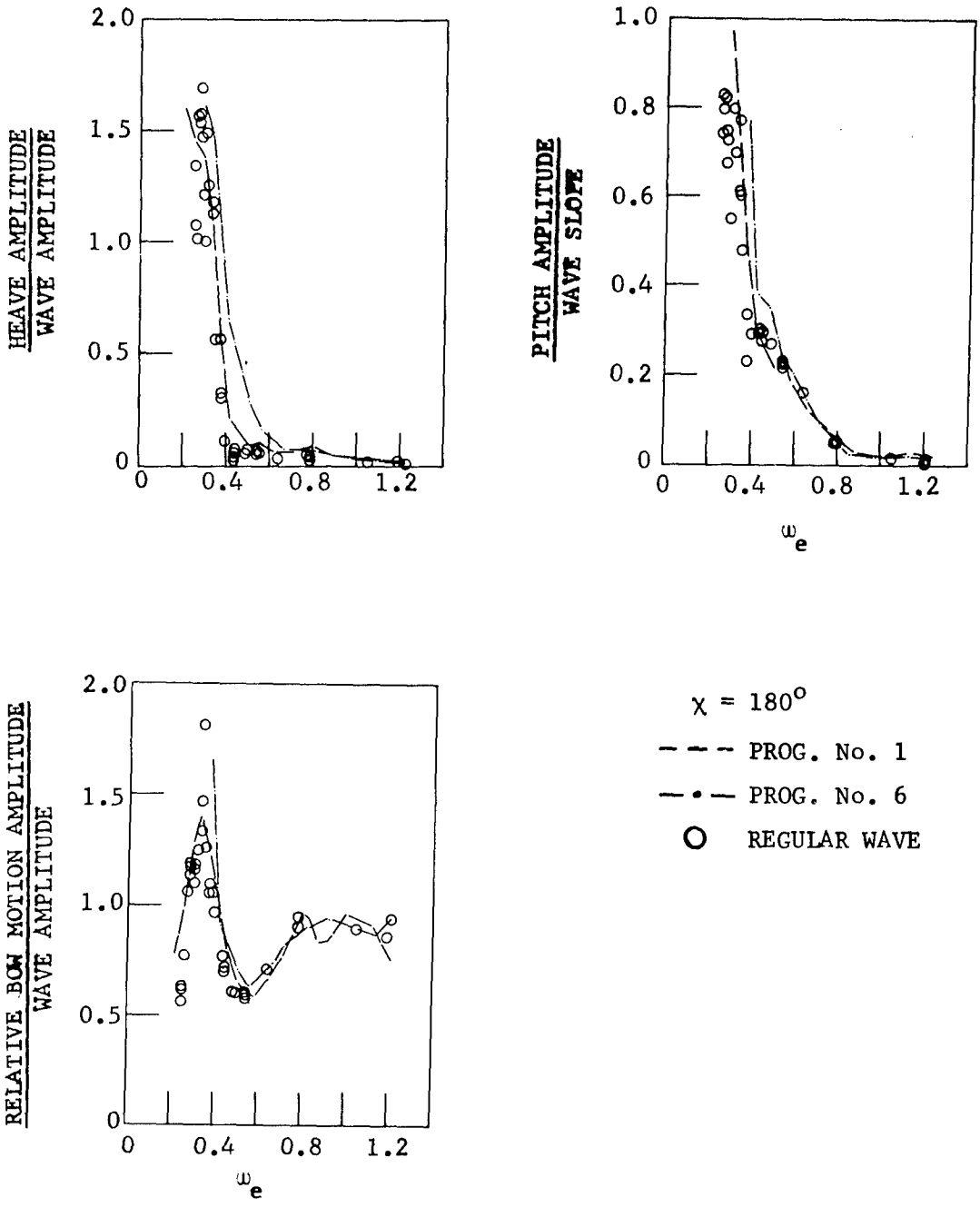

Figure 8 – Nondimensional Heave, Pitch, and Relative Bow-Motion Transfer Functions versus Frequency of Encounter from Irregular and Regular Wave Experiments for F_n = 0.153, Full Scale

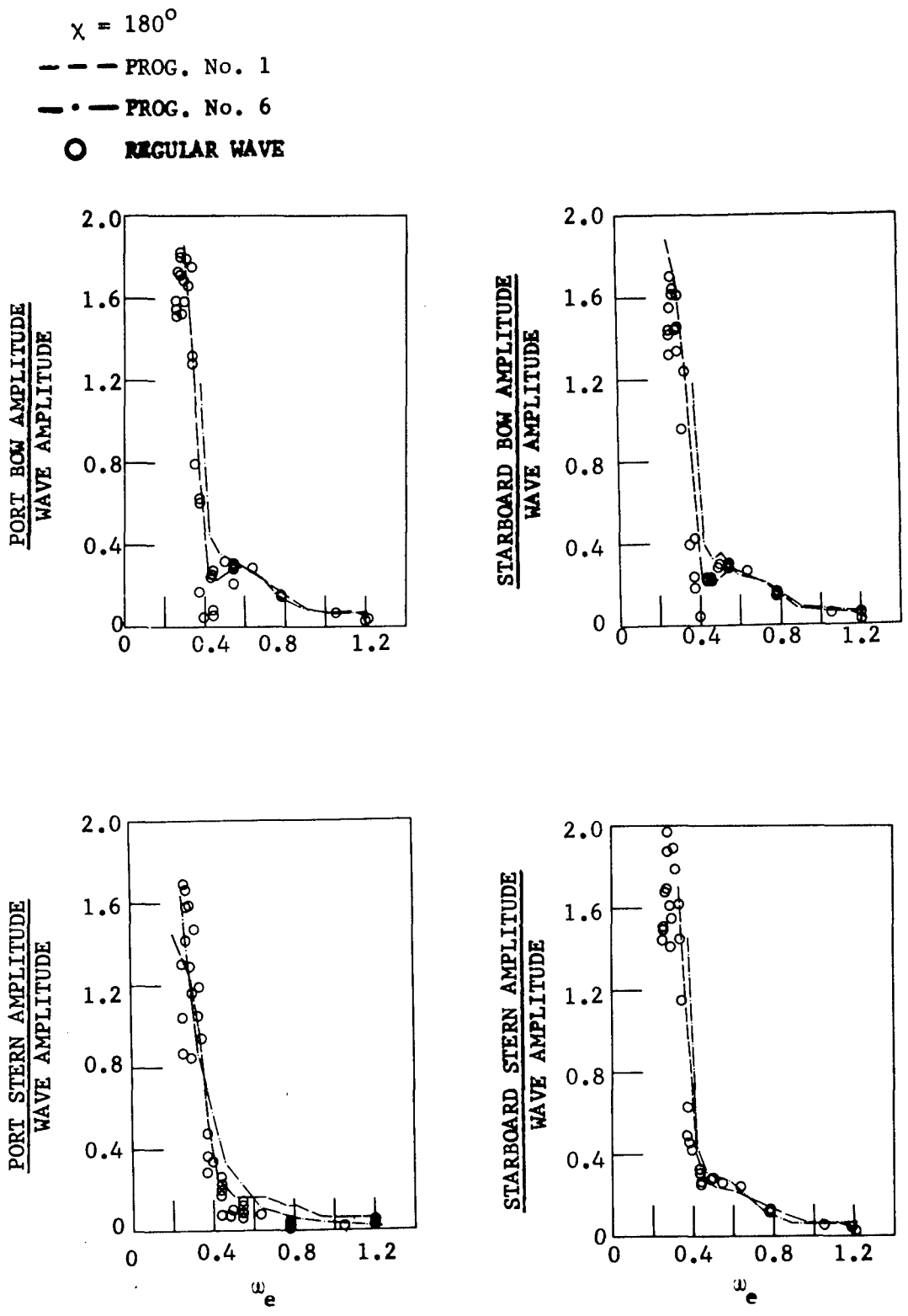

Figure 9 – Nondimensional Port Bow and Stern and Starboard Bow and Stern Transfer Functions versus Frequency of Encounter from Irregular and Regular Wave Experiments for F_n = 0.153, Full Scale

$\chi = 90^{o}$

SIGNIFICANT WAVE HEIGHTS

Prog. 1 - 8.2'	Prog. 1 - 19.4'
Prog. 6 - 6.1'	Prog. 6 - 17.2'
Pierson - 7.1'	Pierson- 18.3'

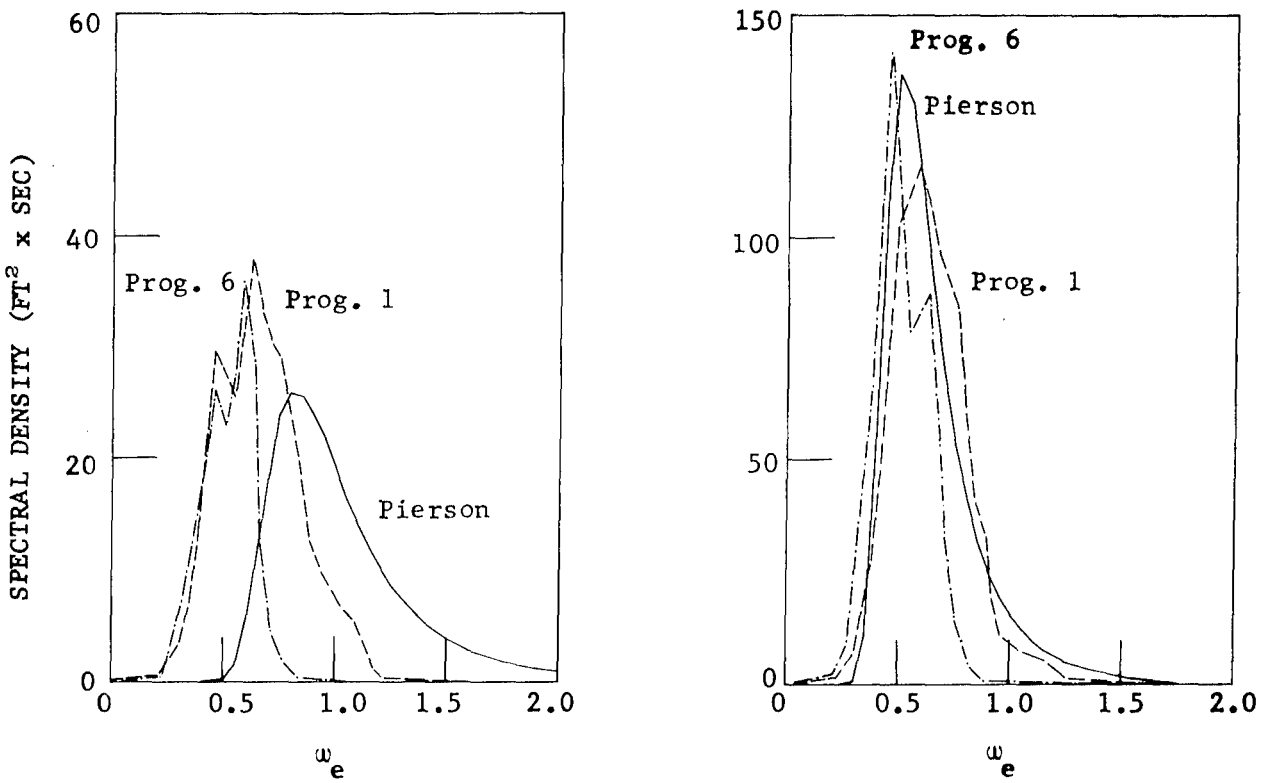

Figure 10 – Spectral Energy of Long-Crested, Irregular Sea-Test Conditions with Theoretical Pierson Predictions for F_n = 0.153, Full Scale

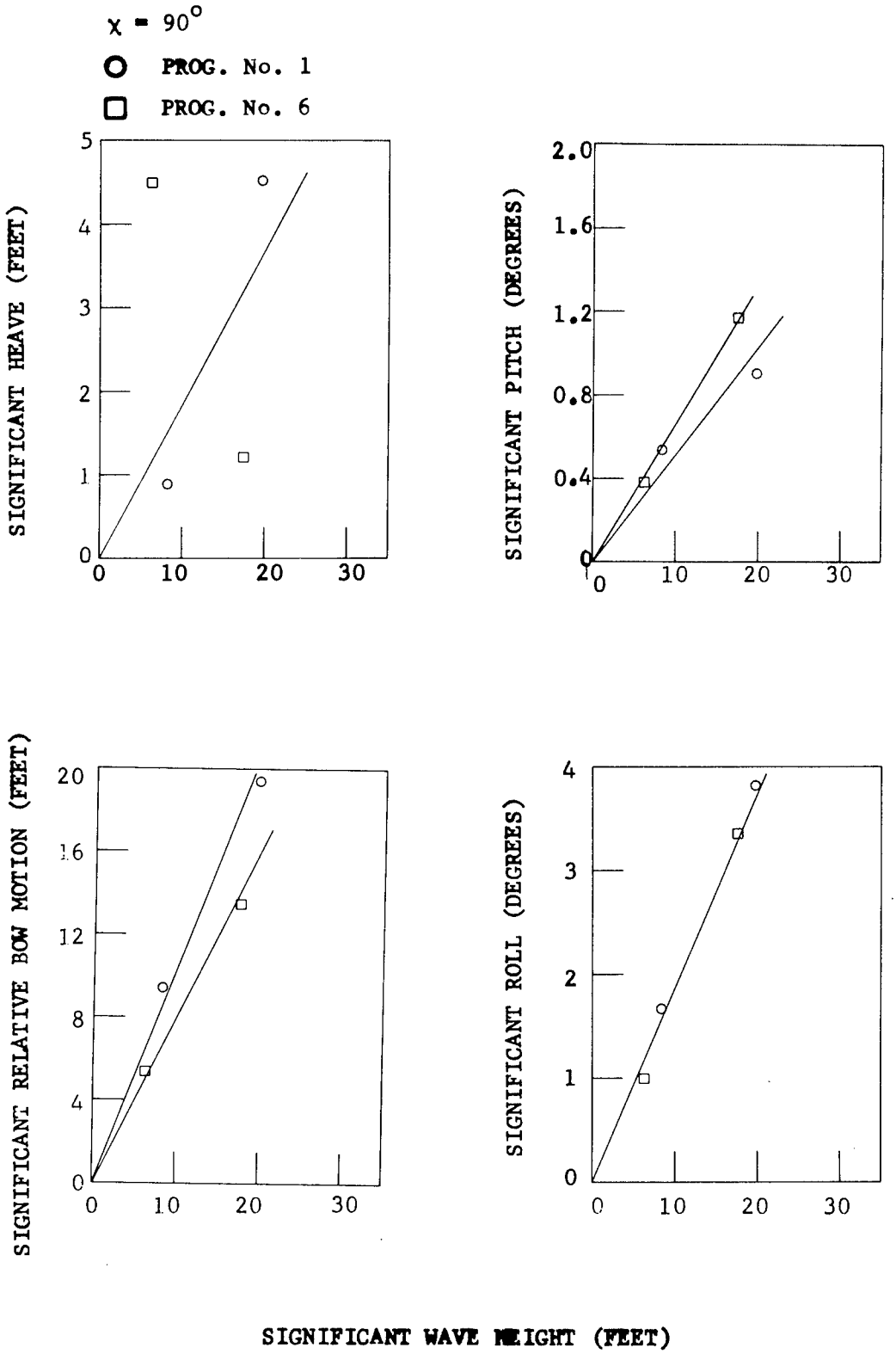

Figure 11 – Significant Heave, Pitch, Relative Bow Motion, and Roll versus Significant Wave Height for F_n = 0.153, Full Scale

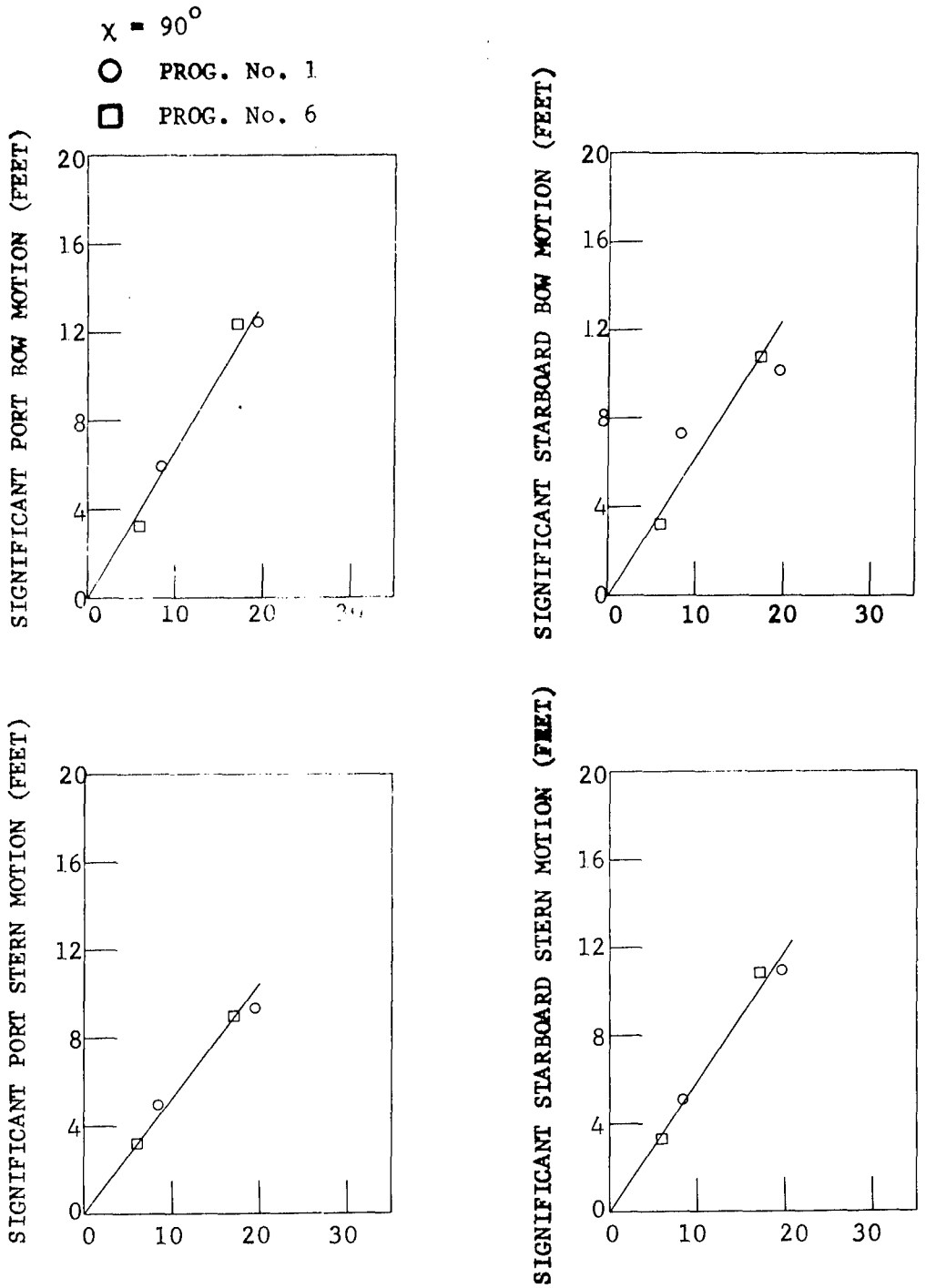

Figure 12 – Significant Port Bow and Stern and Starboard Bow and Stern Motions versus Significant Wave Height for F_n = 0.153

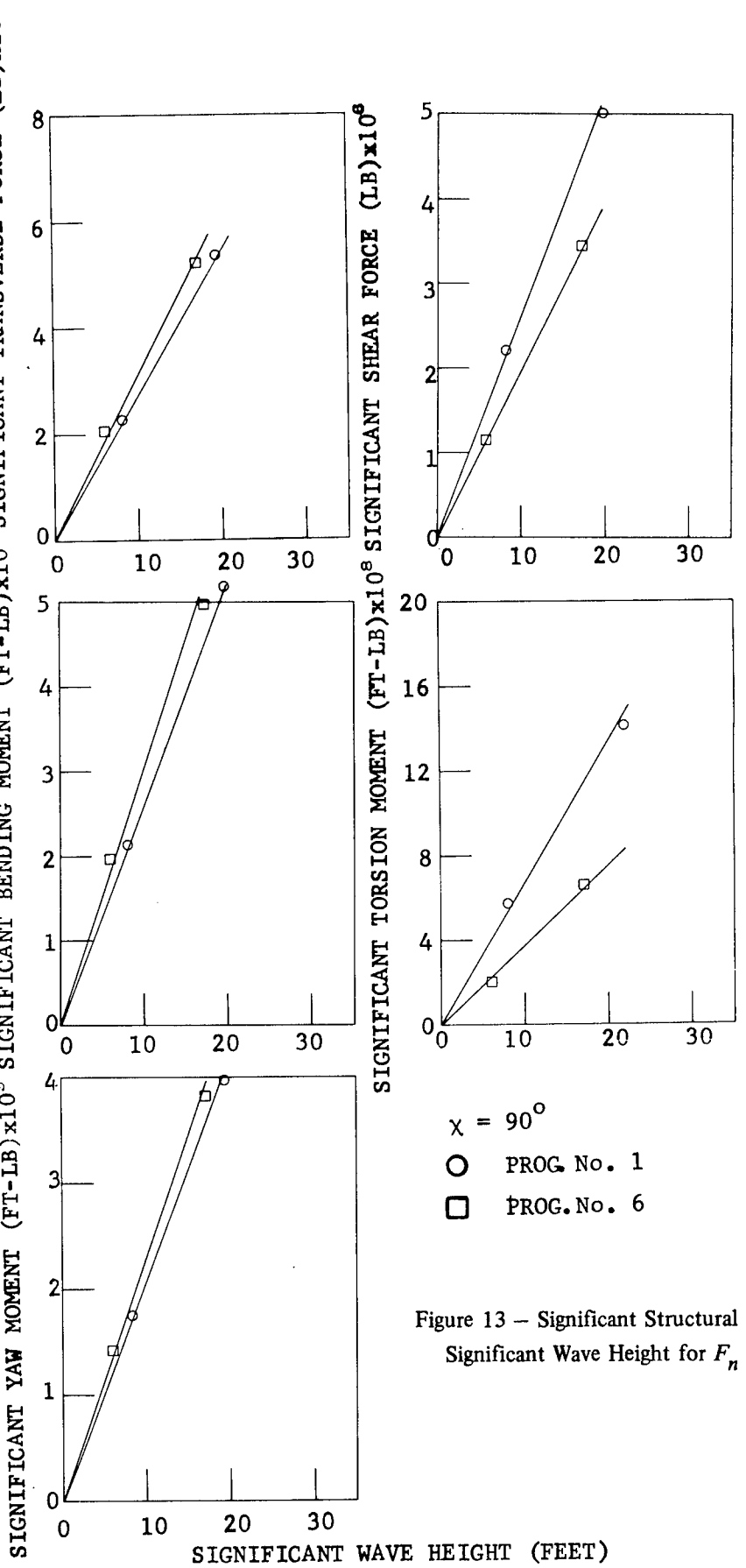

Figure 13 – Significant Structural Loads versus Significant Wave Height for F_n = 0.153

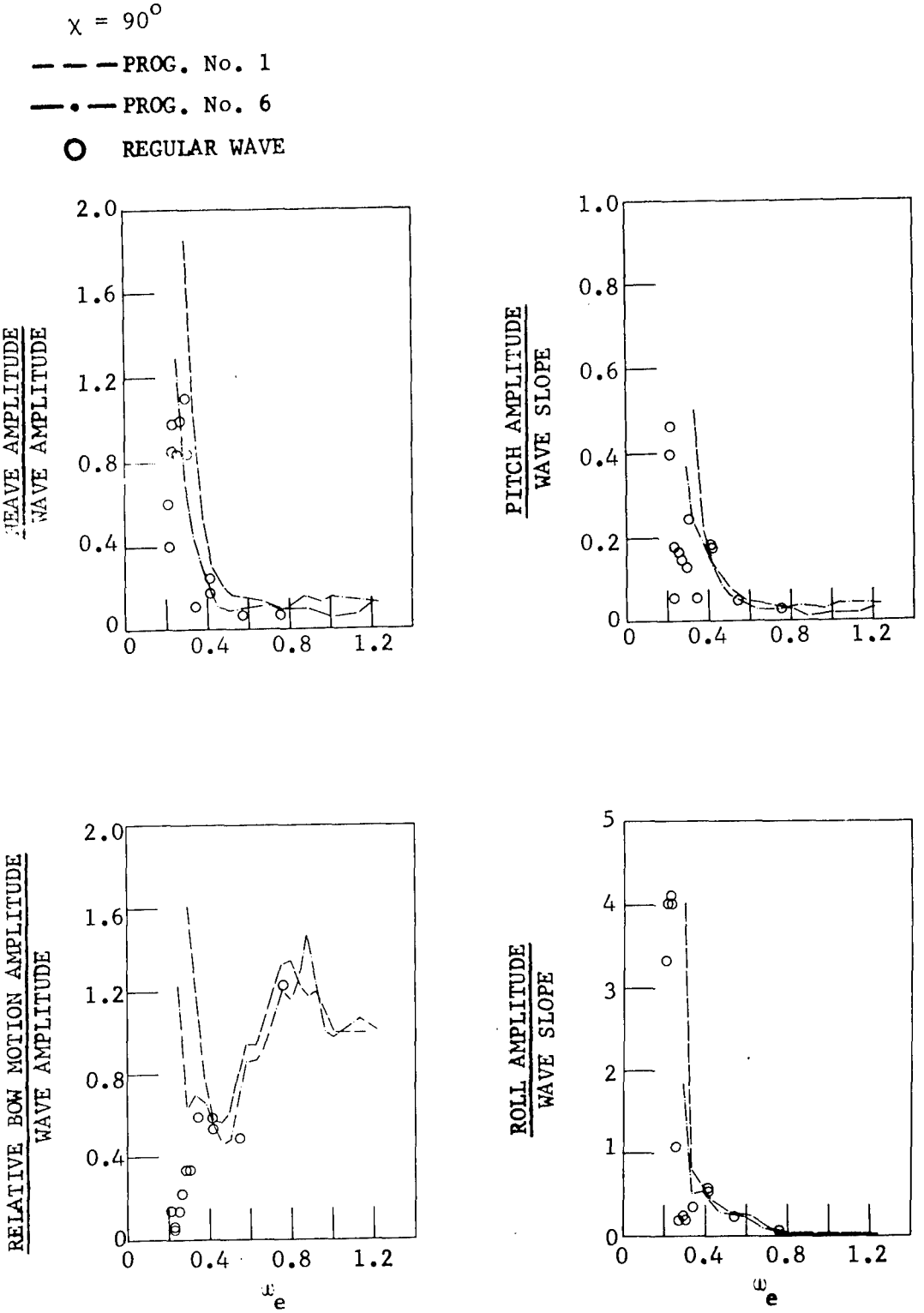

Figure 14 – Nondimensional Heave, Pitch, Relative Bow Motion, and Roll-Transfer Functions versus Frequency of Encounter from Irregular and Regular Wave Experiments for F_n = 0.153, Full Scale

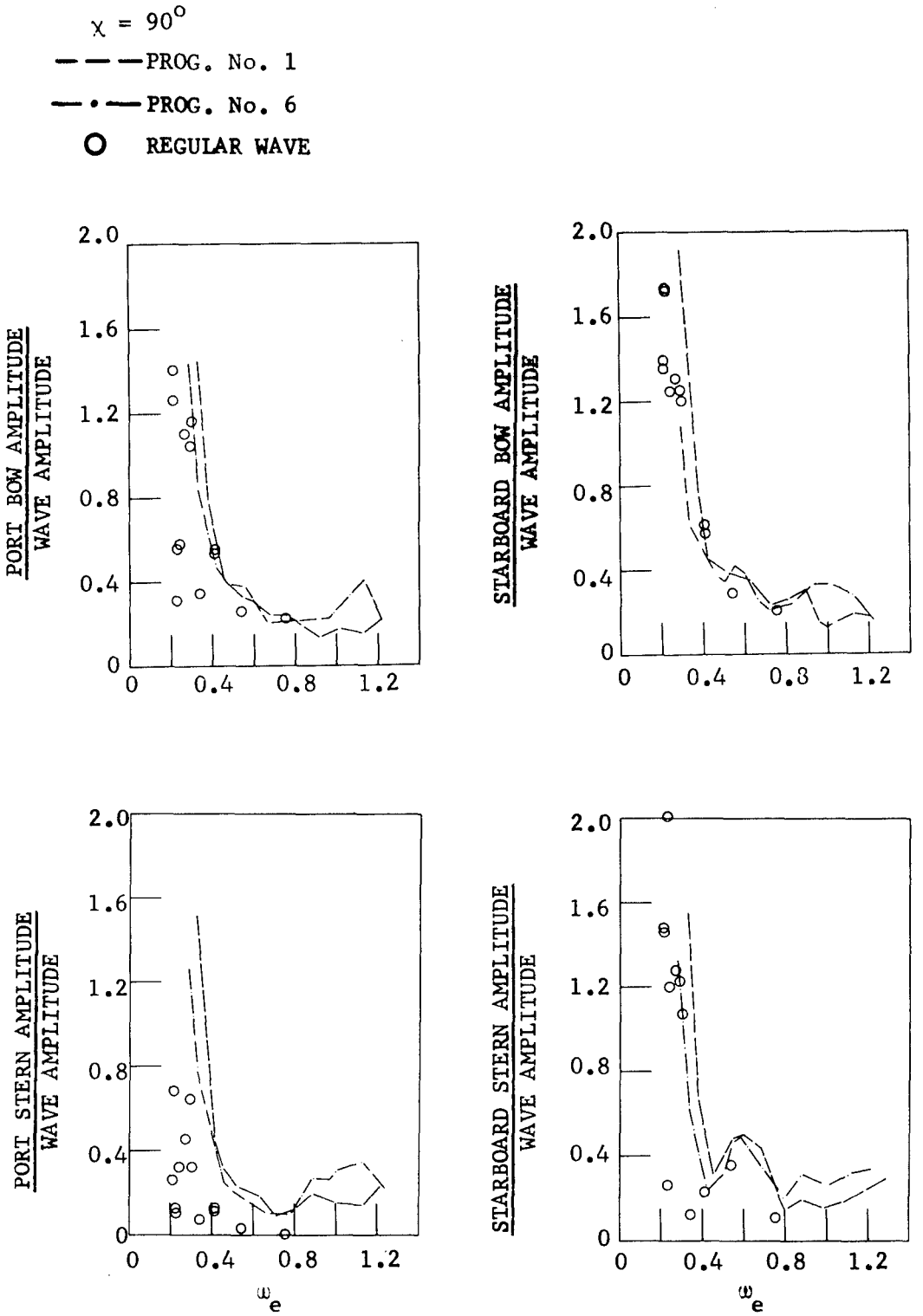

Figure 15 – Nondimensional Port Bow and Stern and Starboard Bow and Stern Transfer Functions versus Frequency of Encounter from Irregular and Regular Wave Experiments for F_n = 0.153, Full Scale

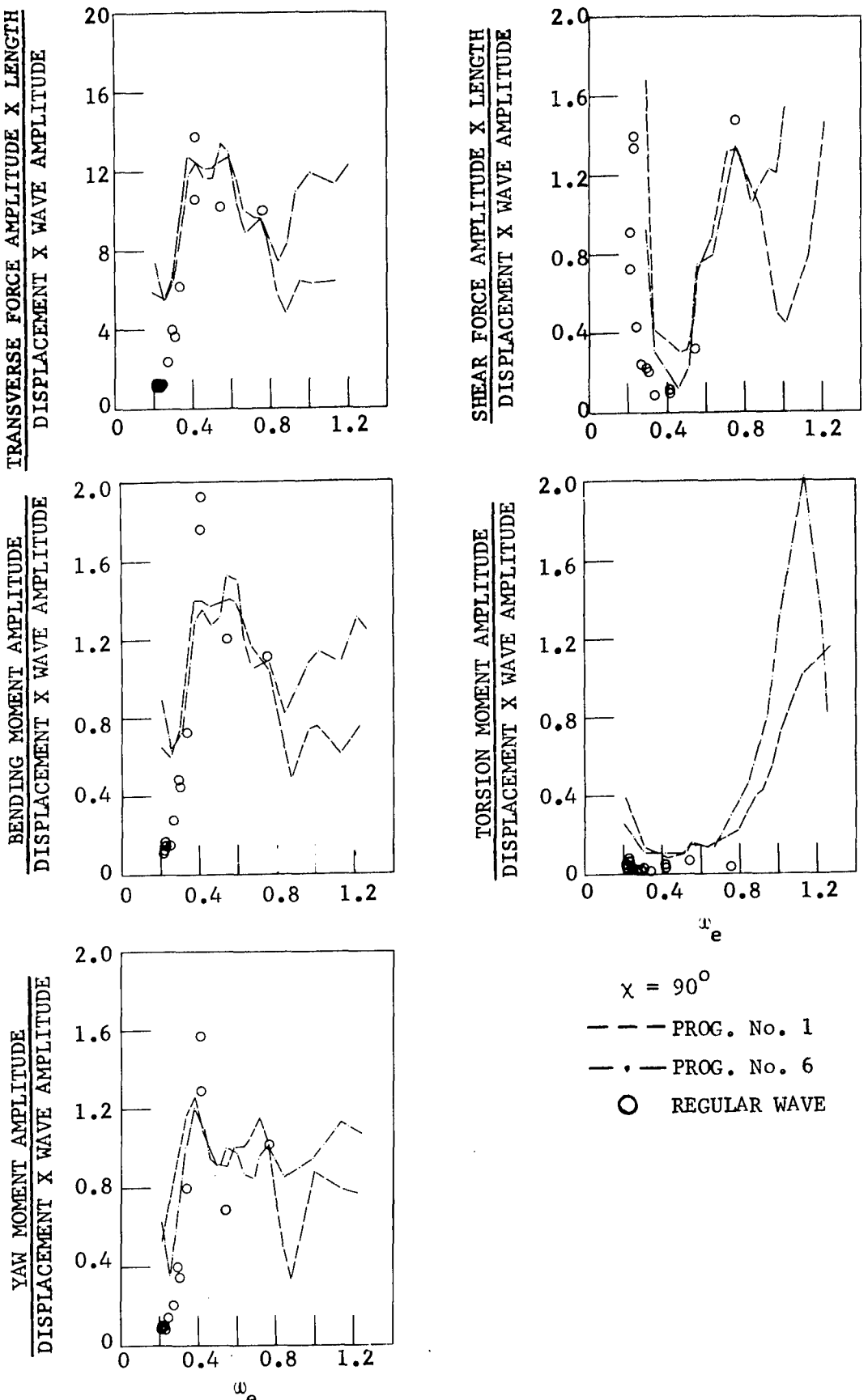

Figure 16 – Nondimensional Structural Loads versus Frequency of Encounter from Irregular and Regular Wave Experiments for F_n = 0.153, Full Scale

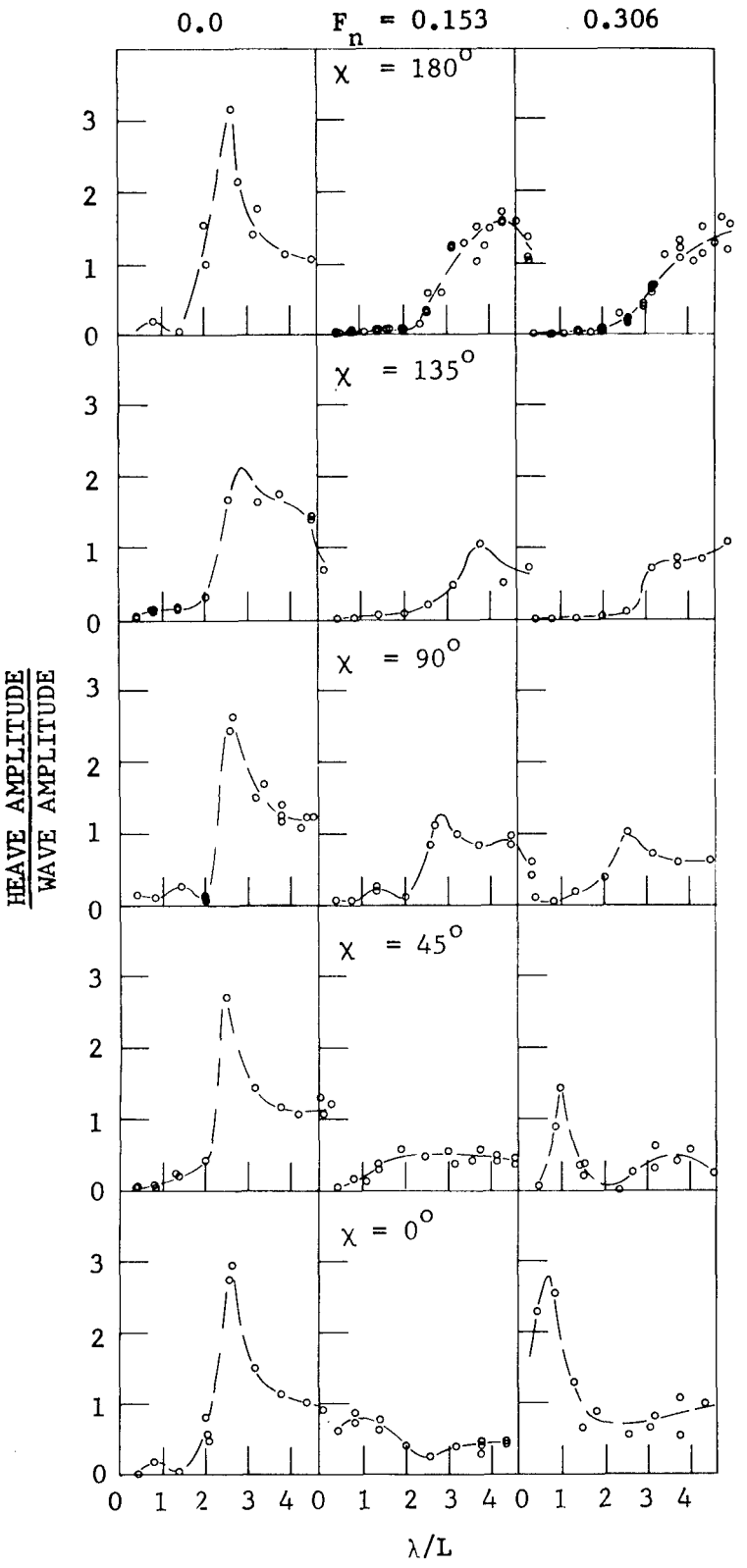

Figure 17 – Nondimensional Amplitude of Heave for a Hull Separation of 207 Feet

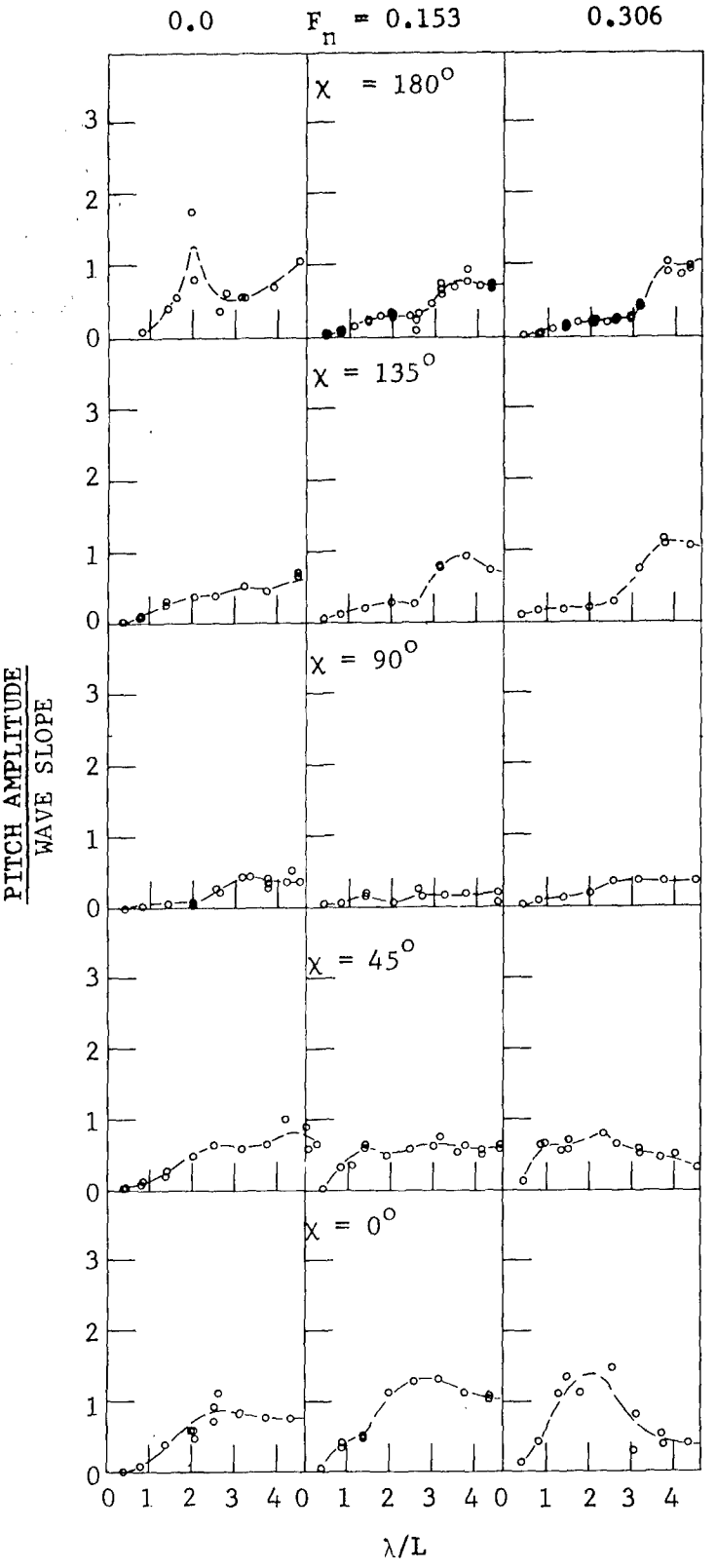

Figure 18 – Nondimensional Amplitude of Pitch for a Hull Separation of 207 Feet

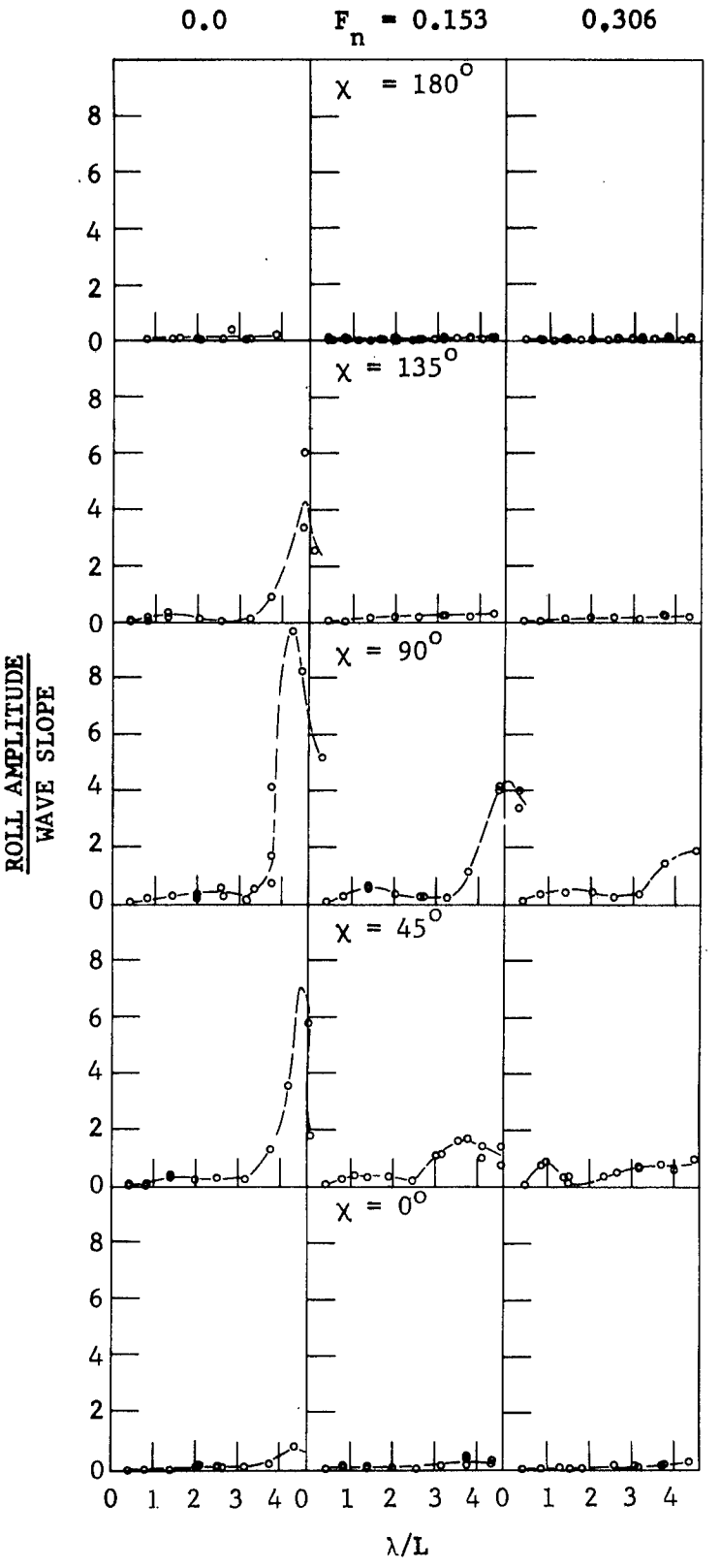

Figure 19 – Nondimensional Amplitude of Roll for a Hull Separation of 207 Feet

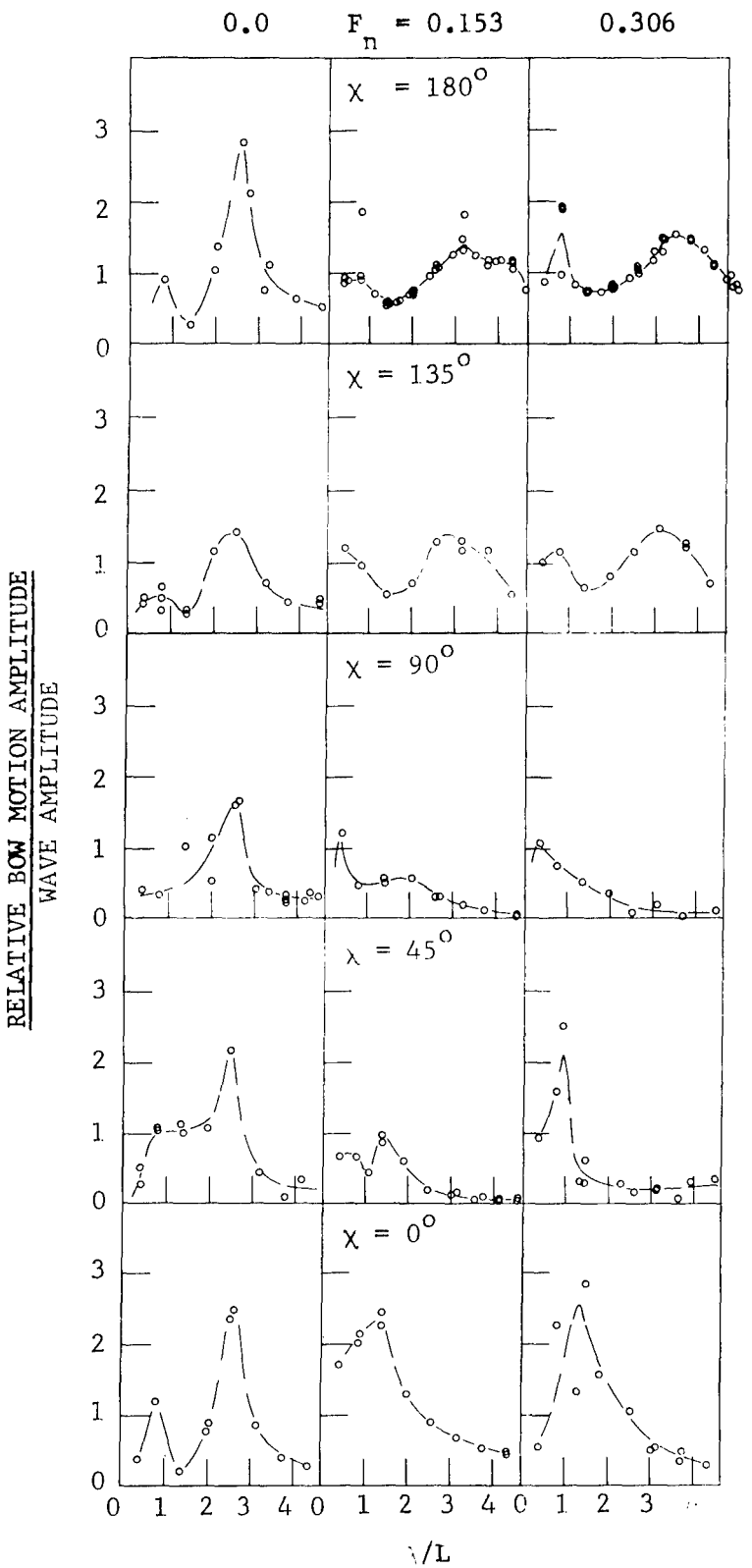

Figure 20 – Nondimensional Amplitude of Relative Bow Motion for a Hull Separation of 207 Feet

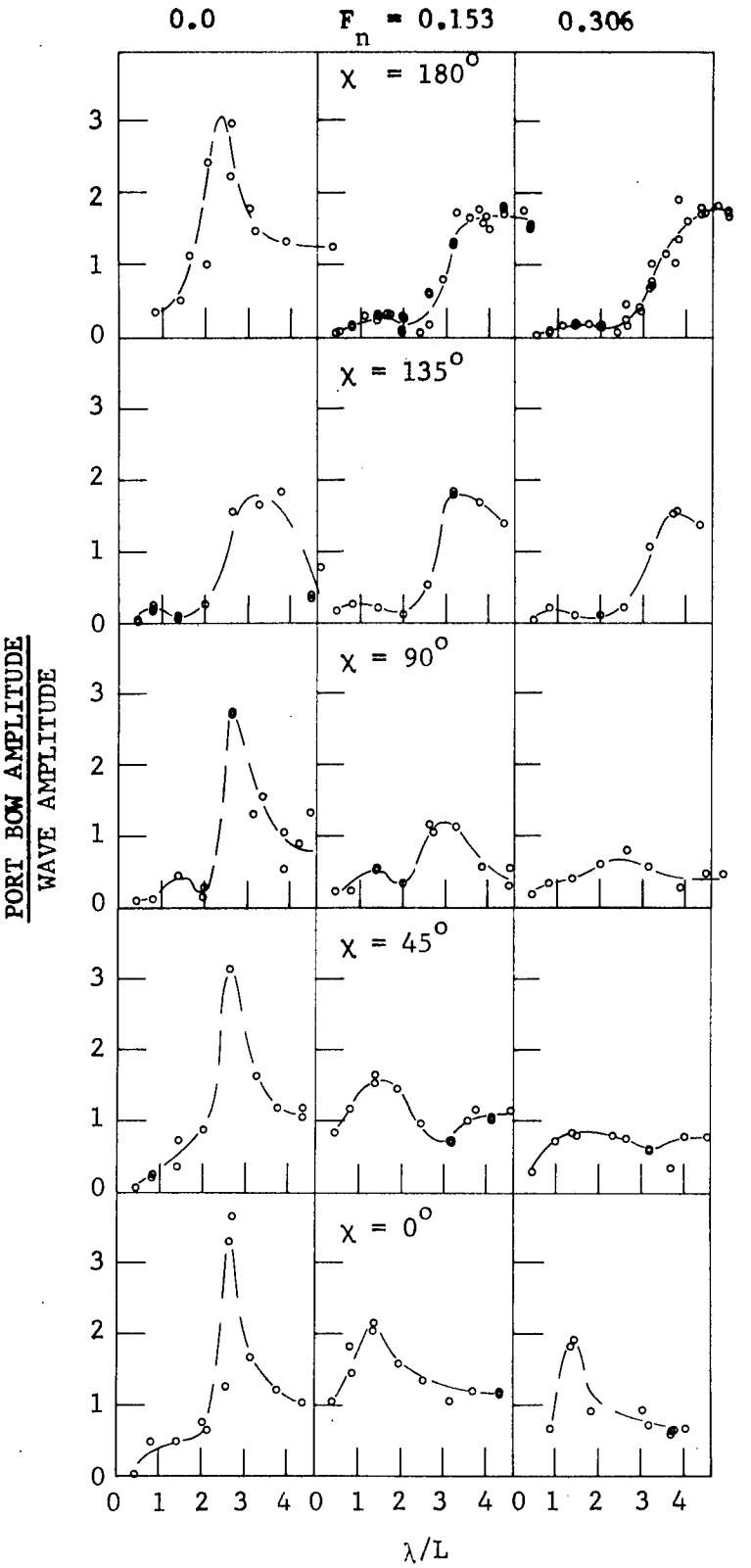

Figure 21 – Nondimensional Amplitude of Port Bow Motion for a Hull Separation of 207 Feet

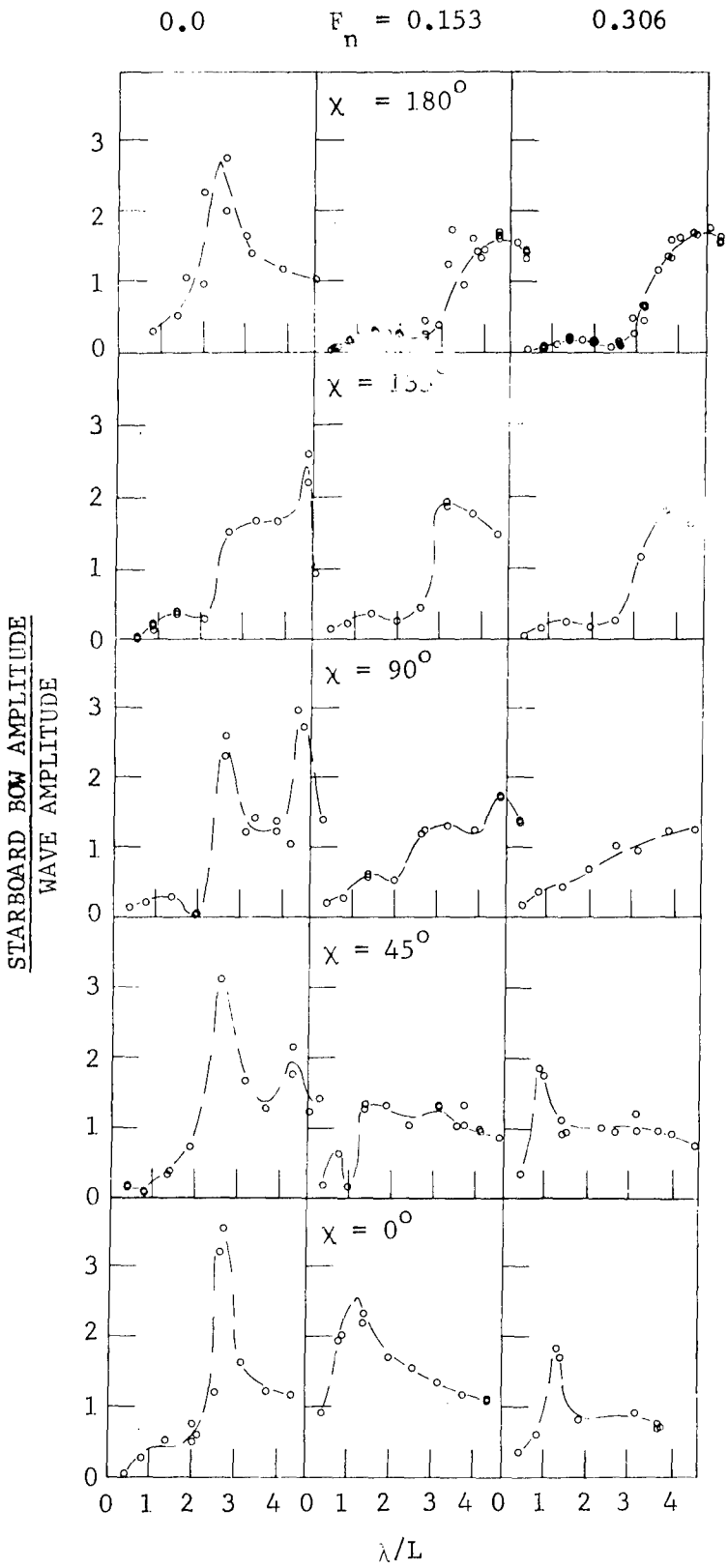

Figure 22 – Nondimensional Amplitude of Starboard Bow Motion for a Hull Separation of 207 Feet

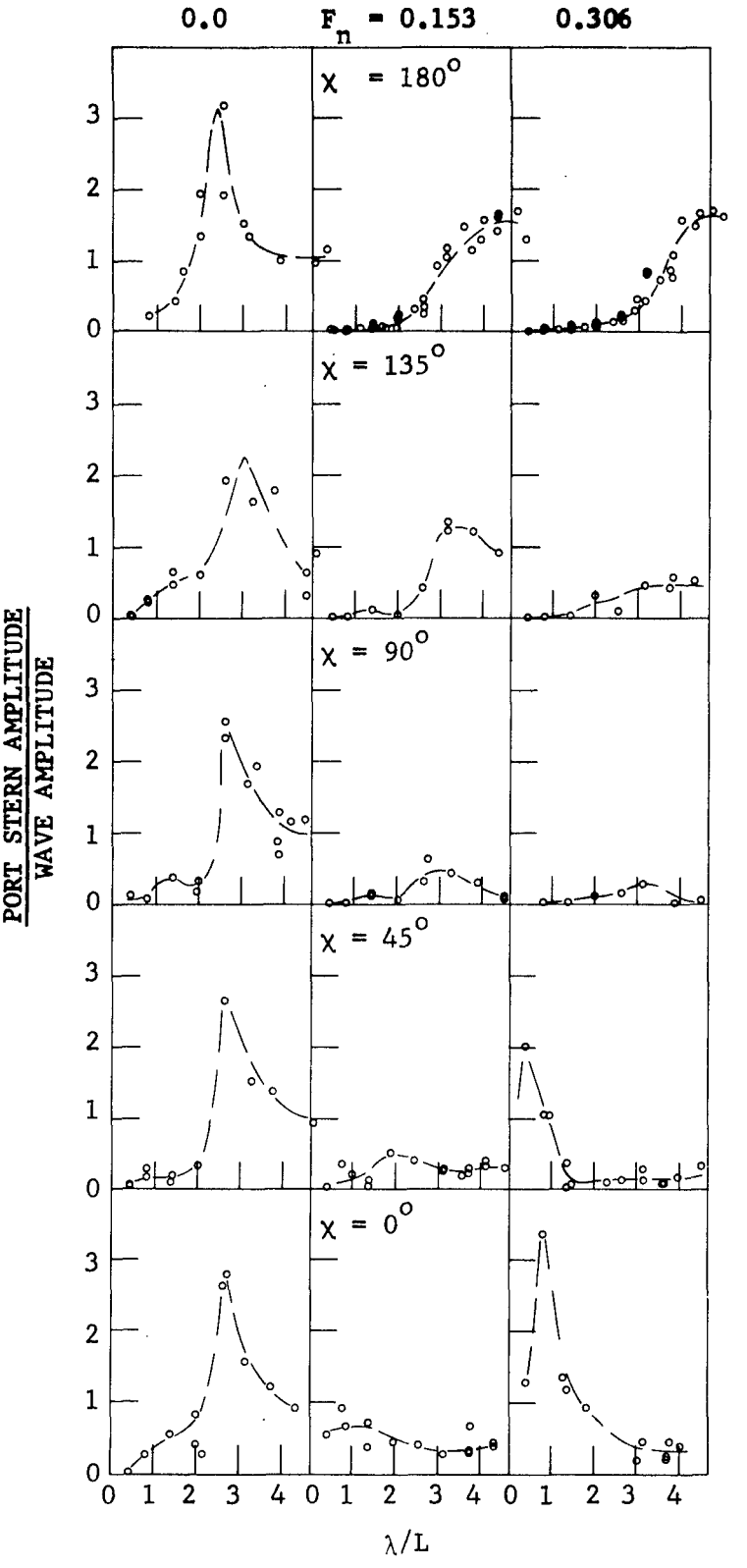

Figure 23 – Nondimensional Amplitude of Port Stern Motion for a Hull Separation of 207 Feet

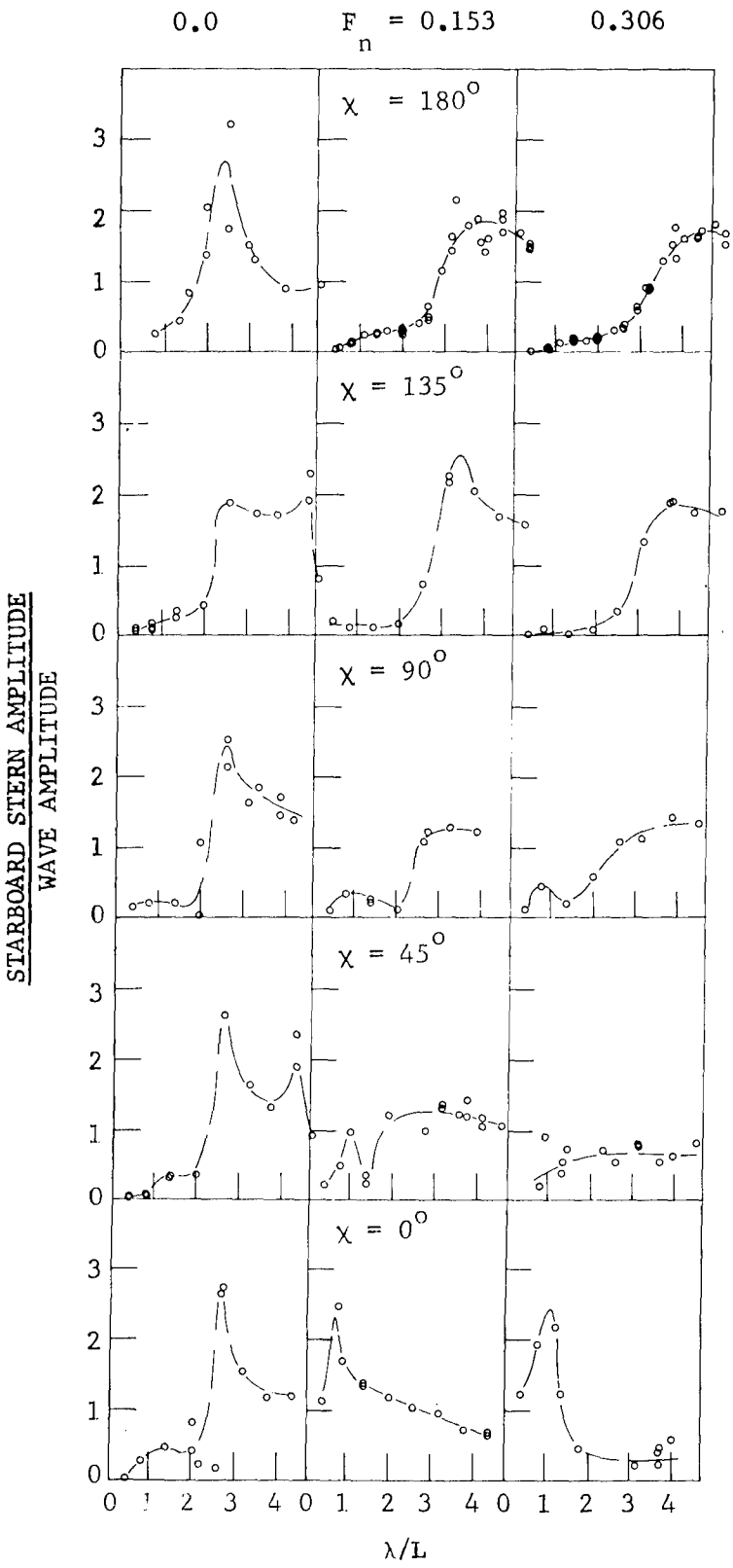

Figure 24 – Nondimensional Amplitude of Starboard Stern Motion for a Hull Separation of 207 Feet

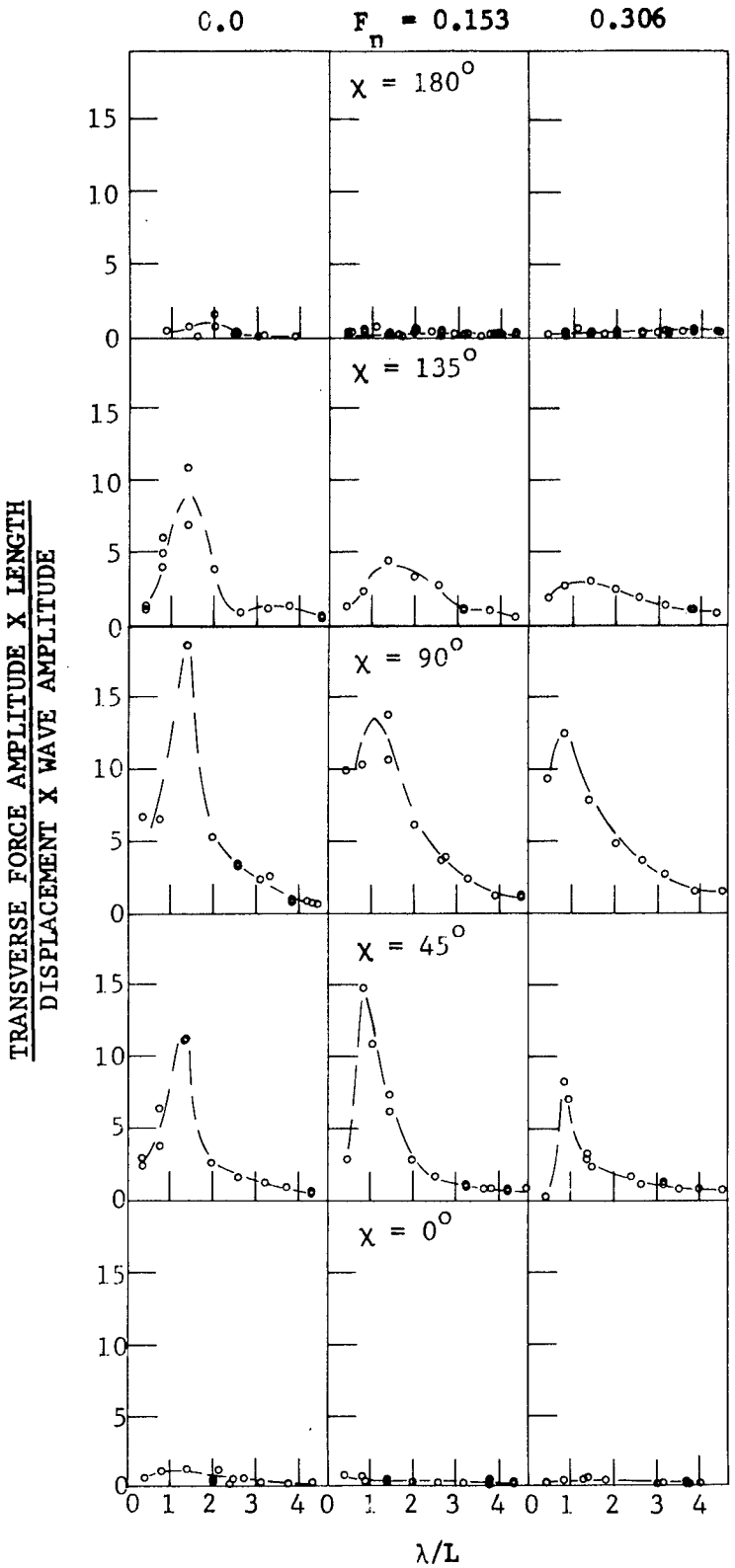

Figure 25 – Nondimensional Amplitude of Transverse Force for a Hull Separation of 207 Feet

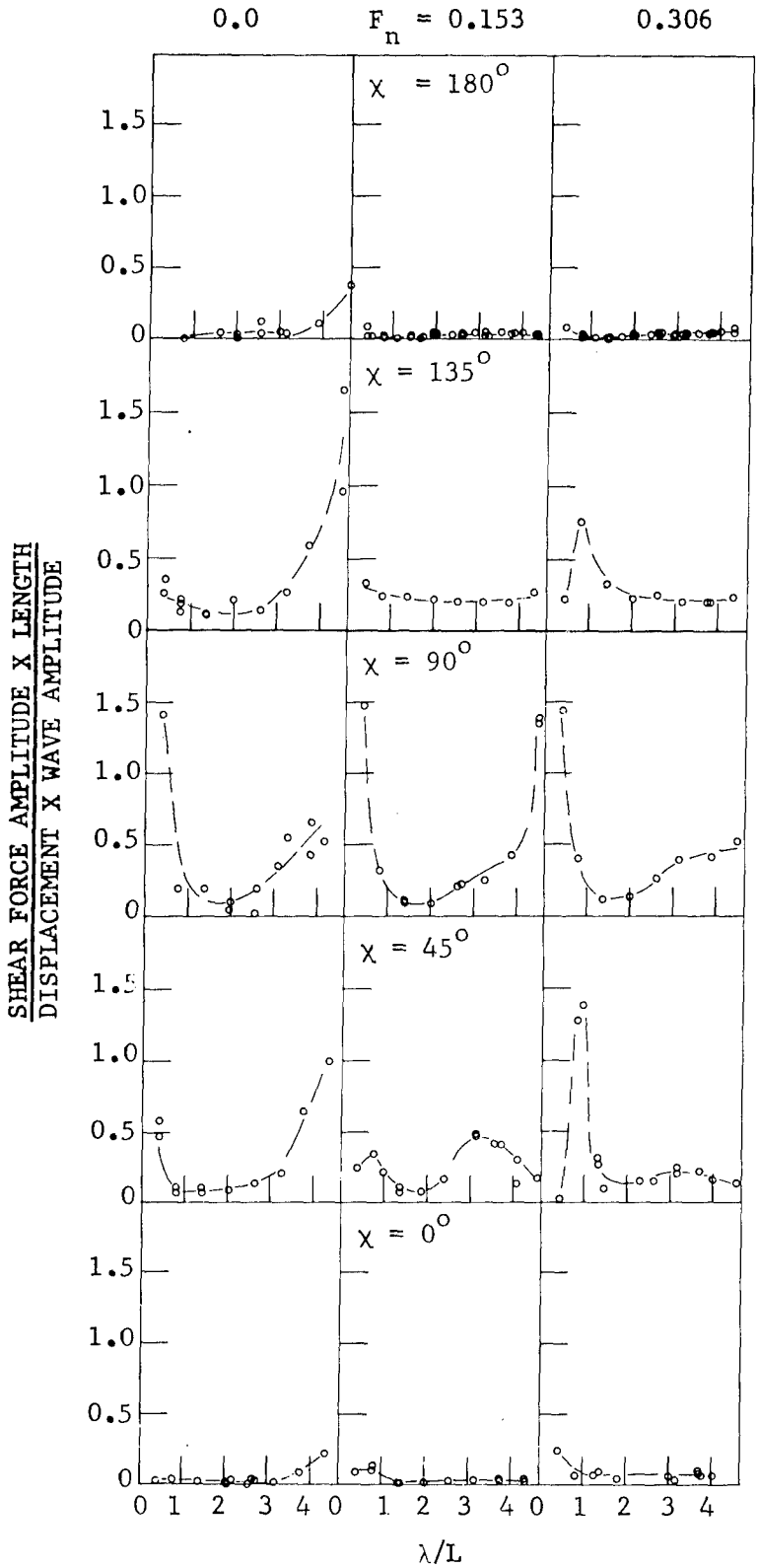

Figure 26 – Nondimensional Amplitude of Shear Force for a Hull Separation of 207 Feet

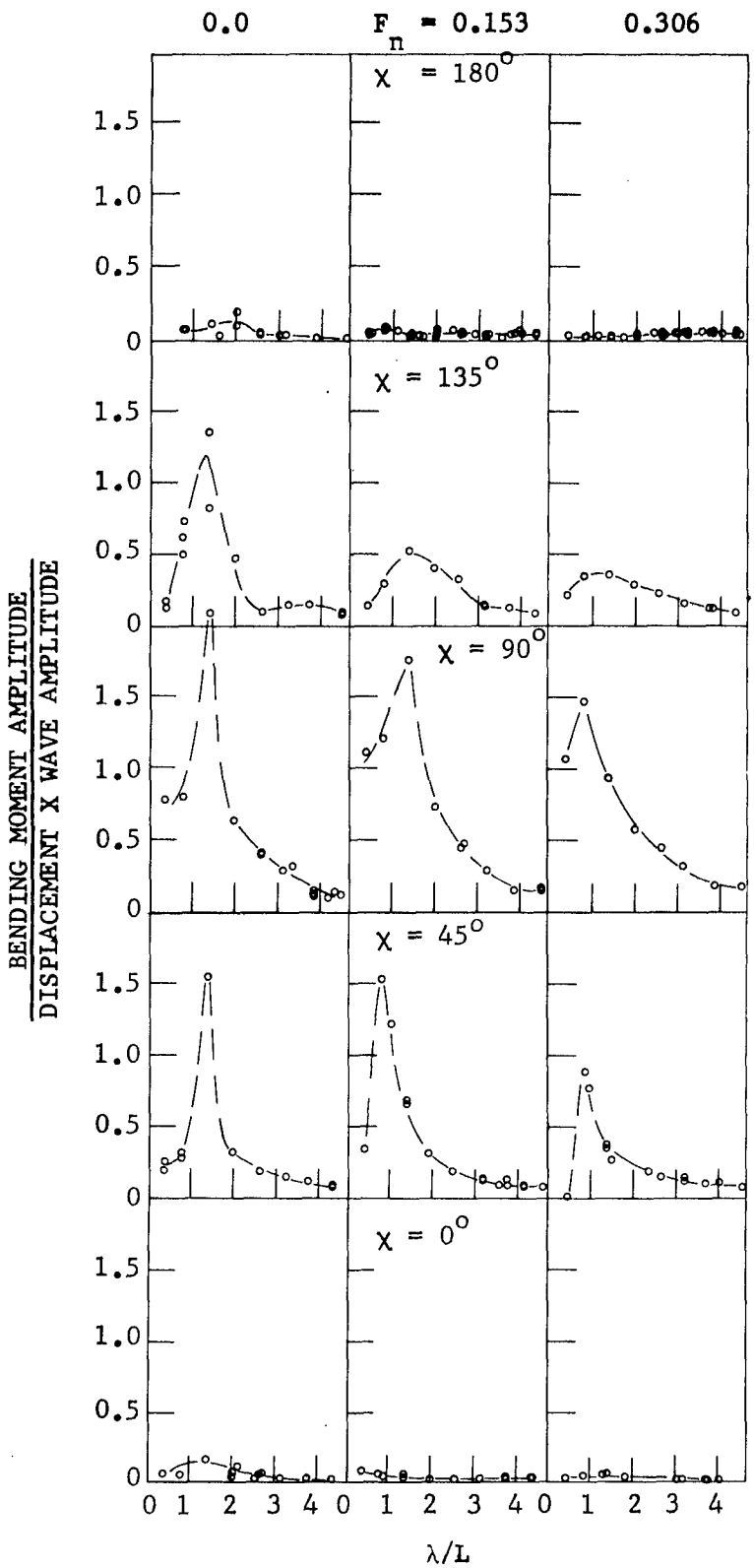

Figure 27 – Nondimensional Amplitude of Bending Moment for a Hull Separation of 207 Feet

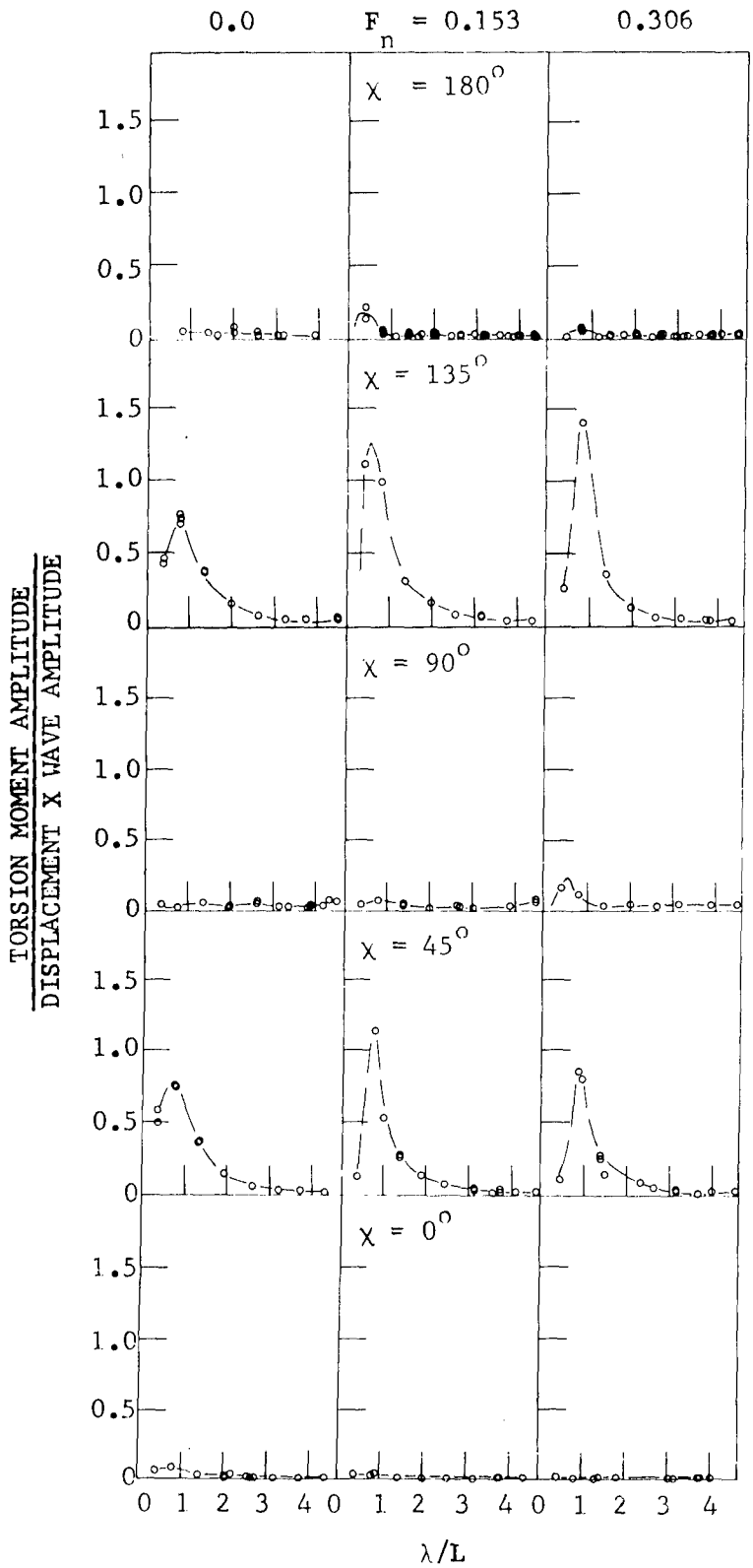

Figure 28 – Nondimensional Amplitude of Torsion Moment for a Hull Separation of 207 Feet

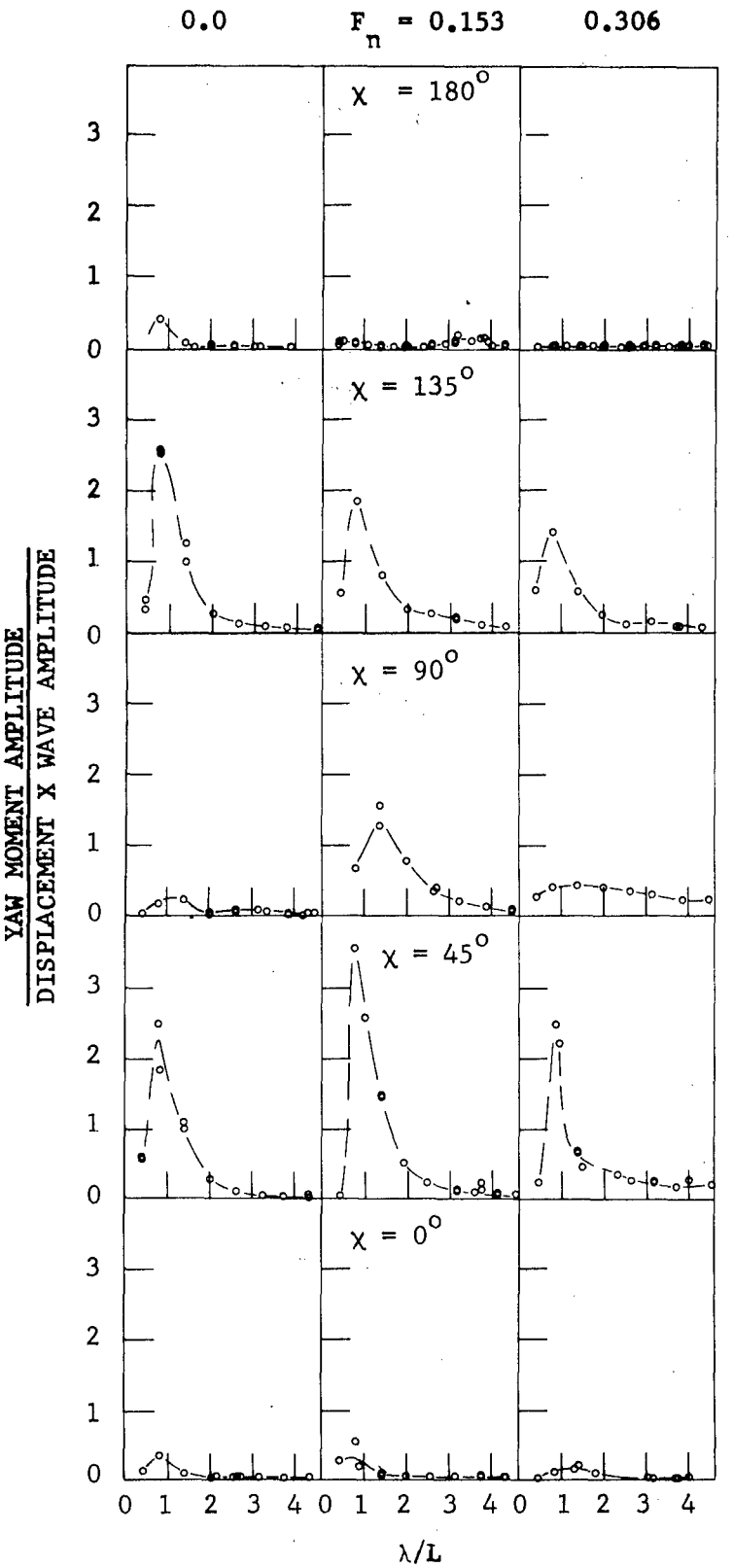

Figure 29 – Nondimensional Amplitude of Yaw Moment for a Hull Separation of 207 Feet

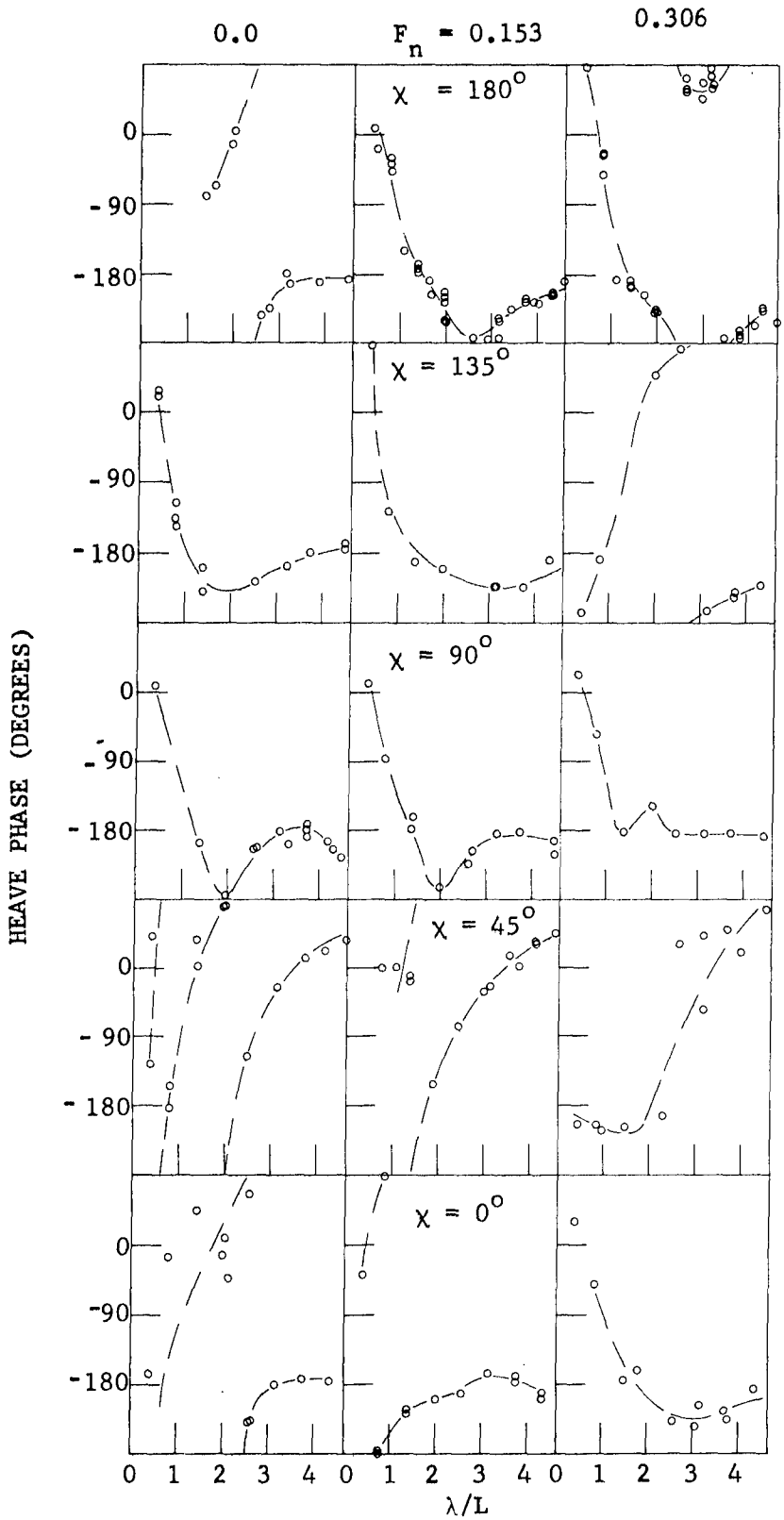

Figure 30 – Phase Angle of Heave for a Hull Separation of 207 Feet

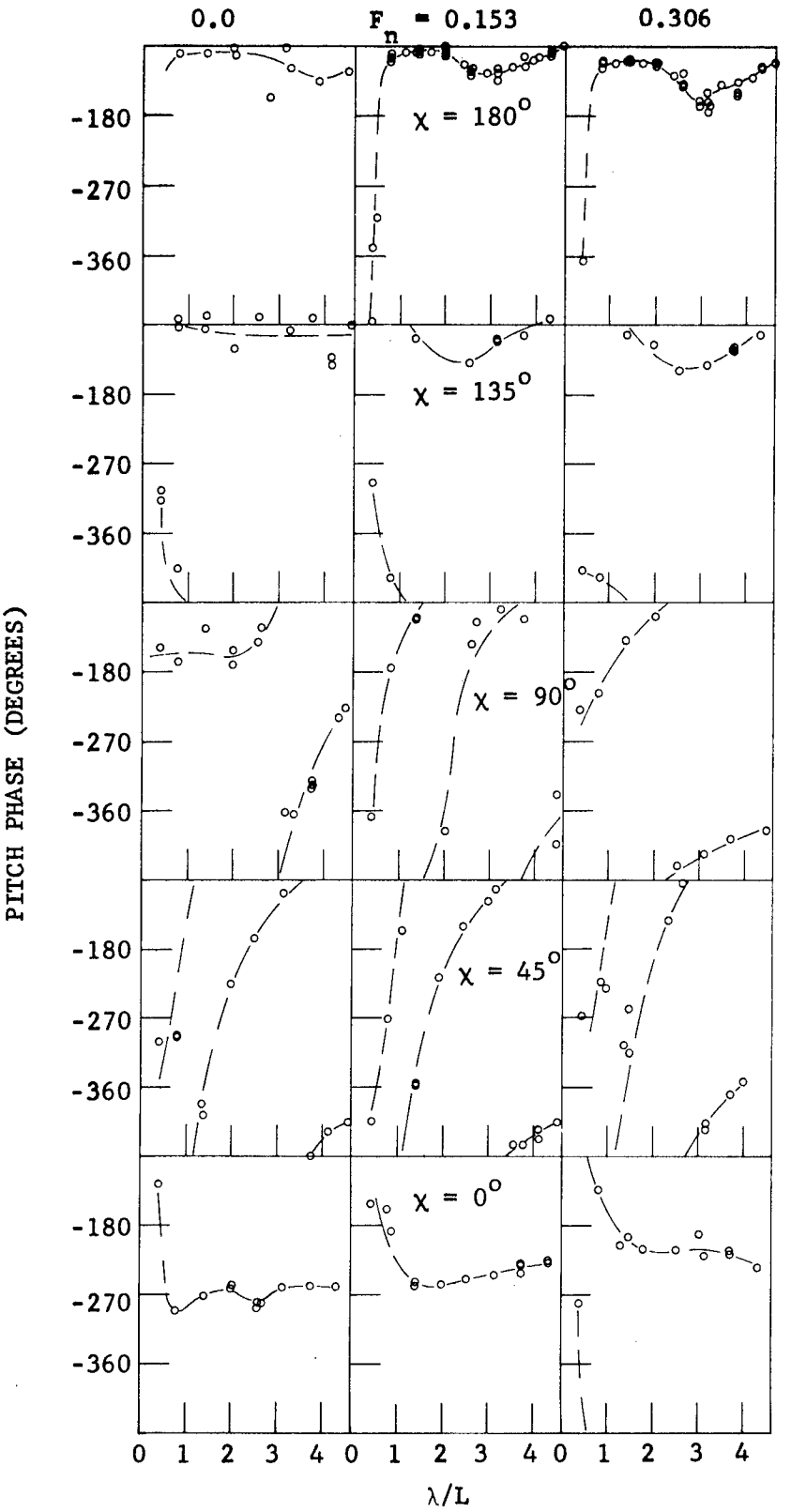

Figure 31 – Phase Angle of Pitch for a Hull Separation of 207 Feet

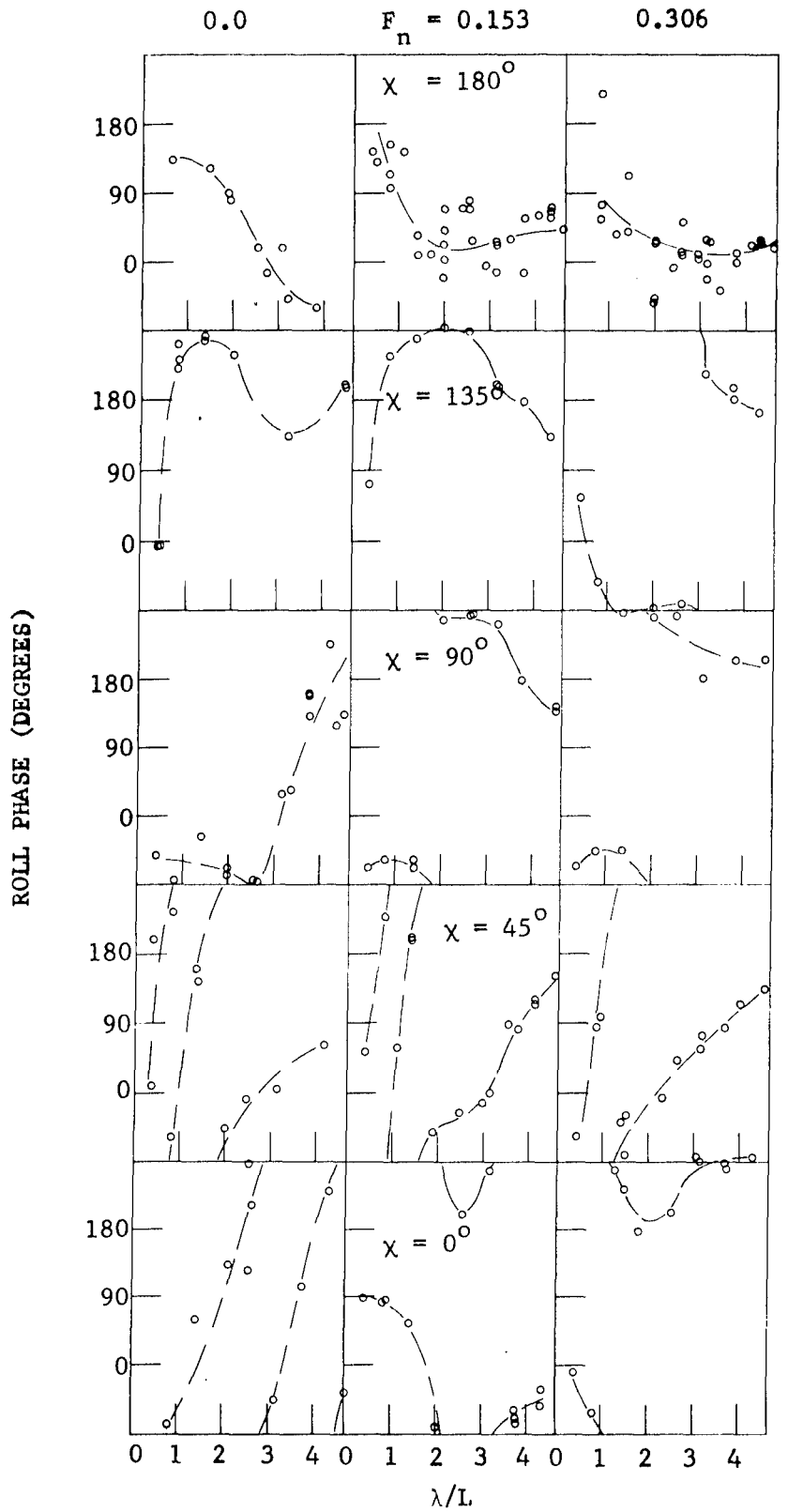

Figure 32 – Phase Angle of Roll for a Hull Separation of 207 Feet

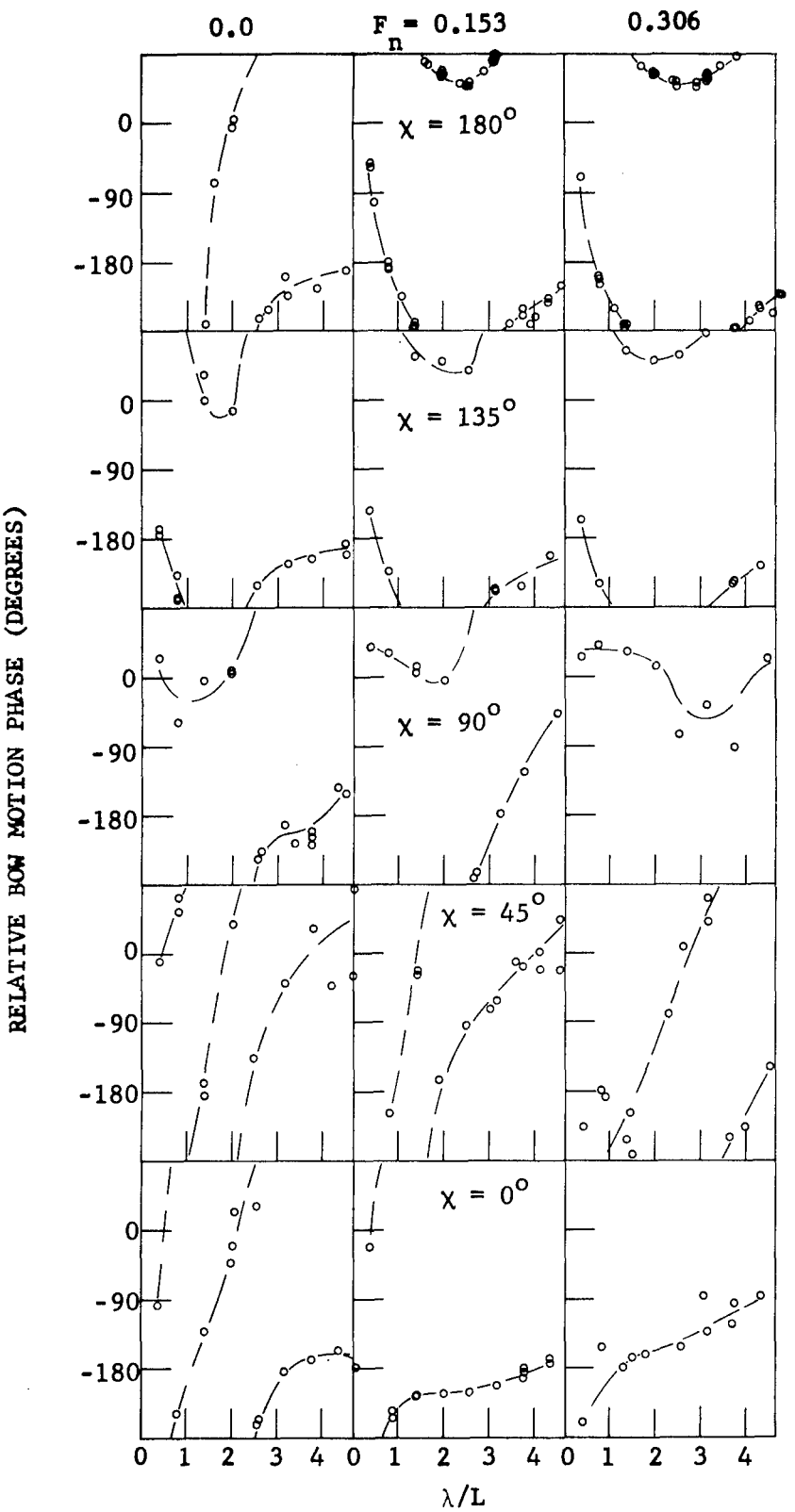

Figure 33 – Phase Angle of Relative Bow Motion for a Hull Separation of 207 Feet

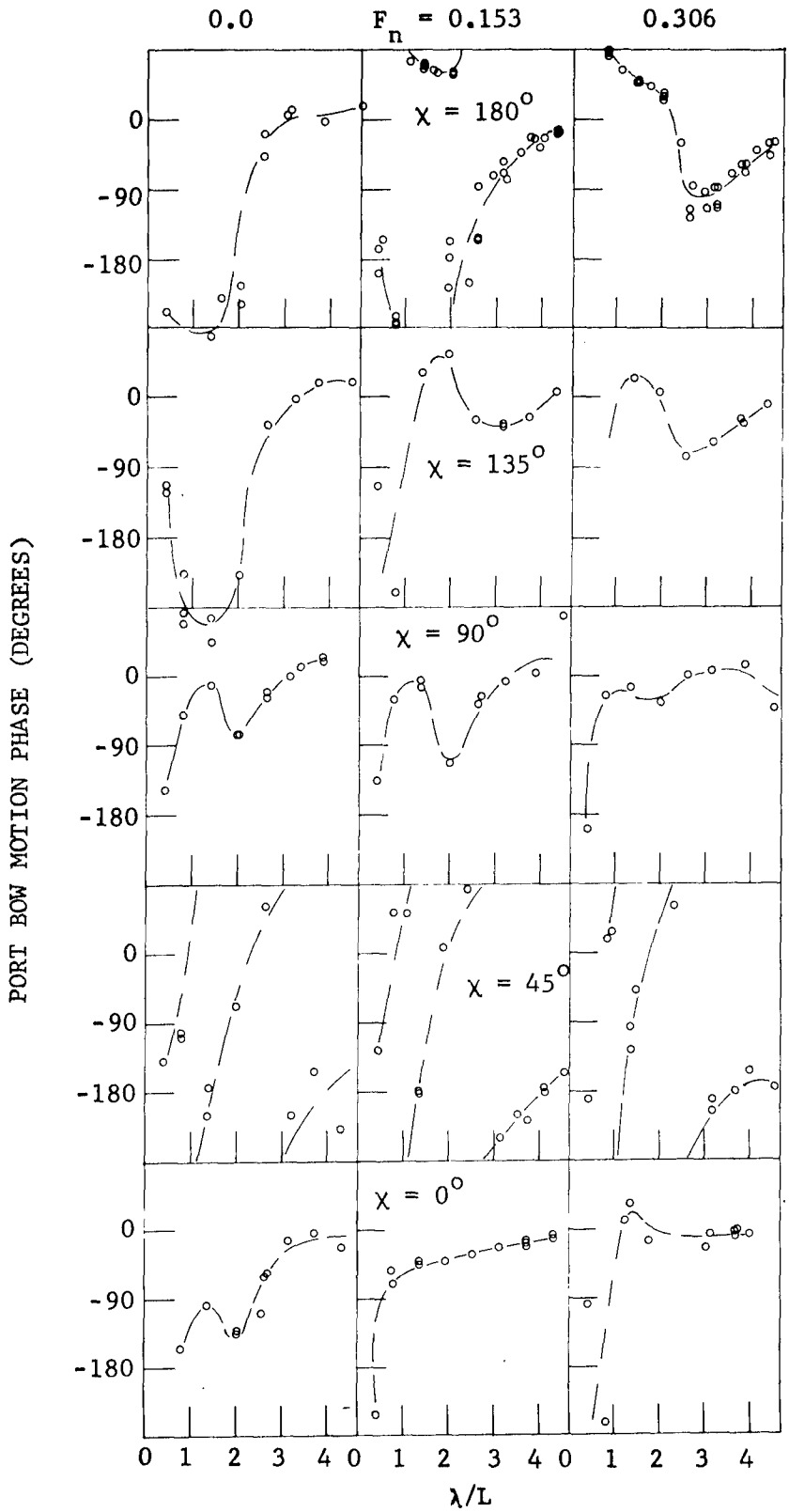

Figure 34 – Phase Angle of Port Bow Motion for a Hull Separation of 207 Feet

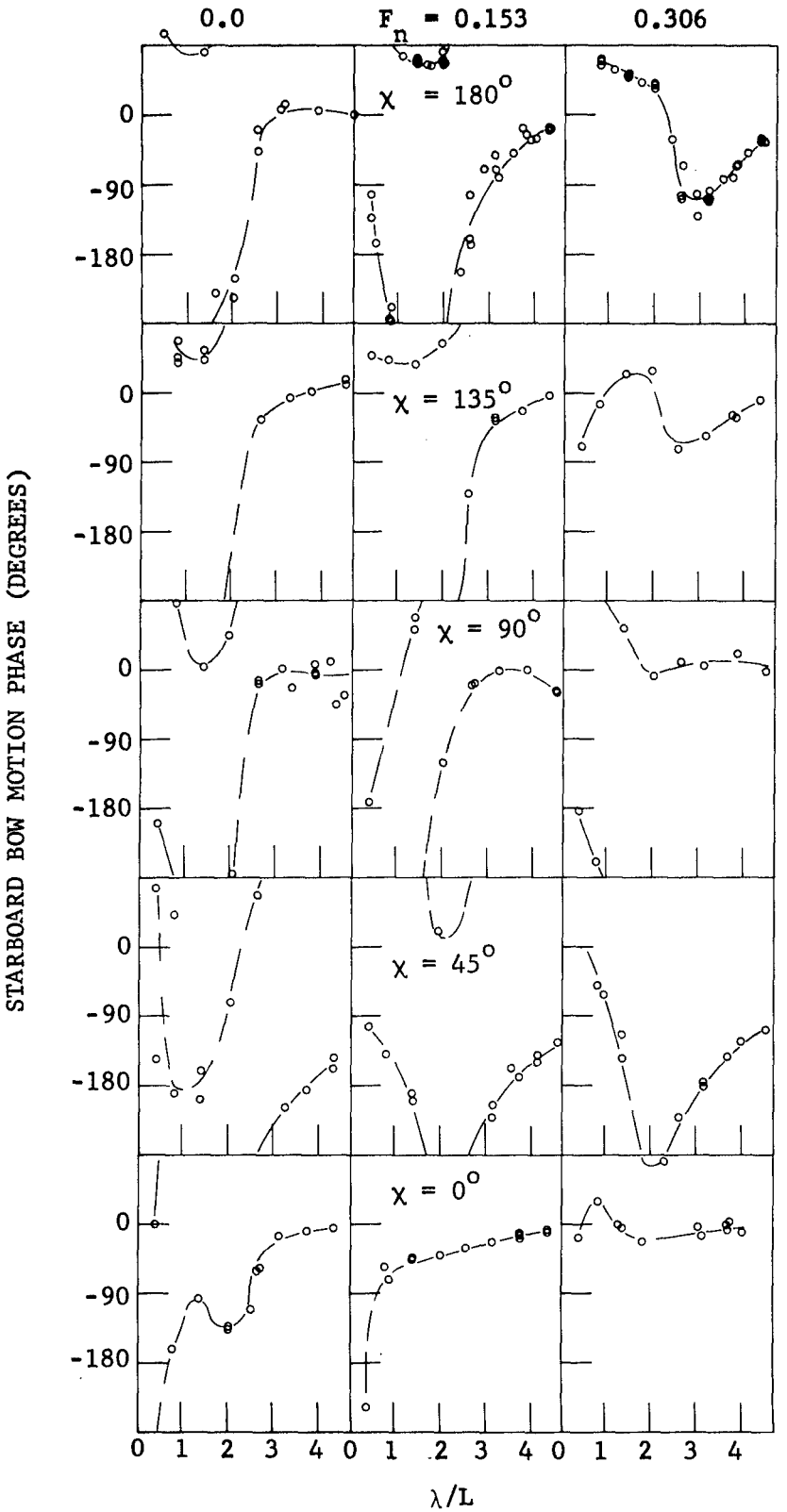

Figure 35 – Phase Angle of Starboard Bow Motion for a Hull Separation of 207 Feet

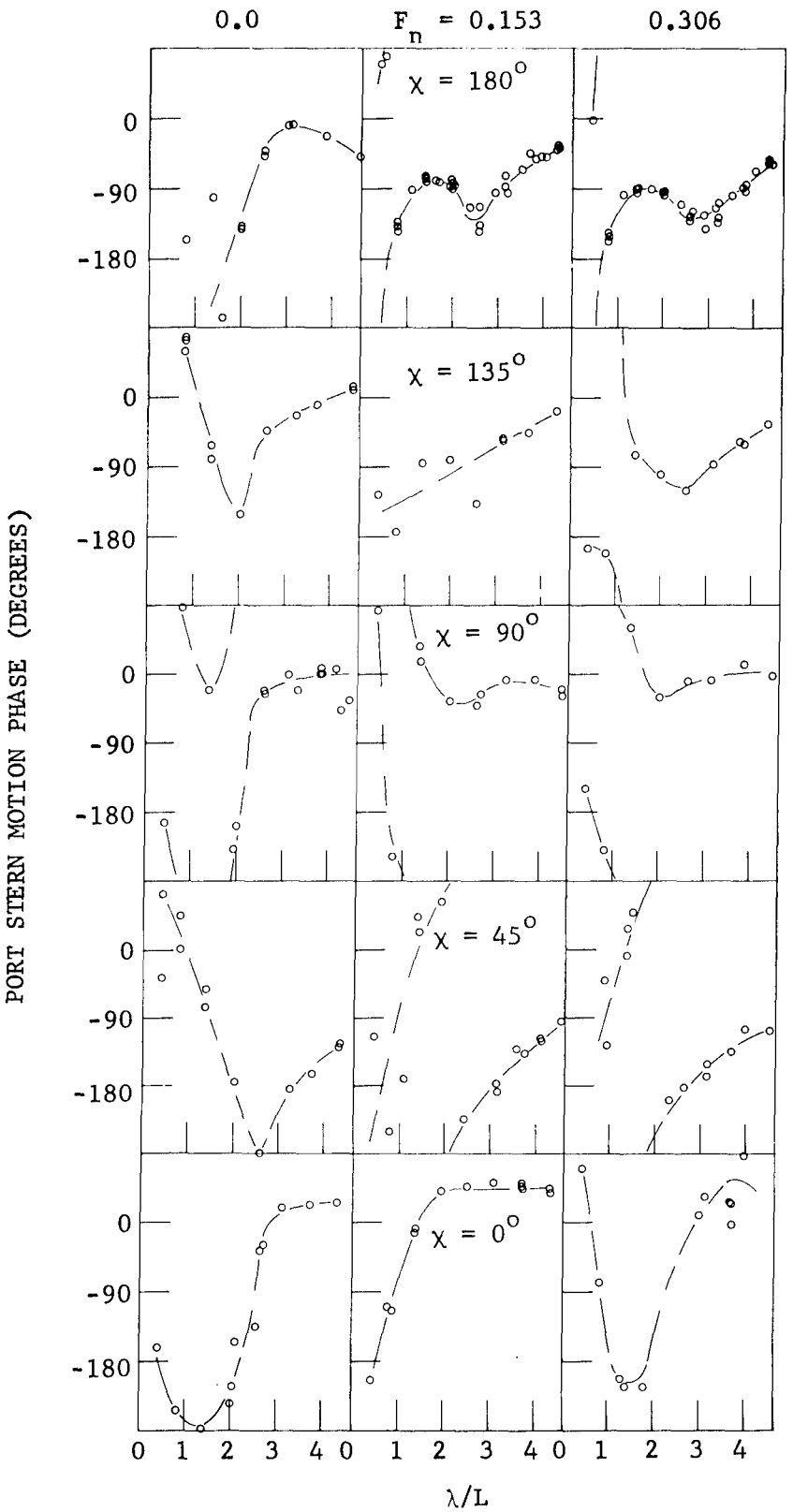

Figure 36 – Phase Angle of Port Stern Motion for a Hull Separation of 207 Feet

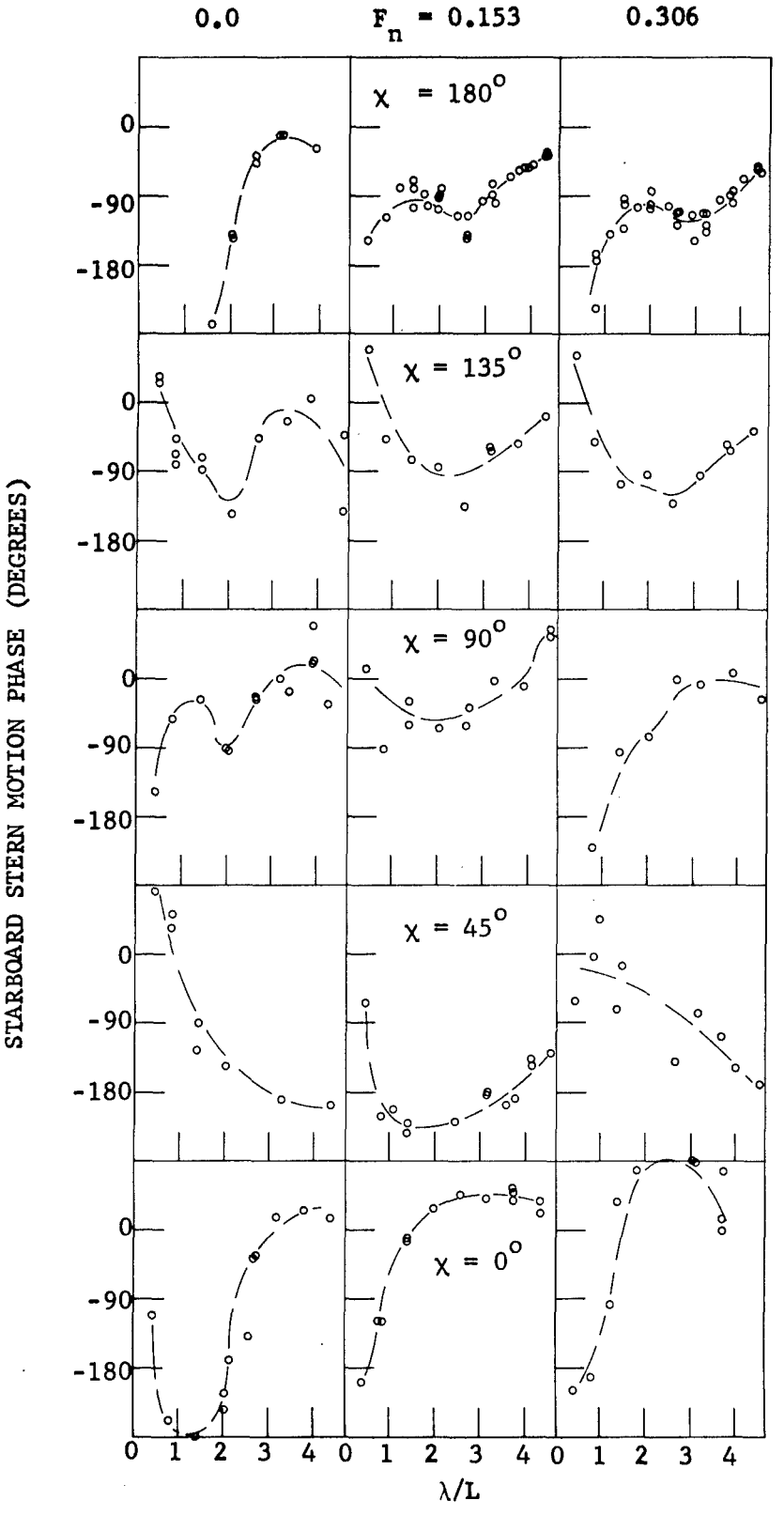

Figure 37 – Phase Angle of Starboard Stern Motion for a Hull Separation of 207 Feet

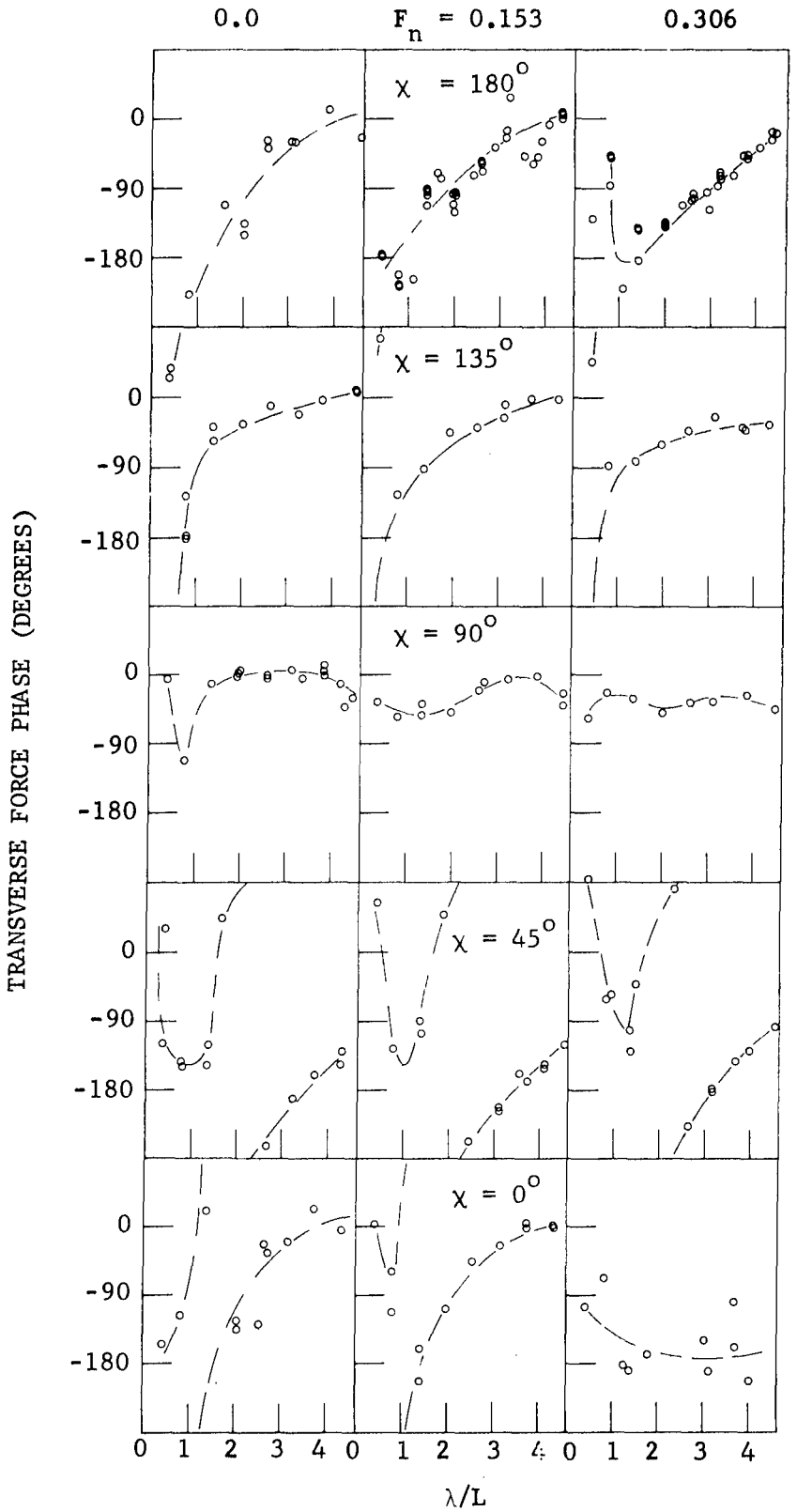

Figure 38 – Phase Angle of Transverse Force for a Hull Separation of 207 Feet

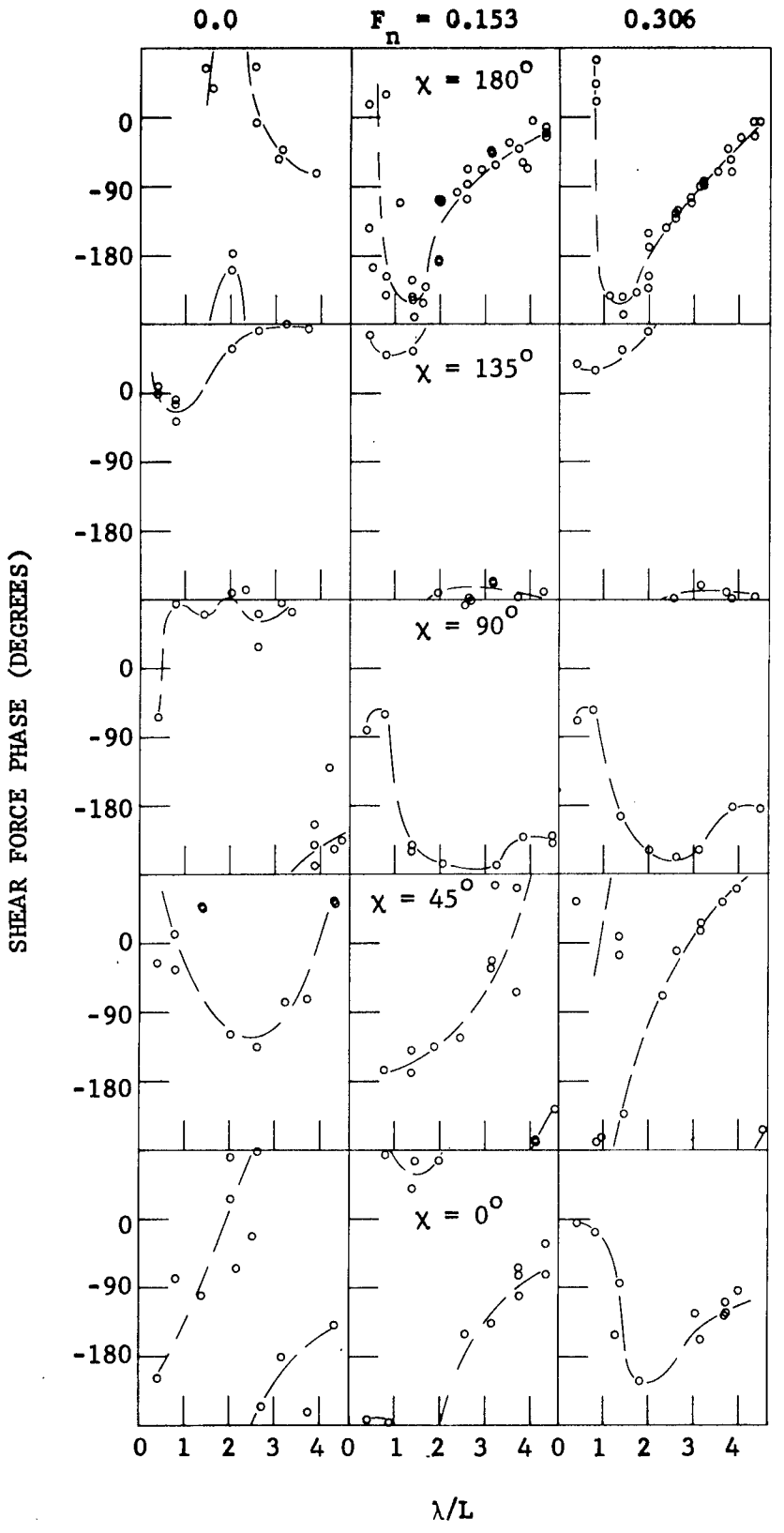

Figure 39 – Phase Angle of Shear Force for a Hull Separation of 207 Feet

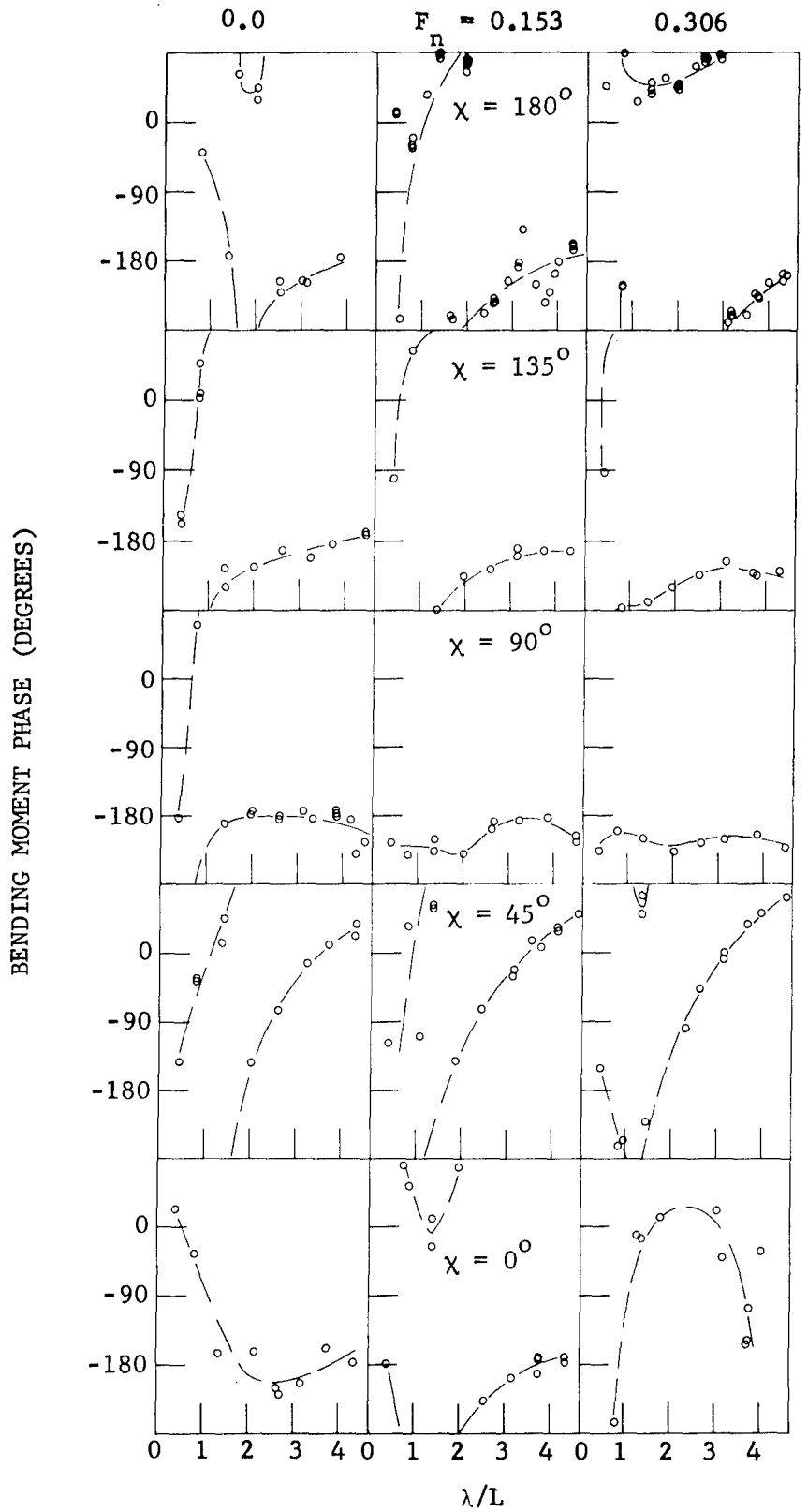

Figure 40 – Phase Angle of Bending Moment for a Hull Separation of 207 Feet

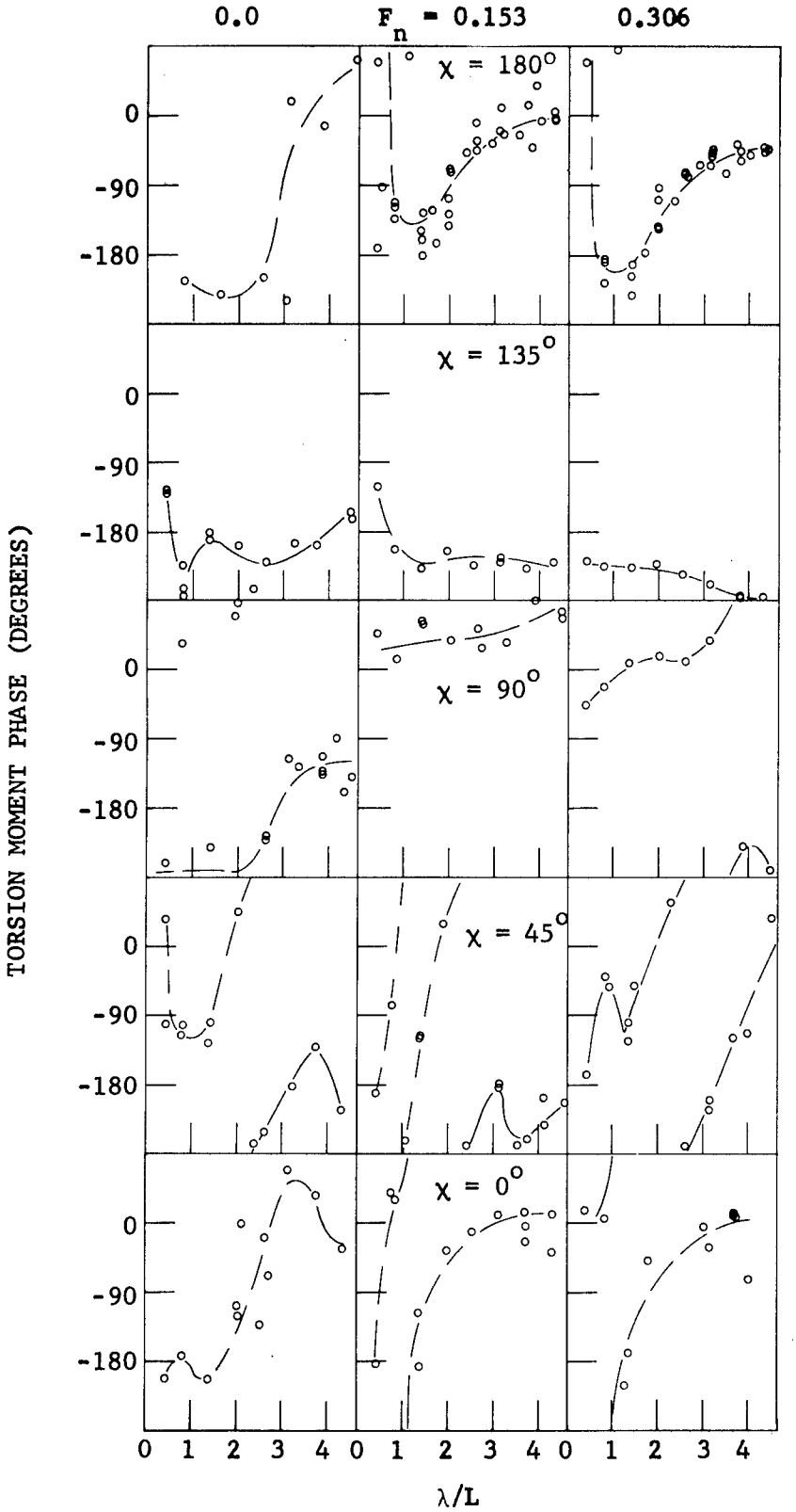

Figure 41 – Phase Angle of Torsion Moment for a Hull Separation of 207 Feet

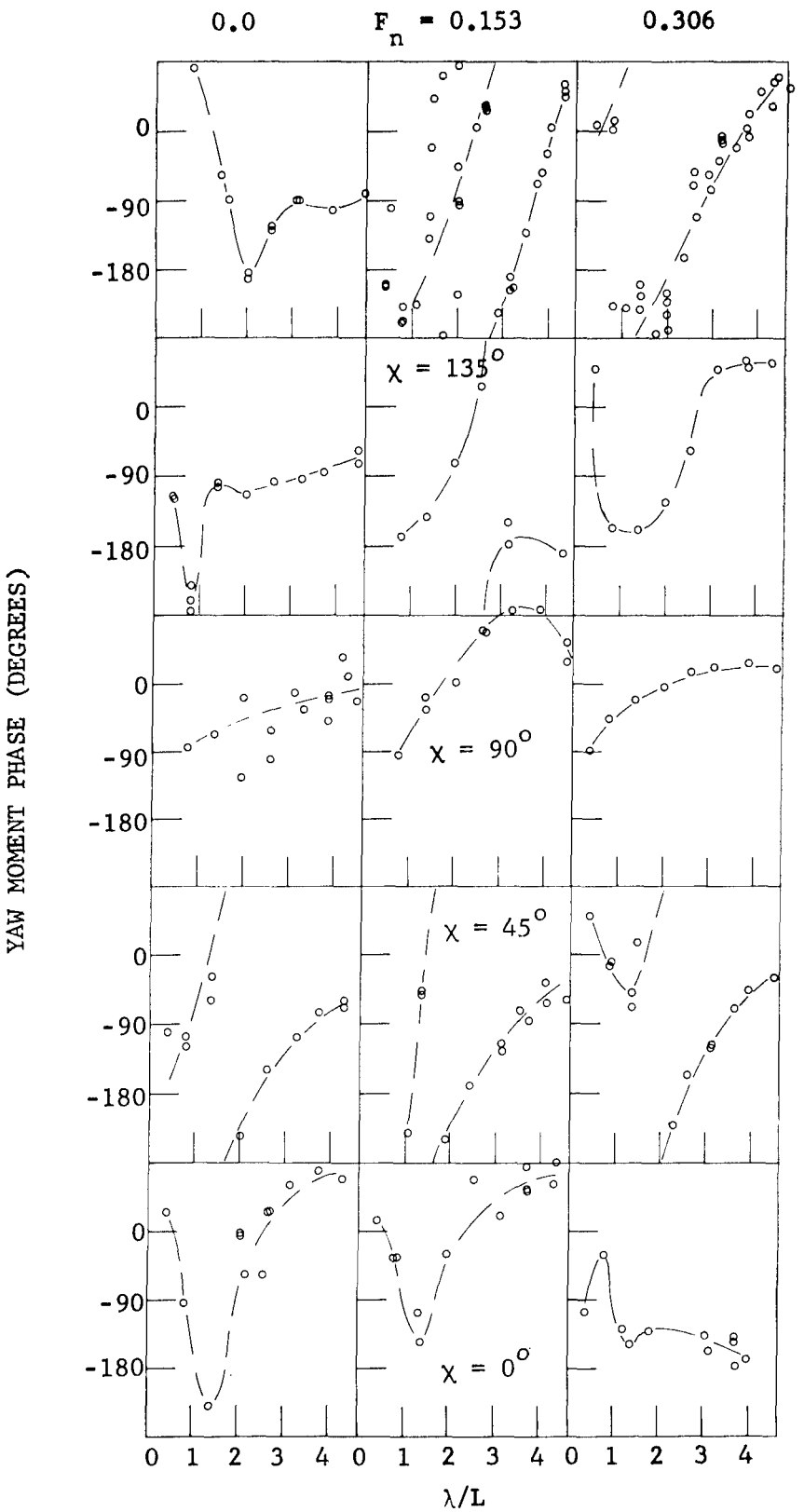

Figure 42 – Phase Angle of Yaw Moment for a Hull Separation of 207 Feet

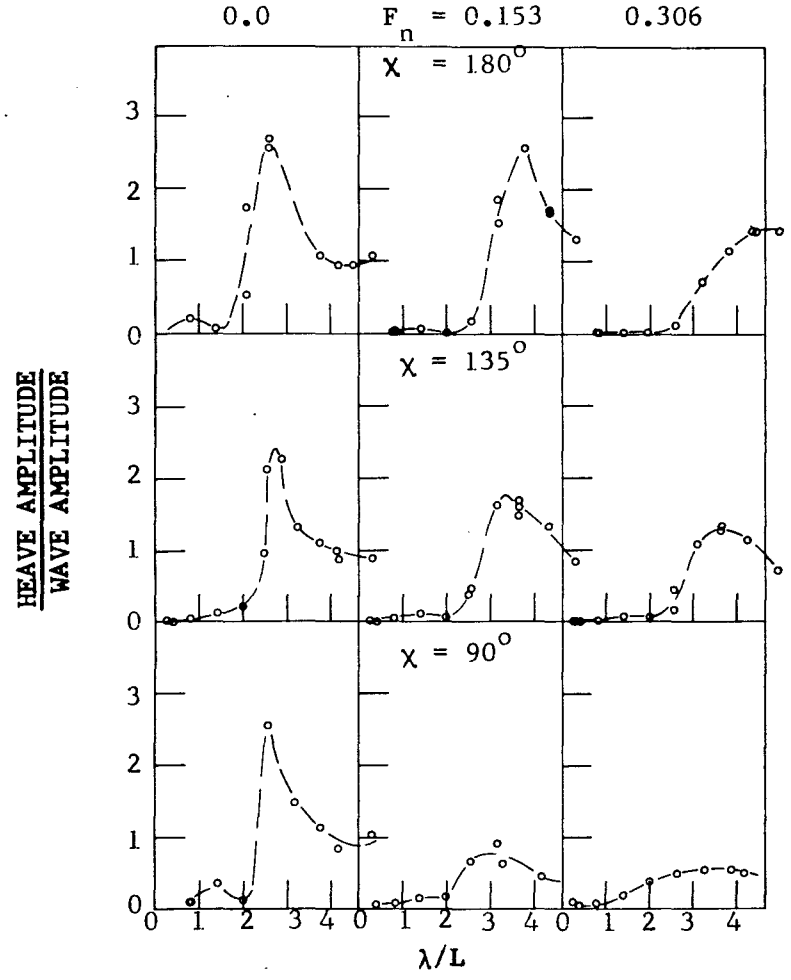

Figure 43 – Nondimensional Amplitude of Heave for a Hull Separation of 157 Feet

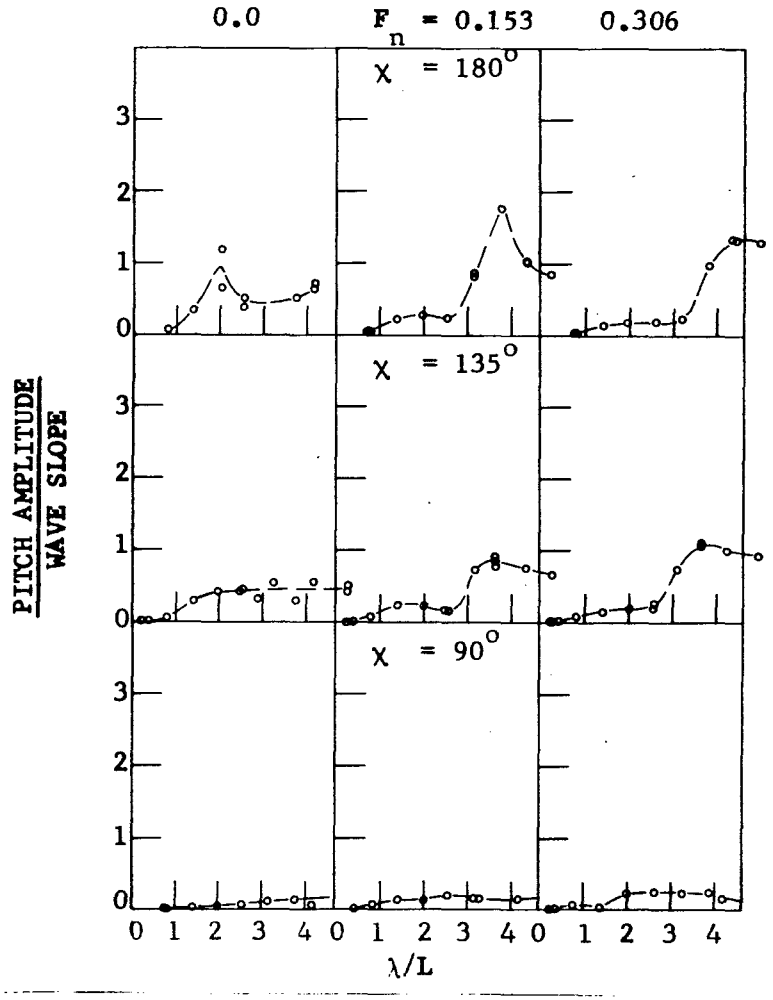

Figure 44 – Nondimensional Amplitude of Pitch for a Hull Separation of 157 Feet

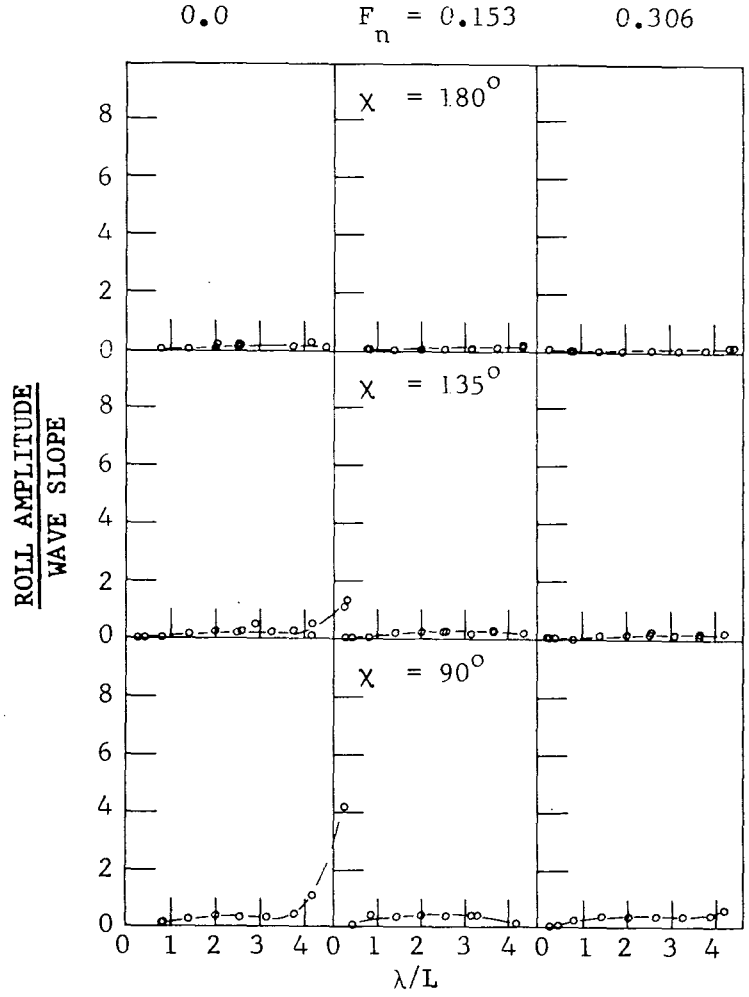

Figure 45 – Nondimensional Amplitude of Roll for a Hull Separation of 157 Feet

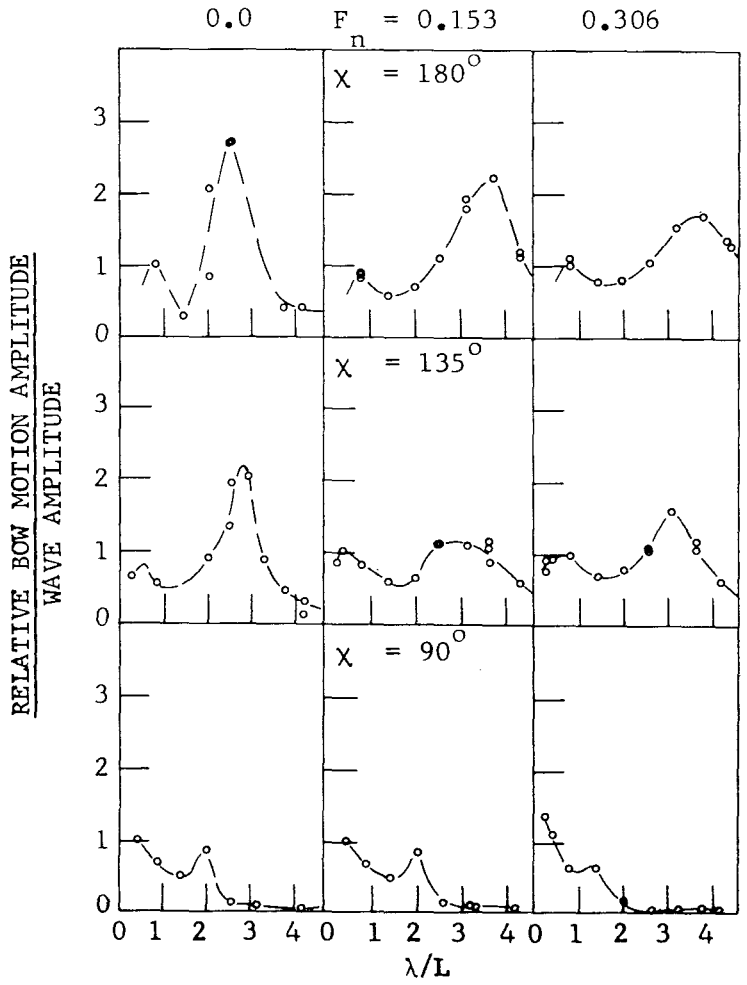

Figure 46 – Nondimensional Amplitude of Relative Bow Motion for a Hull Separation of 157 Feet

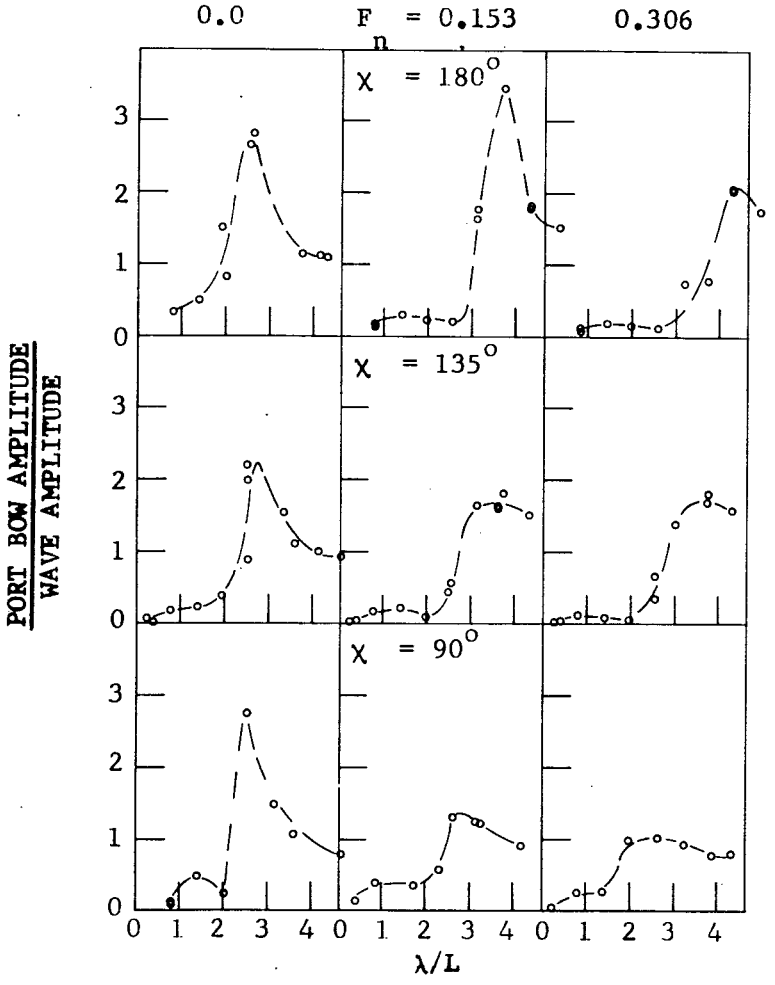

Figure 47 – Nondimensional Amplitude of Port Bow Motion for a Hull Separation of 157 Feet

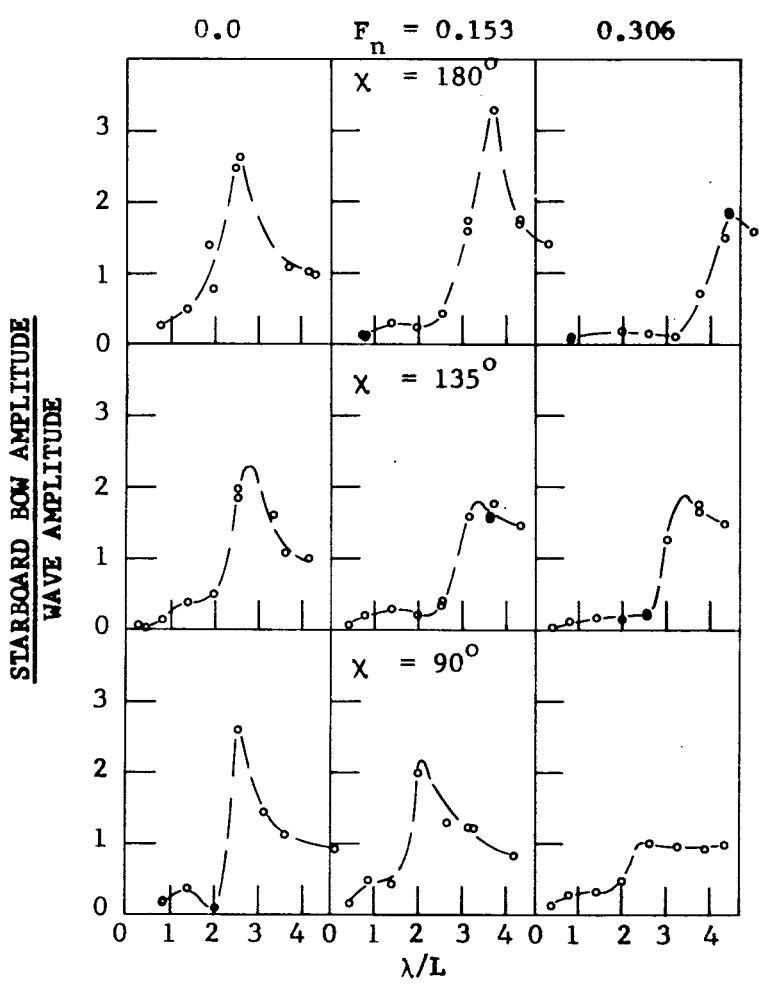

Figure 48 – Nondimensional Amplitude of Starboard Bow Motion for a Hull Separation of 157 Feet

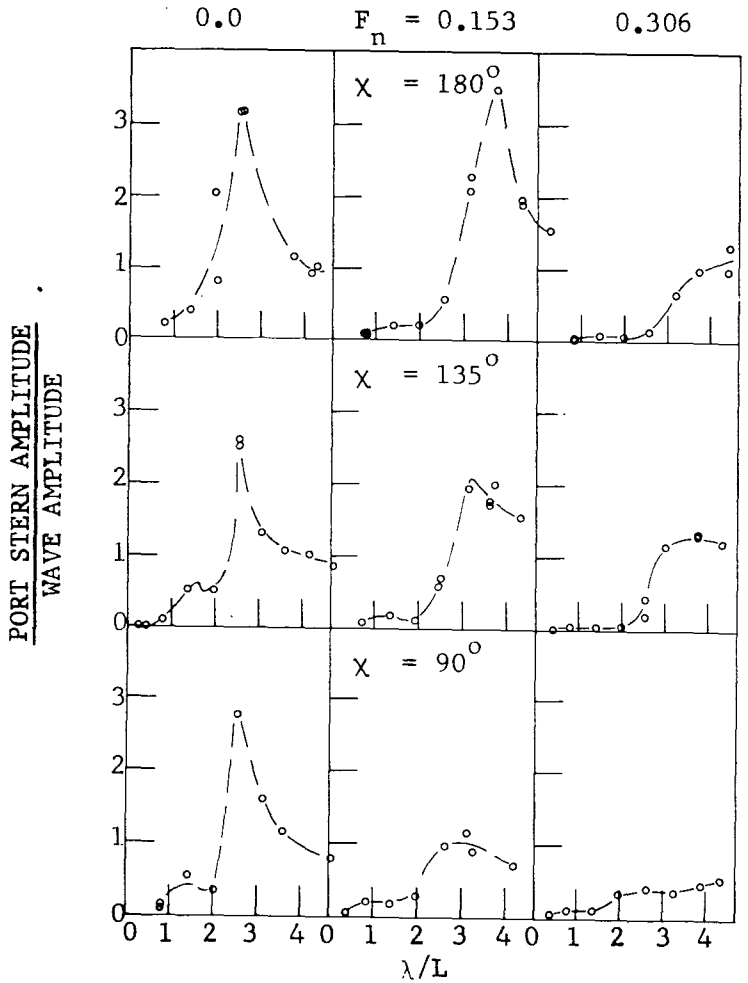

Figure 49 – Nondimensional Amplitude of Port Stern Motion for a Hull Separation of 157 Feet

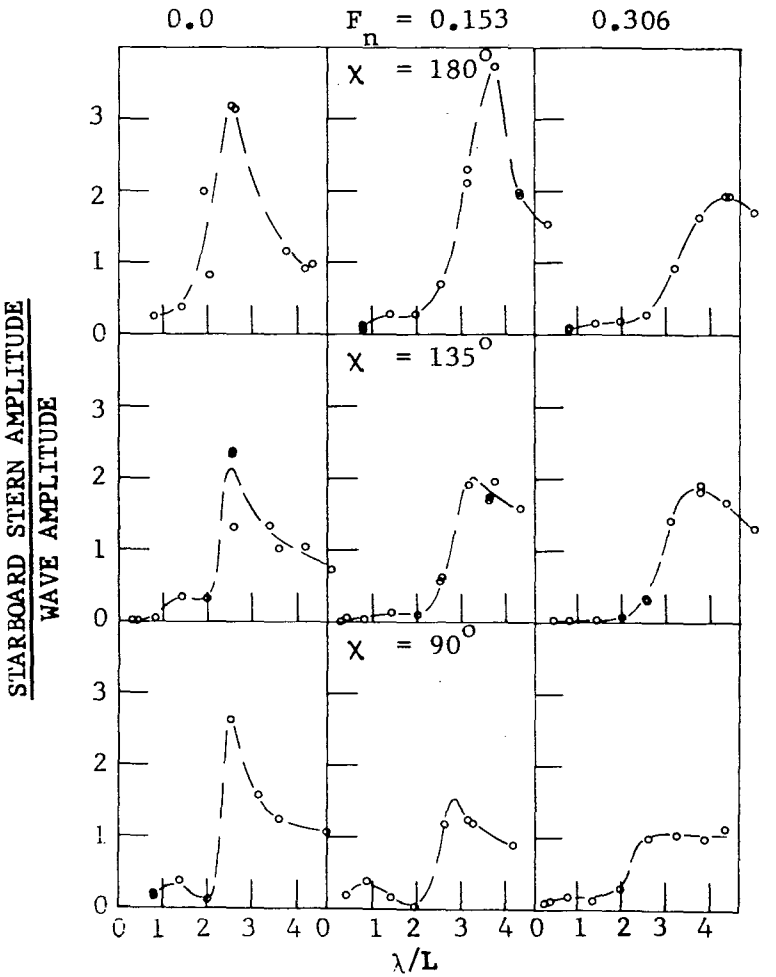

Figure 50 – Nondimensional Amplitude of Starboard Stern Motion for a Hull Separation of 157 Feet

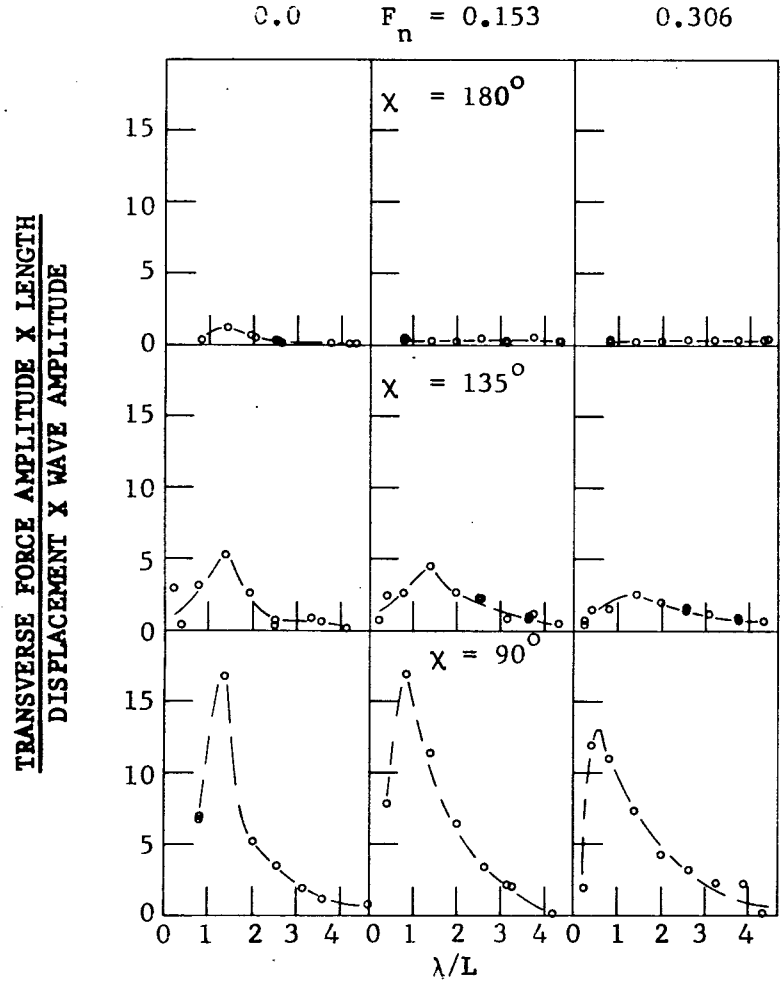

Figure 51 – Nondimensional Amplitude of Transverse Force for a Hull Separation of 157 Feet

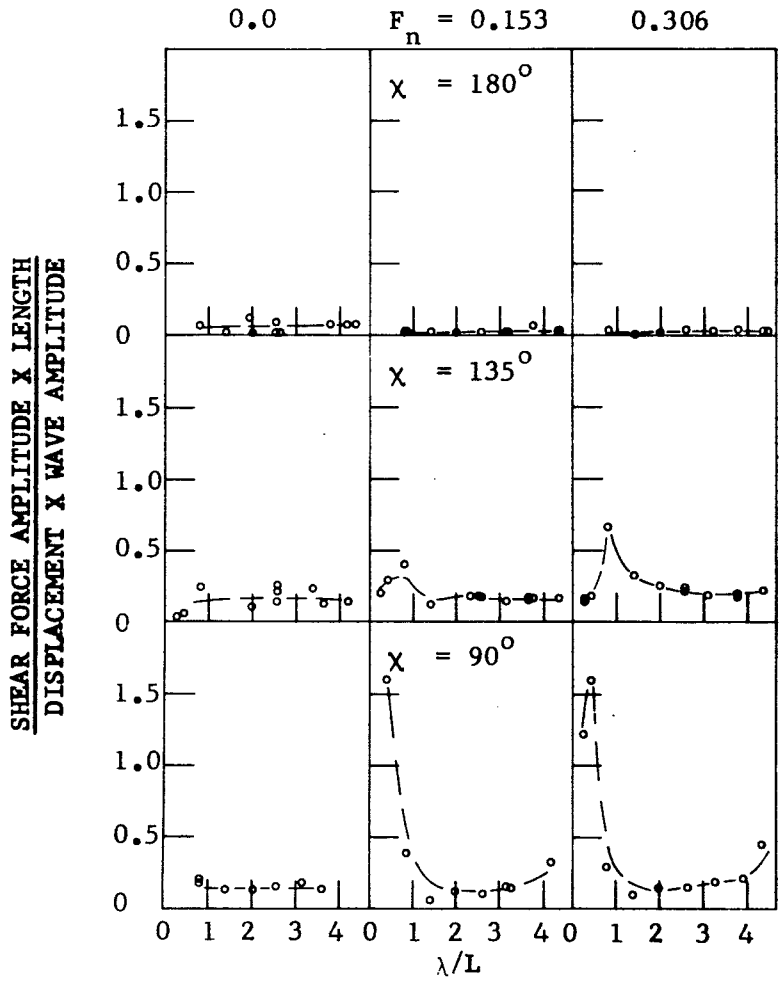

Figure 52 – Nondimensional Amplitude of Shear Force for a Hull Separation of 157 Feet

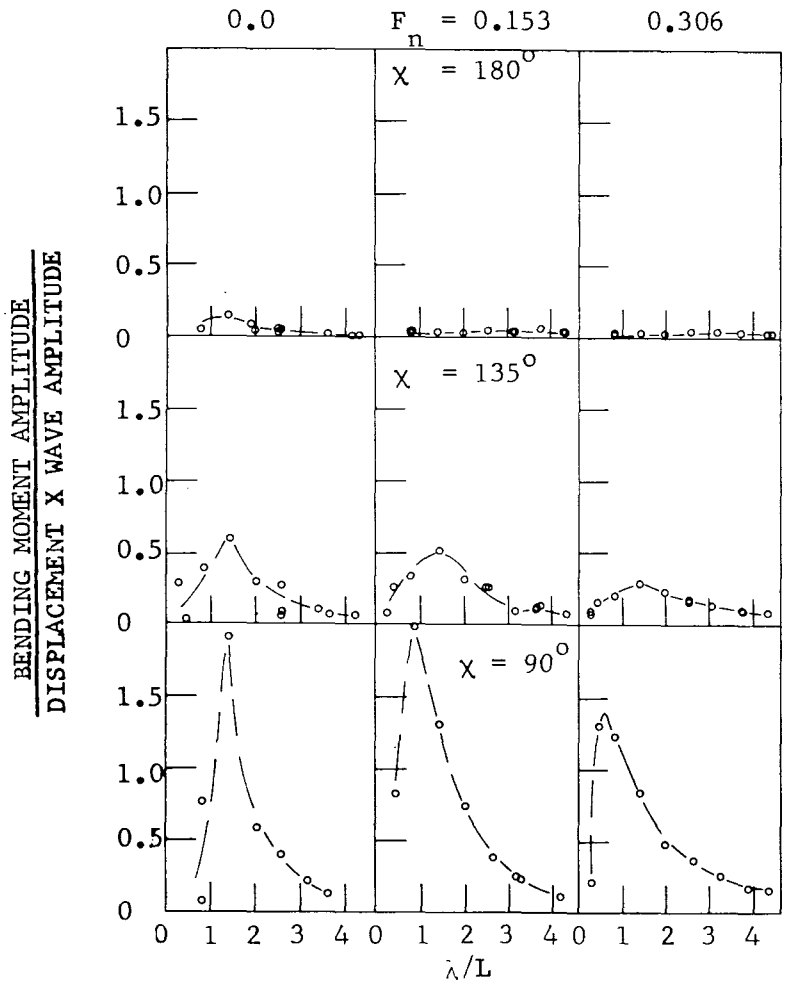

Figure 53 – Nondimensional Amplitude of Bending Moment for a Hull Separation of 157 Feet

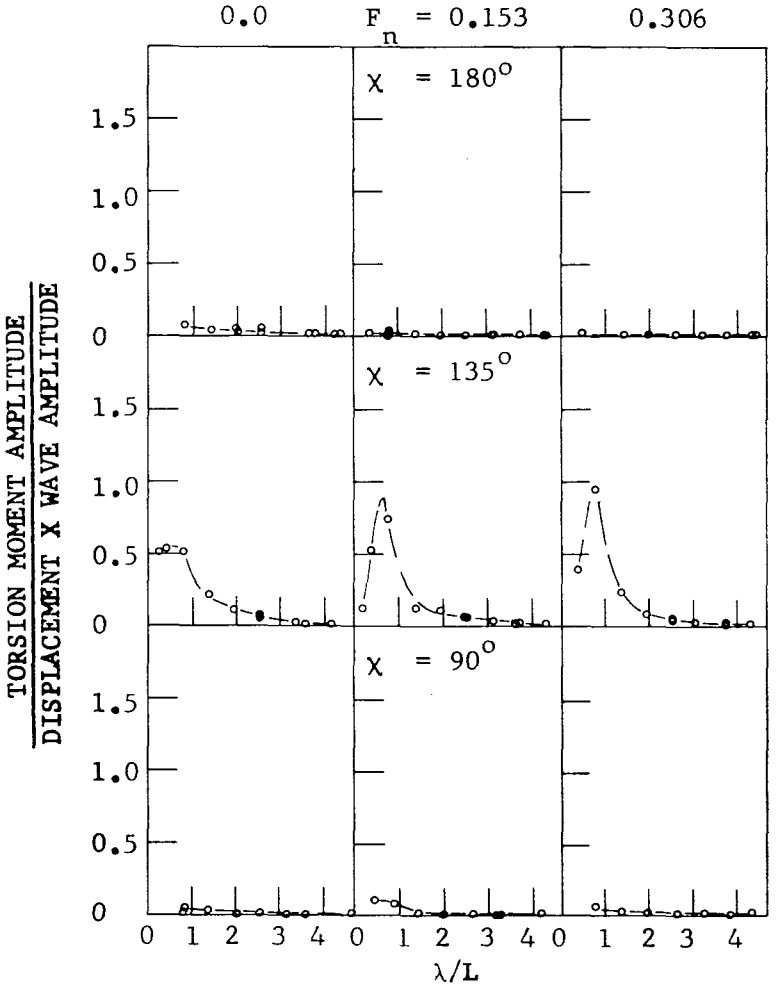

Figure 54 – Nondimensional Amplitude of Torsion Moment for a Hull Separation of 157 Feet

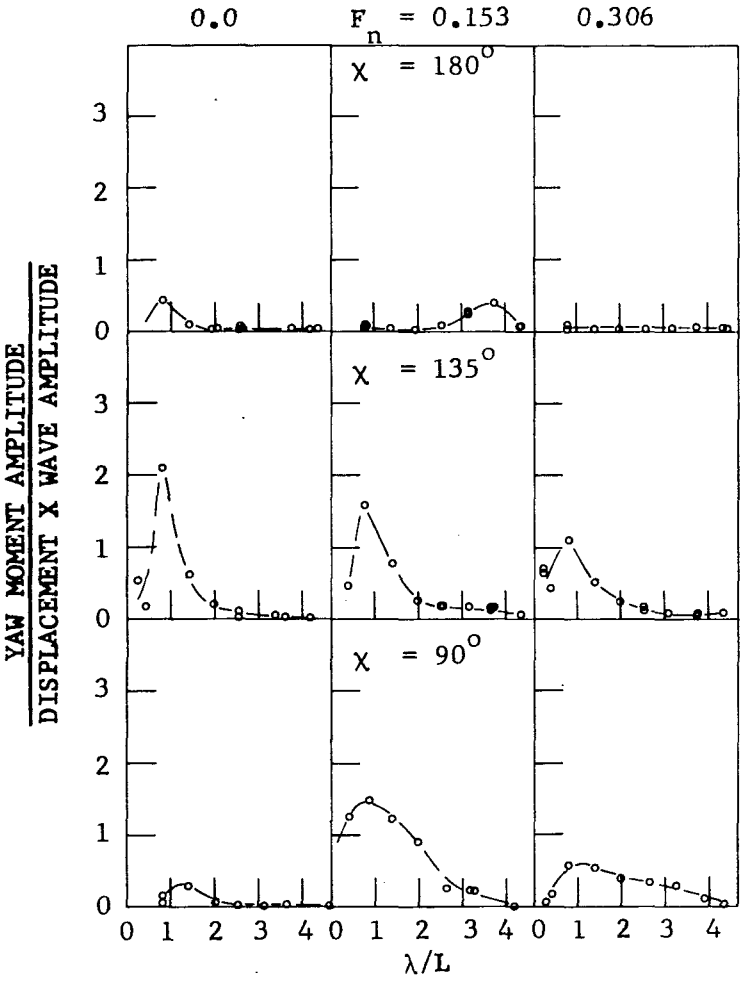

Figure 55 – Nondimensional Amplitude of Yaw Moment for a Hull Separation of 157 Feet

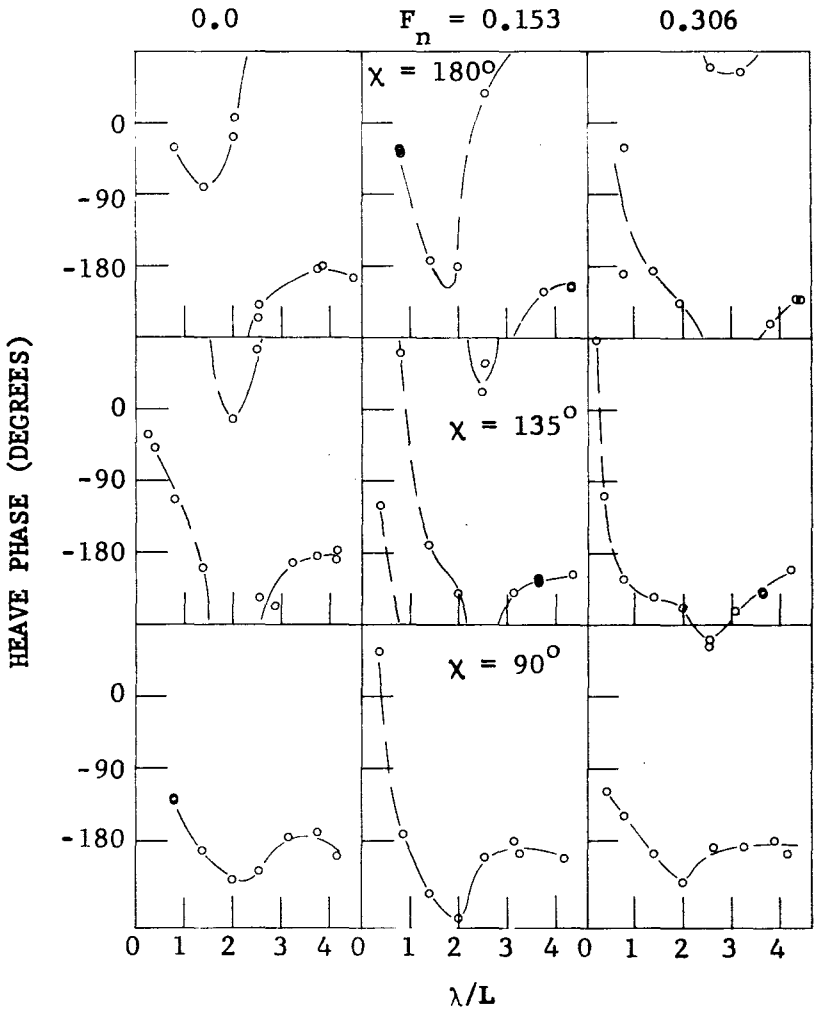

Figure 56 – Phase Angle of Heave for a Hull Separation of 157 Feet

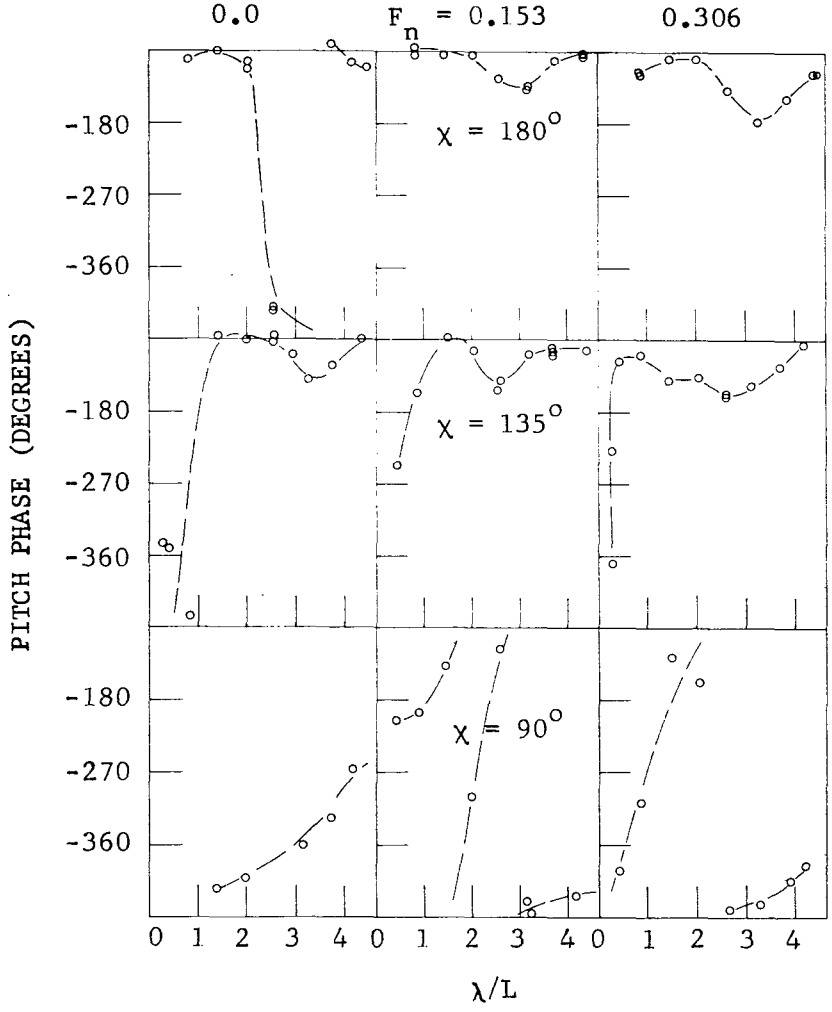

Figure 57 – Phase Angle of Pitch for a Hull Separation of 157 Feet

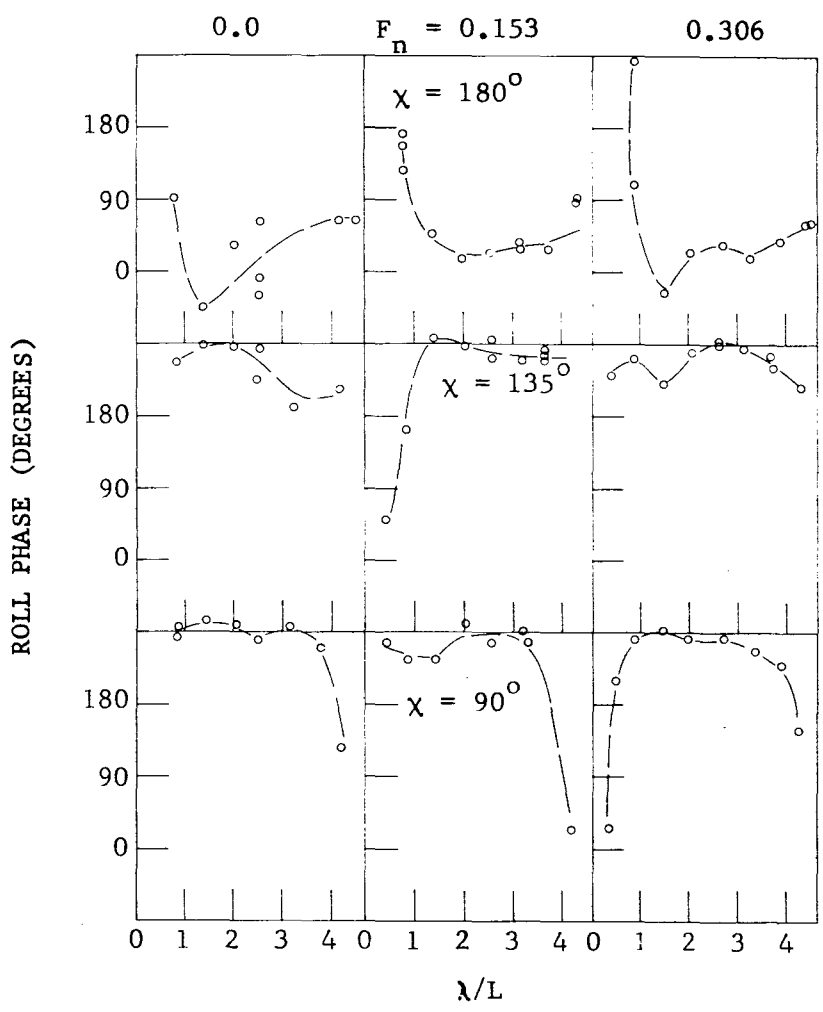

Figure 58 – Phase Angle of Roll for a Hull Separation of 157 Feet

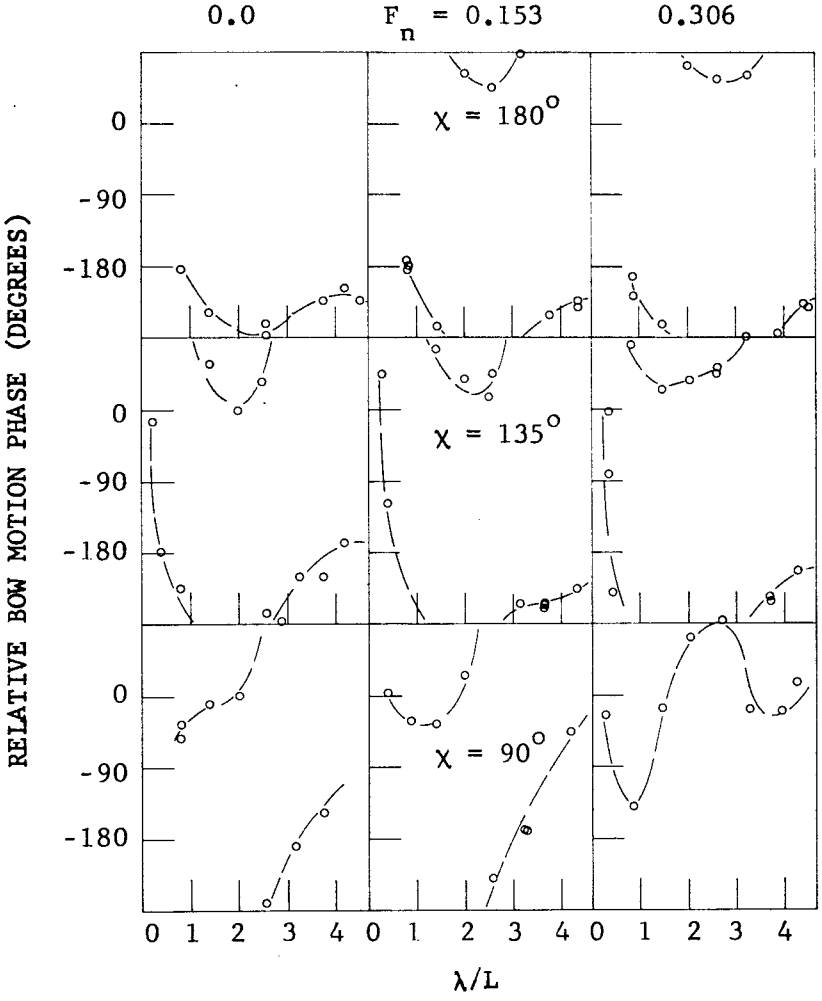

Figure 59 – Phase Angle of Relative Bow Motion for a Hull Separation of 157 Feet

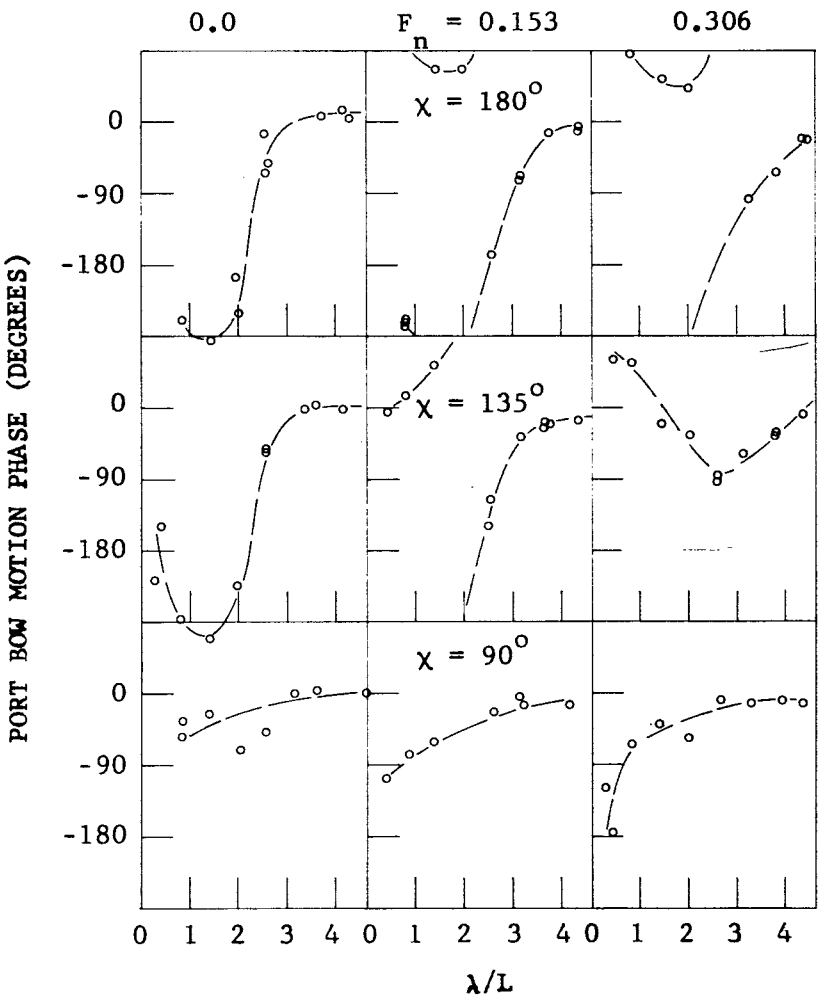

Figure 60 – Phase Angle of Port Bow Motion for a Hull Separation of 157 Feet

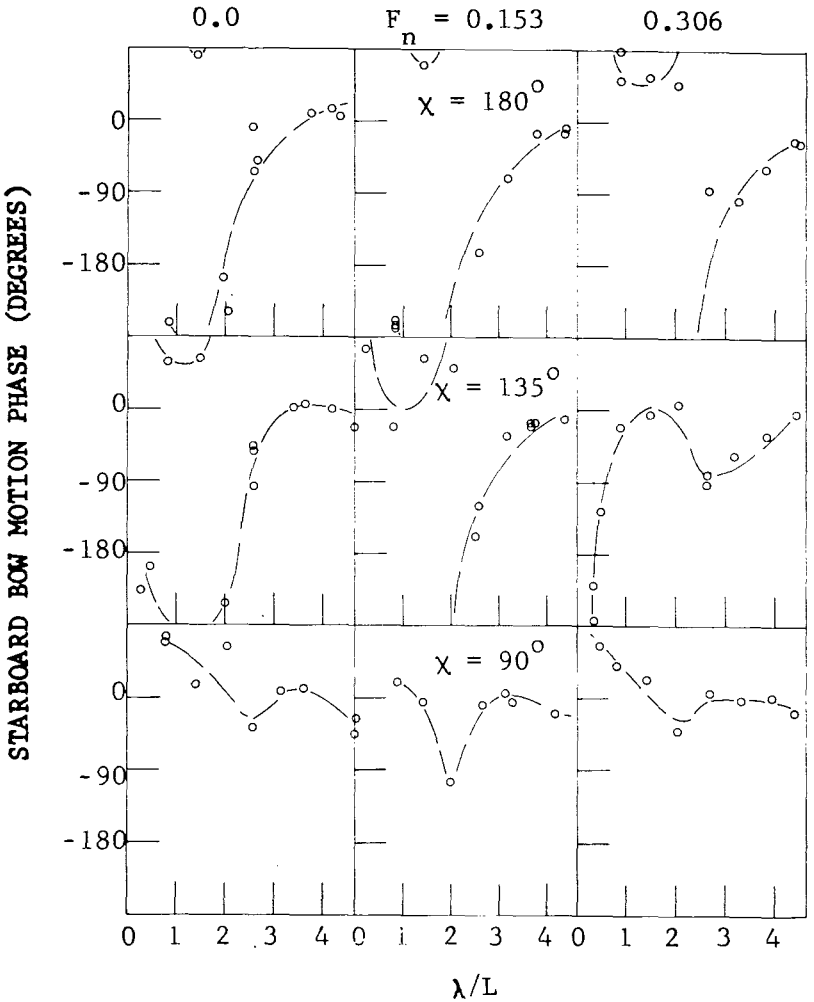

Figure 61 – Phase Angle of Starboard Bow Motion for a Hull Separation of 157 Feet

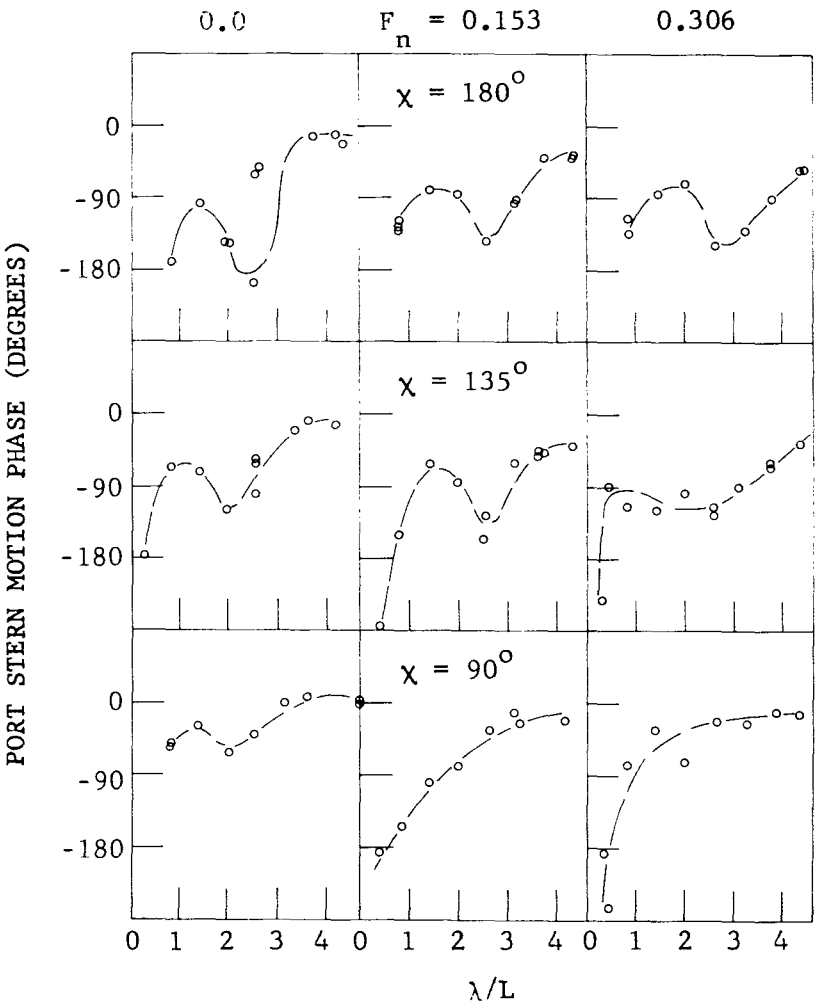

Figure 62 – Phase Angle of Port Stern Motion for a Hull Separation of 157 Feet

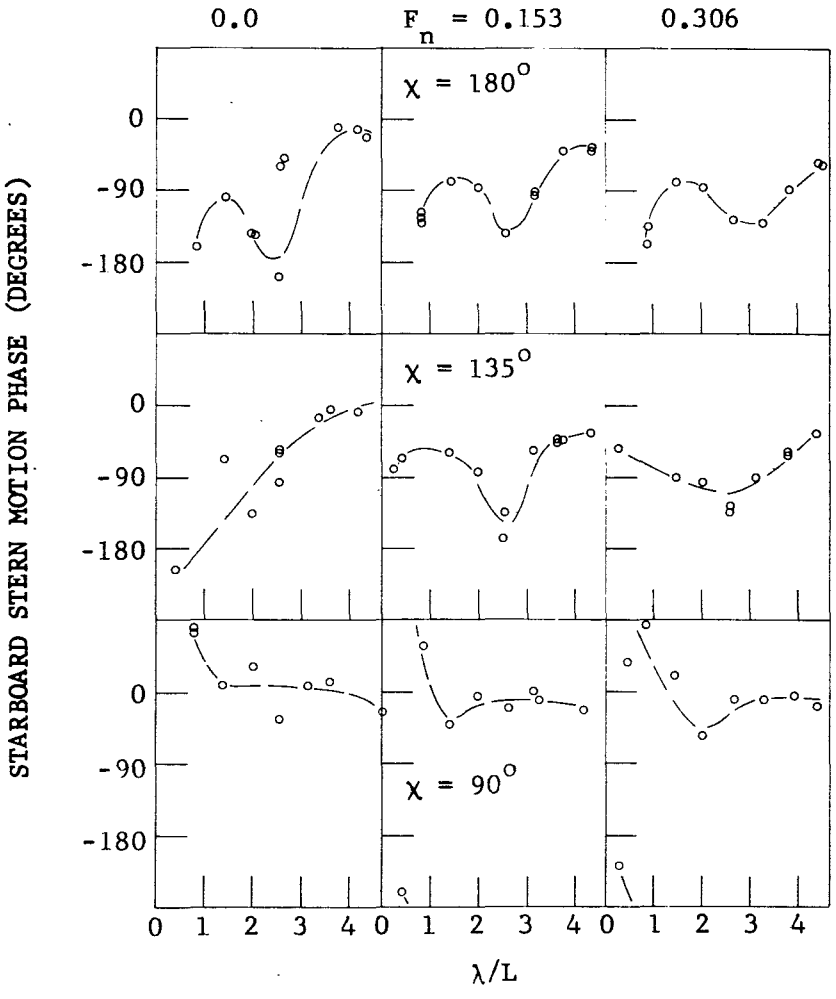

Figure 63 – Phase Angle of Starboard Stern Motion for a Hull Separation of 157 Feet

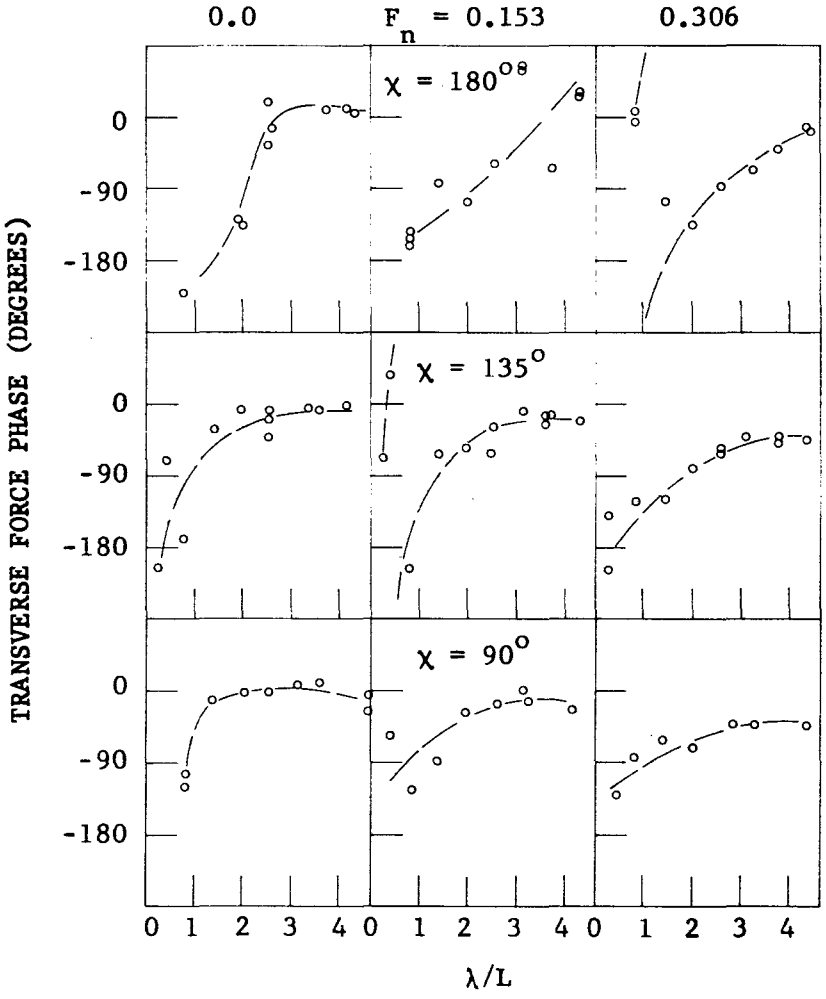

Figure 64 – Phase Angle of Transverse Force for a Hull Separation of 157 Feet

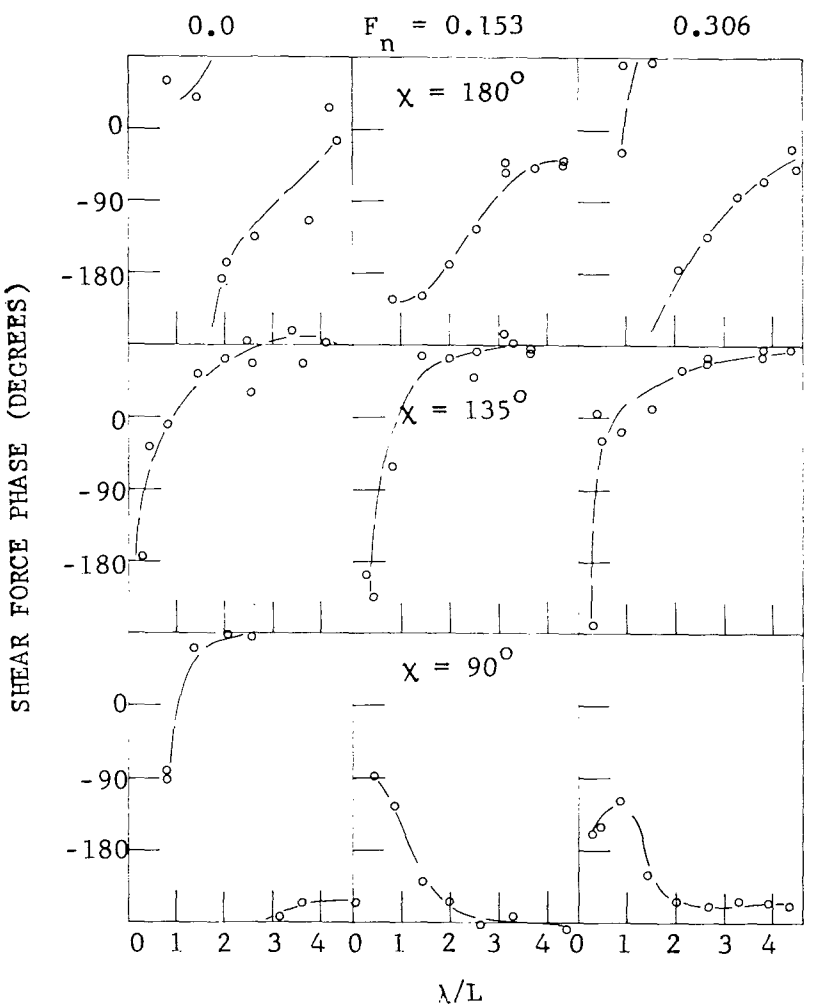

Figure 65 – Phase Angle of Shear Force for a Hull Separation of 157 Feet

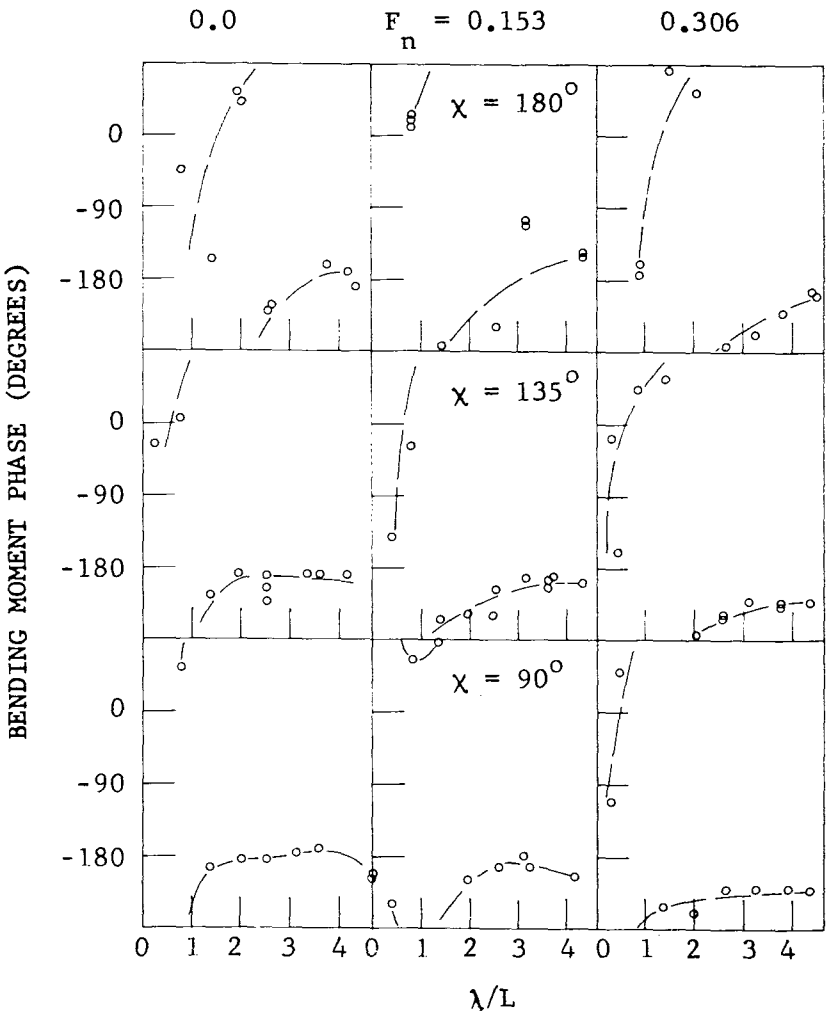

Figure 66 – Phase Angle of Bending Moment for a Hull Separation of 157 Feet

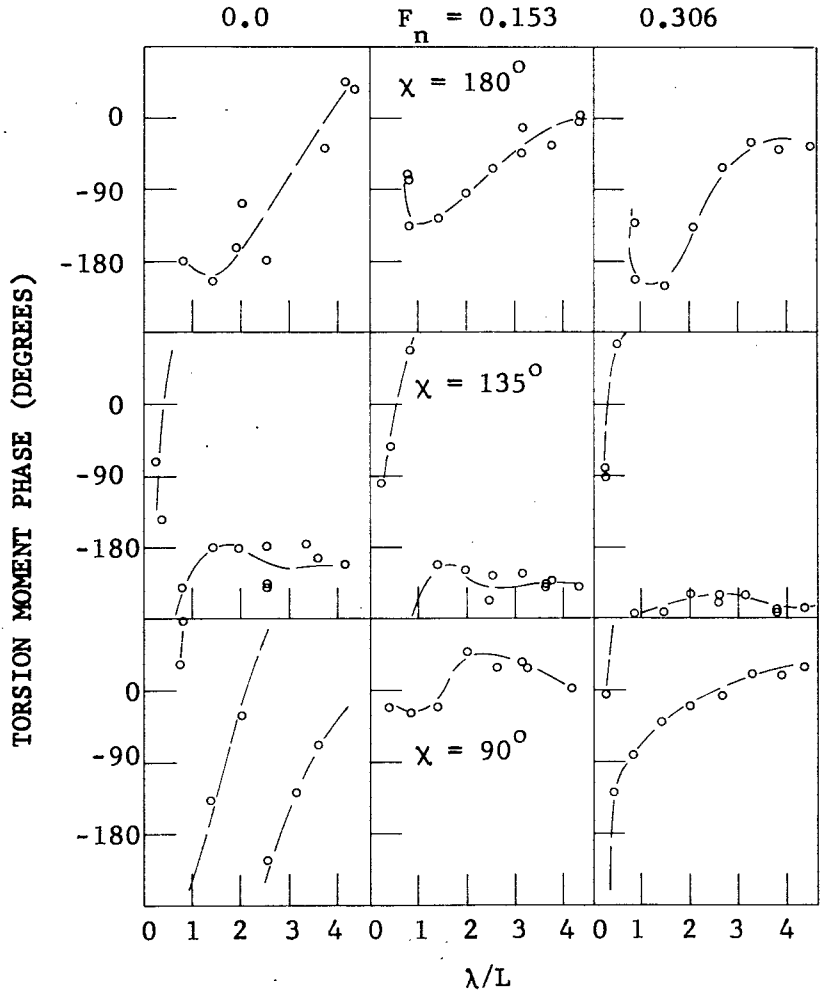

Figure 67 – Phase Angle of Torsion Moment for a Hull Separation of 157 Feet

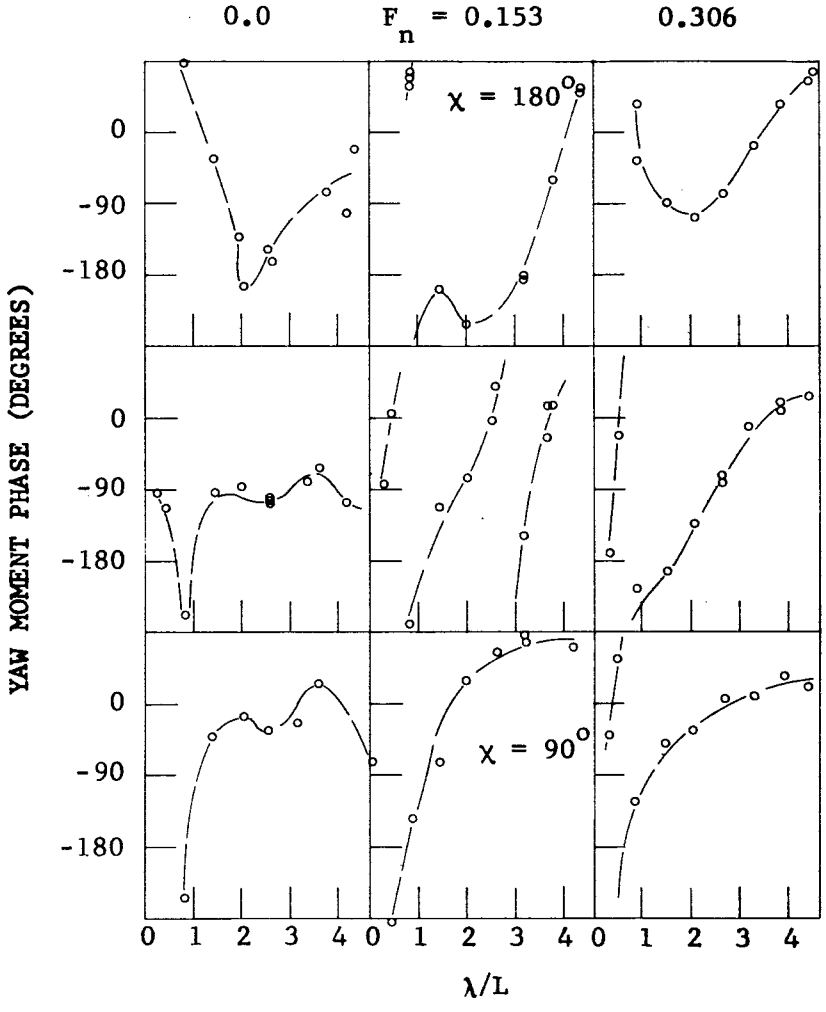

Figure 68 – Phase Angle of Yaw Moment for a Hull Separation of 157 Feet

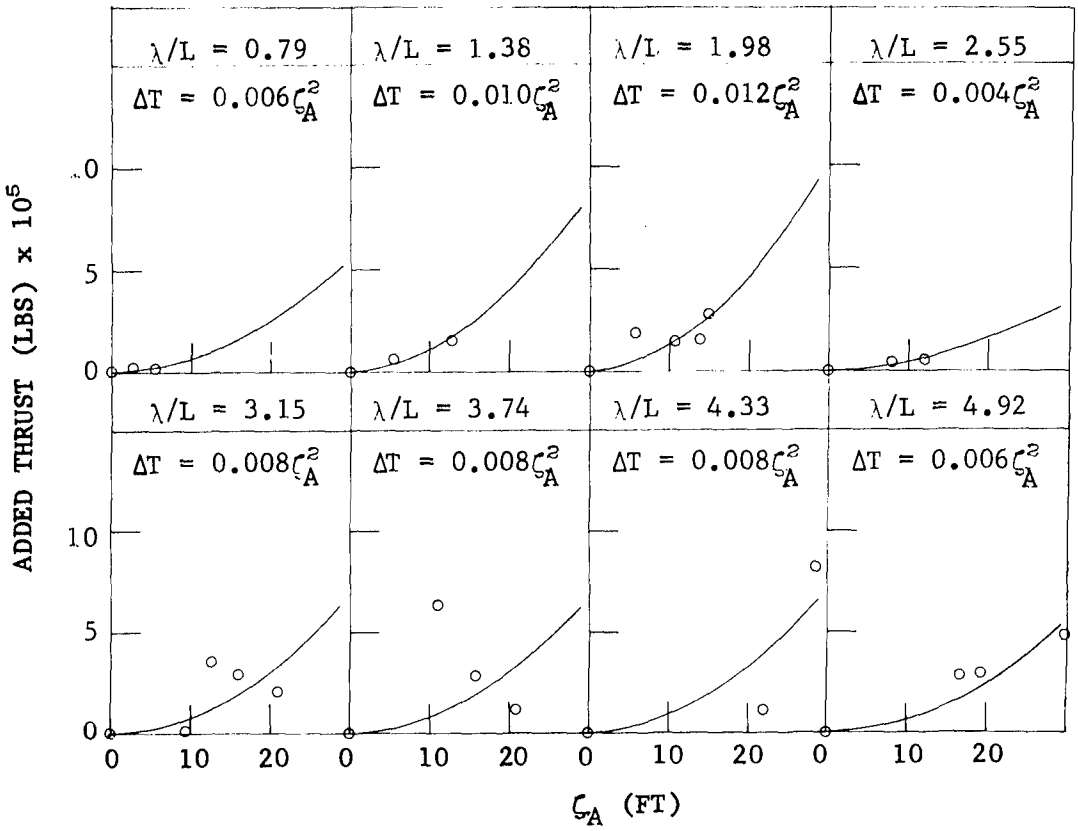

Figure 69 – Added Thrust versus Wave Amplitude for a Froude Number of 0.153, with Least-Square-Fit Parabolas of the Form $\Delta T = A\,\zeta_A{}^2$, Full Scale

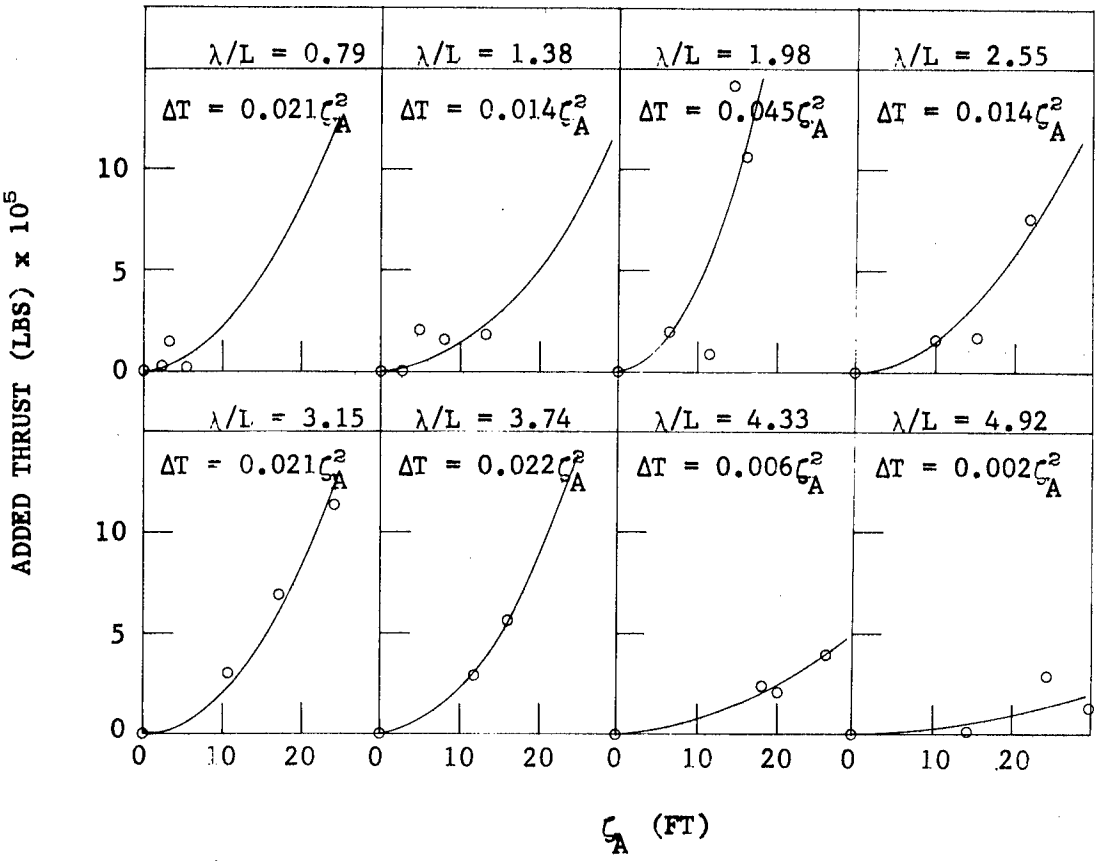

Figure 70 – Added Thrust versus Wave Amplitude for a Froude Number of 0.306, with Least-Square-Fit Parabolas of the Form $\Delta T = A\zeta_A^2$, Full Scale

INITIAL DISTRIBUTION

Copies		Copies	
1	Army Waterways Exp Station	1	NAVSHIPYD PUGET
1	CHONR 438	2	SEC 6034B
1	ONR BOSTON	1	SEC 6110
1	ONR CHICAGO	1	SEC 6114H
1	ONR PASADENA	1	SEC 6120
1	NRL	1	SEC 6136
1	USNA	1	SEC 6144G
1	NAVPGSCOL	1	SEC 6660.03 NORVA
1	NROTC & NAVADMINU, MIT	12	DDC
1	NAVWARCOL	1	LC
2	SHIPS 2052	1	MMA Lib
1	SHIPS 03412	1	MMA Mar Res Cen
1	SHIPS 0342	1	DOT
1	FAC 032C	1	U Cal Berkeley NAME
1	NAVOCEANO	1	U Cal Berkeley NAME/Paulling
1	NAVAIRDEVCEN	1	U Cal Berkeley NAME/Webster
1	NELC	1	U Cal Berkeley NAME/Wehausen
1	NAVWPNSCEN	1	U Cal Scripps
1	NAVUSEACEN SAN DIEGO	1	CIT Aero Lib
1	NAVUSEACEN PASADENA	1	CIT/Wu
1	CIVENGRLAB	1	Florida Atlantic U/Ocean Engr
1	NOL	1	U Hawaii Ocean Engr/Bretschneider
1	NWL	1	U Iowa Inst of Hydr Res
1	NPTLAB NUSC	1	Long Island U Mar Sci/Price
1	NLONLAB NUSC	1	MIT Ocean Engr
1	NAVSHIPYD BSN	1	MIT Ocean Engr/Abkowitz
1	NAVSHIPYD CHSN	1	MIT Ocean Engr/Mandel
1	NAVSHIPYD HUNTERS PT	1	MIT Ocean Engr/Newman
1	NAVSHIPYD LBEACH	1	U Michigan NAME
1	NAVSHIPYD MARE	1	U Michigan NAME/Couch
1	NAVSHIPYD MARE 250	1	U Michigan NAME/Hammitt
1	NAVSHIPYD PEARL	1	U Michigan NAME/Ogilvie
1	NAVSHIPYD PHILA	1	U Michigan Will Run Labs
1	NAVSHIPYD PTSMH	1	U Minnesota St. Anthony Falls/Son

Copies	
1	U Notre Dame Engr Lib
1	New York U/Pierson
1	SWRI Appl Mech Rev
1	SWRI/Abramson
1	Stanford U/Street
1	Stanford Res Inst
1	SIT Davidson Lab
1	SIT Davidson Lab/Breslin
1	SIT Davidson Lab/Tsakonas
1	U Washington Appl Phys Lab
1	Webb Inst/Lewis
1	Webb Inst/Ward
1	Woods Hole/Ocean Engr
1	SNAME
1	Bethlehem Steel New York
1	Bethlehem Steel Sparrows
1	Bolt Beranek & Newman
1	Eastern Res Group
1	Esso International
1	Gen Dyn Elec Boat/Boatwright
1	Gibbs & Cox
1	Hydronautics
1	Lockheed Miss & Space/Waid
1	Newport News Shipbuilding
1	Oceanics
1	Sperry Sys Mgmt
1	Sun Shipbuilding Aero/Hydro
1	Robbert Taggart
1	Tracor

CENTER DISTRIBUTION

Copies	Code	
1	15	W. Cummins
1	1502	G. Stuntz
1	1506	M. Ochi
1	1509	H. Pollard
1	152	R. Wermter
1	1528	H. Yeh
1	154	W. Morgan
1	1552	N. Salvesen
1	156	J. Hadler
1	1561	G. Hagen
1	1562	M. Martin
1	1564	J. Beldman
1	1564	C. Lee
1	1564	R. Curphey
1	1568	G. Cox
1	1568	L. Ruth
1	1568	E. Zarnick
1	1568	E. Baitis
1	1568	D. Gerzina
1	1568	H. Jones
1	1568	E. Foley
1	1572	M. Ochi
1	1572	J. Kallio
1	1576	W. Smith
1	117	S. Hawkins
1	117	R. Stevens
1	117	G. Lamb
1	117	J. Bloom
1	1173	B. Nakonechny

UNCLASSIFIED

Security Classification

DOCUMENT CONTROL DATA - R & D

(Security classification of title, body of abstract and indexing annotation must be entered when the overall report is classified)

1. ORIGINATING ACTIVITY *(Corporate author)*

Naval Ship Research and Development Center
Bethesda, Maryland 20034

2a. REPORT SECURITY CLASSIFICATION

Unclassified

2b. GROUP

3. REPORT TITLE

MOTIONS AND HULL-INDUCED BRIDGING-STRUCTURE LOADS FOR A SMALL WATERPLANE AREA, TWIN-HULLED, ATTACK AIRCRAFT CARRIER IN WAVES

4. DESCRIPTIVE NOTES *(Type of report and inclusive dates)*

5. AUTHOR(S) *(First name, middle initial, last name)*

Harry D. Jones and David M. Gerzina

6. REPORT DATE	7a. TOTAL NO. OF PAGES	7b. NO. OF REFS
August 1973	73	1

8a. CONTRACT OR GRANT NO.	9a. ORIGINATOR'S REPORT NUMBER(S)
b. PROJECT NO. 1-1568-205	3819
c.	9b. OTHER REPORT NO(S) *(Any other numbers that may be assigned this report)*
d.	

10. DISTRIBUTION STATEMENT

APPROVED FOR PUBLIC RELEASE: DISTRIBUTION UNLIMITED

11. SUPPLEMENTARY NOTES	12. SPONSORING MILITARY ACTIVITY
	NAVSHIPS

13. ABSTRACT

An experimental investigation was performed with a model in the maneuvering and seakeeping facility at the Naval Ship Research and Development Center to determine the characteristics of a proposed small waterplane area, twin-hulled, attack aircraft carrier in waves. Motions of the model were measured, together with the forces and moments induced by the hulls on the cross structure spanning the two hulls. Experimental data were compiled in head, bow, beam, quartering, and following regular waves in addition to long-crested, irregular head and beam waves. Some powering measurements were also made in regular head waves.

DD FORM 1 NOV 65 1473 (PAGE 1)

S/N 0101-807-6801

UNCLASSIFIED

Security Classification

14 KEY WORDS	LINK A		LINK B		LINK C	
	ROLE	WT	ROLE	WT	ROLE	WT
SWATH (Small Waterplane Area, Twin-Hulled, Attack Aircraft Carrier)						
Motions						
Loads						
Added Thrust						
Catamaran						